Addis Ababa University

College of Technology and Built Environment

School of Built Environment

Department of Urban and Regional Planning

Comparative Analysis of Urban Heat Island Effect Before and After Corridor Development From 'Piassa' to 'Megenagna' Route, Addis Ababa, Ethiopia

Author: Robel Kassahun Bogale

June, 2025

Addis Ababa, Ethiopia

COMPARATIVE ANALYSIS OF URBAN HEAT ISLAND EFFECT BEFORE AND AFTER CORRIDOR DEVELOPMENT FROM PIASSA TO MEGENAGNA ROUTE, ADDIS ABABA, ETHIOPIA

AUTHOR: ROBEL KASSAHUN BOGALE

A THESIS SUBMITTED TO THE DEPARTMENT OF URBAN AND REGIONAL PLANNING, SCHOOL OF BUILT ENVIRONMENT, COLLEGE OF TECHNOLOGY AND BUILT ENVIRONMENT, ADDIS ABABA UNIVERSITY IN PARTIAL FULFILLMENT OF THE REQUIREMENTS FOR THE DEGREE OF MASTER OF SCIENCE IN ENVIRONMENTAL PLANNING AND LANDSCAPE DESIGN.

JUNE, 2025

ADDIS ABABA, ETHIOPIA

Declaration

I, the undersigned, declare that this thesis is my original work and has not been presented for a degree in any other university. All sources of material used for the thesis have been duly acknowledged, following the scientific guidelines of the University.

Student Name: Robel Kassahun

Enrolment Number: GSR/8618/15

Signature: _______________ Date: _______________

Confirmation

The thesis is submitted with my approval as the Institute's supervisor.

Supervisor’s Name: Aramde Fetene (Ph.D.)

Signature: _______________ Date: _______________

Addis Ababa, Ethiopia

Approval sheet

This is to certify that the thesis prepared by Robel Kassahun titled: ***Comparative analysis of urban heat island effect before and after corridor development from 'Piassa' to 'Megenagna' route Addis Ababa, Ethiopia*** and submitted in fulfillment of the requirements for the degree of Master of Science in Environmental Planning and Landscape Design complies with the regulations of the University and meets the accepted standards concerning originality and quality.

Approved By the Board of Examiners

Aramde Fetene (PhD) Signature: ____________________ Date: __________________

Advisor

_________________________ Signature: ____________________ Date: __________________

Internal Examiner

_________________________ Signature: ____________________ Date: __________________

External Examiner

________________________ Signature: ____________________ Date: __________________

Chairperson

_________________________ Signature: ____________________ Date: __________________

Head, Department of Urban and Regional Planning

Acknowledgement

First and foremost, I would like to express my deepest gratitude to GOD almighty for his support in my lifetime journey. I am profoundly thankful to my advisor, Aramde Fetene (PhD), for dedicating his time to insightful guidance, constructive advice, and fruitful feedback for shaping my paper until the final stage of submission with remarkable patience. Furthermore, I sincerely acknowledge Government officials i.e. Addis Ababa city Land development and administration bureau, Addis Ababa city road authority, Ethiopian metrological institute, Plan preparation & administration bureau, and Urban beautification & green development bureau, who specifically supported me in providing data for the research and their willingness for an interview regarding the corridor development. Finally, I would like to give my special thanks to my family for their unconditional love and encouragement throughout my whole life.

Table of Contents

Declaration ... ii

Approval sheet ... i

Acknowledgement ... ii

List of Figures ... vi

List of tables ... vii

List of Annex ... viii

Acronyms ... ix

Abstract ... x

CHAPTER ONE: INTRODUCTION ... 1

1.1 Background of the Study ... 1

1.2. Statement of the Problem ... 2

1.3. Objectives of the Study ... 4

1.3.1. General Objective ... 4

1.3.2. Specific Objectives ... 4

1.4. Research Questions ... 4

1.5 Scope of the Study ... 4

1.6 Significance of the Study ... 5

1.7 Research Limitations ... 5

1.8 Organization of the paper ... 6

CHAPTER TWO: LITERATURE REVIEW ... 7

2.1. Definition of Terms ... 7

Streetscapes ... 7

2.2. Theoretical Review ... 7

2.2.1. The Complexity Theory ... 7

2.2.2. Modernization theory ... 8

2.2.3. Urban system theory ... 8

2.2.4. Urban Heat Island Theory ... 8

2.2.5. Urban Canopy ... 8

2.2.6. Wind Blocking ... 9

2.2.7. Urban rural Energy Balance ... 9

2.2.8. Urban evapotranspiration 9
2.2.9. Spatial Analysis 10
2.3. Conceptual review 10
2.3.1. Land surface temperature (LST) 10
2.3.2. Normalized difference vegetation index/NDVI/ 11
2.3.3. Normalized difference built-up index/NDBI/ 12
2.3.4. Urban heat island intensity 12
2.3.5. Planning strategies and models 14
2.3.6. Urban Road 17
2.3.6.1. Environmental impacts of Urban Road 17
2.3.6.2. Urbanization, Urban Road, and UHIE 17
2.3.6.3. Urban Road Expansion, corridor development and UHIE 18
CHAPTER THREE: MATERIALS AND METHODS 19
3.1. Description of the Study Area 19
3.1.1. Site selection criteria 19
3.2. Research design 20
3.3. Data types and sources 20
3.4. Method of data analysis 23
3.4.1. Spatial analysis 23
3.4.2. Temporal analysis 23
3.4.3. Correlation analysis 26
3.4.4. Regression analysis 27
3.5. Method of data presentation 28
3.6. Methodological Framework 29
3.7. Reliability and Validity 29
3.8. Ethical Consideration 31
CHAPTER FOUR: RESULT AND DISCUSSION 32
4.1. Results 32
4.1.1. Spatial and temporal patterns in LST 32
4.1.2. Spatial and temporal patterns in NDVI 39
4.1.3. Spatial and temporal patterns in NDBI 43
4.1.4. Combined result of variations on UHIE 46

4.2 Discussions ... 50
4.2.1. Spatial and temporal patterns in LST ... 50
4.2.2. Spatial and temporal patterns in NDVI ... 52
4.2.3. Spatial and temporal patterns in NDBI ... 54
4.2.4. Trends on urban heat island intensity (UHII) ... 55
CHAPTER 5: CONCLUSION AND RECOMMENDATIONS ... 57
5.1. Conclusion ... 57
5.2. Recommendation ... 59
Reference ... 63
Annex 1 **Publishable Manuscript** ... 76

List of Figures

Figure 3.1. Location map of the study area 19
Figure 3.2. LST Analysis workflow chart in Arc Gis ……………………………………..24
Figure 3.3. Code script of a) LST, b) NDVI, c) NDBI, and d) UHIE retrieval ……………..…26
Figure 3.4. Methodological workflow of the study……………………………………..29
Figure 4.1. Spatial patterns on the road before and after corridor Development 32
Figure 4.2. Addis Ababa City: a) LST in 2015, b) LST in 2020, and c) LST in 2024 33
Figure 4.3. Temporal Trend line in LST of Addis Ababa (2015, 2020, and 2024) 33
Figure 4.4. Addis Ababa city minimum, mean, and maximum temperature line 35
Figure 4.5. Study Area LST, a) 2015, b) 2020, and c) 2024... 36
Figure 4.6. Temporal Trend line in LST of the study area in 2015 36
Figure 4.7. Temporal Trend line in LST of the study area in 2020 37
Figure 4.8. Temporal Trend line in LST of the study area in 2024 38
Figure 4.9. Temporal Trend line in LST of study area (2015, 2020, and 2024).......................... 38
Figure 4.10. Addis Ababa city NDVI in a) 2015, b) 2020, and c) 2024..................................... 39
Figure 4.11. Temporal Trend bar in NDVI of Addis Ababa (2015, 2020, and 2024) 40
Figure 4.12. Study Area NDVI in a) 2015, b) 2020, and c) 2024... 41
Figure 4.13. Temporal Trend bar in NDVI of the Study Area (2015, 2020, and 2024) 42
Figure 4.15. Addis Ababa city NDBI in a) 2015, b) 2020, and c) 2024 43
Figure 4.16. Temporal Trend bar in NDBI of Addis Ababa (2015, 2020, and 2024) 44
Figure 4.17. Spatial and temporal patterns of NDBI in the study area, a) 2015, b) 2020, and c) 2024... 45
Figure 4.18. Temporal Trend bar in NDBI of Study Area (2015, 2020, and 2024) 45
Figure 4.19. Addis Ababa city UHIE in 2015, 2020, and 2024.. 46
Figure 4.20. Temporal Trend bar chart in UHIE of Addis Ababa (2015, 2020, and 2024)......... 47
Figure 4.21. Study Area UHII in a) 2015, b) 2020, and c) 2024 47
Figure 4.22. Temporal Trend bar chart in UHII of the study area (2015, 2020, and 2024) 49
Figure 5.1. Green infrastructure, and wind blocking conceptual model..................................... 59
Figure 5.2. Proposed Permeable pavement strategy 60
Figure 5.3. Shades, Nature-based solutions, and case study... 61
Figure 5.4. Proposed strategies with corridor development road 62

List of tables

Table 2.1: NDVI value range description 11

Table 2.2: UHI classification range 13

Table 2.3: Threshold range of UTFVI 13

Table 2.4: Variable classification in urban heat island 18

Table 3.1: Data source, Data set used, spatial resolution, and date of Acquisition 21

Table 3.2: Satellite imagery description 21

Table 3.3: Remote sensing data used in the study 21

Table 3.4: Remote sensing data used in the study for surface reflectance 21

Table 3.5: Key informant for the research interview 22

Table 4.1: Temporal Trends in NDVI of the Study Area (2015, 2020, and 2024) 41

List of Annex

Annex 1 Publishable Manuscript 76

Annex 2 Corridor development roads and Study Area Road 112

Annex 3 Asphalt Pavement heat flow per day 113

Annex 4 Variation of solar reflectance of asphalt and concrete pavement over time 113

Annex 5 Concrete pavement temperature per day 114

Annex 6 Addis Ababa mean, minimum, and maximum temperature 114

Annex 7 Temporal Trends in LST of Addis Ababa (2015, 2020, and 2024) 114

Annex 8 Temporal Trends in LST of study area (2015, 2020, and 2024) 115

Annex 9 Tree, Shrub and grass species recommended for roadside 115

Annex 10 Interview Questions for Key informants 118

Acronyms

AACRA	Addis Ababa City Road Authority
ECSA	Ethiopian Central Statistics Agency
EMI	Ethiopian Meteorological institute
GEE	Google Earth Engine
GW	Global Warming
LST	Land Surface Temperature
NDBI	Normalized difference built-up index
NDVI	Normalized difference vegetation index
UHI	Urban heat island
UHIE	Urban heat island effect
UHII	Urban heat island intensity
UN	United Nation
UNFCCC	United Nations Framework Convention on Climate Change
USGS	United States Geological Survey
UTFVI	Urban thermal field variance index

Abstract

Urban expansion and urbanization in cities like Addis Ababa are increasing the vulnerability of the areas to urban heat island intensity (UHII) phenomena, with an increasing trend in urban thermal dynamics. This research analyzed the spatial and temporal variations along the route from "Piassa" to "Megenagna" before and after corridor development through field observation, using a combination of remote sensing data, and Landsat 8 imagery by the tools Google Earth Engine, and ArcMap. The results demonstrate that the study area's UHII elevated higher during the research period due to increased land surface temperature (LST), fluctuation in normalized difference built-up index (NDBI), and reduced normalized difference vegetation index (NDVI). The annual average mean LST in 2024, with a value of 32.82467^{0}C, shows an increasing trend with a value of 31.226^{0}C from 2015 and 30.84431^{0}C from the result in 2020. The NDVI result shows a consistently decreasing trend over time. In 2015, the NDVI was 0.34475; in 2020, it declined to 0.265243; by 2024, it further dropped to 0.199966, indicating a reduction of vegetation cover. The mean annual NDBI in 2015 was -0.03495, which increased to 0.001339 in 2020, which indicates built-up area expansion, but in 2024, the value dropped to -0.02705 due to the demolished residence in the area. From the combined impacts of these results, the most negative UHII annual mean average value was recorded in 2015 with the value of 0.246969, which increased in 2020 to -0.257157 and further increased to -0.273355. These results revealed that surface urban heat island intensity (SUHI) was more concentrated in the ‘urban’ area than in the ‘rural’ area. The findings also reveal a significant inverse relationship between NDVI and LST, highlighting the role of sustainable corridor design and Green infrastructure for mitigating the impact of UHII. Future studies should explore in-depth analysis through adaptive advanced approaches by integrating satellite imagery data with the baseline situation (ground truth) for the accuracy and spatially detailed results to develop an effective mitigation strategy.

Key Words: Corridor development, impervious surfaces, street scape, and urban heat island effect

CHAPTER ONE: INTRODUCTION

1.1 Background of the Study

Roads are spreading all across the world due to major factors, including rising populations and improved connectivity. With the right planning and placement, they can benefit the environment rather than damaging it (Laurance et al., 2009; Balmford et al., 2012). The infrastructure of roads and highways plays a pivotal role in facilitating the movement of individuals and goods over extensive distances, which underscores the profound reliance that both developed and developing nations exhibit towards road transportation, as this mode of transit is not only integral to the functionality of contemporary society but also contributes significantly to economic growth, social connectivity, and cultural exchange on a global scale (Mlambo, 1994). The demand for more minerals, fossil fuels, lumber, and agricultural land, as well as the efforts of developing countries to upgrade their energy and transportation infrastructure, all contribute to this worldwide road rush.

The accelerated pace of urbanization is a defining feature of the 21st century. According to the World Bank, urban populations are growing at an annual rate of approximately 1.8%. Due to this growth, metropolitan road networks require expansion and modifications to handle rising traffic loads and a variety of transportation requirements. The development and operation of these routes also greatly contribute to climate change by altering the natural environment. Metropolitan regions are now grappling with two severe environmental problems: flooding and a rise in the urban Heat Island effect (UHI) under the favorable influence of larger-scale flow Therefore, a smaller city with upstream urbanization can have a larger UHI than a larger city with no upstream urbanization (Zhang et al. 2009, and 2011).

In Ethiopia, roadways serve as the principal infrastructure that has developed drastically, accounting for more than 95% of both passenger and freight transportation (AACRA, 2009). The Ethiopian government emphasizes the need to develop high-quality infrastructure to support the country's rapid urban expansion, as well as the significance of building organizational frameworks to ensure infrastructure sustainability.

Urban road networks are essential for environmental sustainability in addition to being crucial for transportation. The metropolis of Addis Ababa, which has been the driving force behind the robust 8 economic growth, is rapidly urbanizing and constructing several roadways. Furthermore, the city of Addis Ababa encourages the building and upgrading of city roadways as part of its long-term development strategy presented on the Addis Ababa City Structure Plan (AACRA, 2009).

Hence, the purpose of this research is to enhance urban resilience through sustainable urban planning by developing a research-based alternative strategic approach on the theme of urban roads by investigating the urban heat island effect before and after corridor development. Finally, it will provide a recommendation to mitigate the imposed impacts.

1.2. Statement of the Problem

The proportion of the world’s population living in urban areas was only 30% in 1950 but reached 55% in 2018, and is projected to be 68% by 2050 (World Urbanization Prospects, 2018). The population of developing countries' metropolitan areas will rise from 2.6 billion in 2010 to 5.3 billion in 2050 (Madlener et al., 2011). Sub-Saharan Africa (SSA) has the highest urban growth rate, at around 3.6% per year (Yiral et al., 2020; Bocquier, 2005). It is widely recognized as the world's fastest-urbanizing area, with an urban population of around 472 million, which is expected to double within the next 25 years (Saghir & Santoro, 2018).

According to the Ethiopian Central Statistics Agency in 2011, the country was grouped among the fastest urbanization processes in the world. In the agencies' Projection for the year 2007, the urban population in Ethiopia will triple to 42.3 million by 2037, growing at 3.8% a year. According to the Ethiopian urbanization review report in 2015, the rate of urbanization will be even faster, at about 5.4% a year. Addis Ababa City, which has been driving the robust economic growth (7~8% of GDP) of the country in recent years, is rapidly urbanizing, and many new roads are being developed (AACRA, 2019).

Urbanization has led to a rapid expansion in road construction and extension. Ethiopia has a total road network of approximately 3,761 km, of which only 26.3% (about 990 km) are paved (AACRA, 2019). The asphalt pavement ratio varies by road type, and the arterial roads have high ratio of 95.7% in average, while the others (Collector Streets and Local Streets) have low ratio of 15.9%. Although AACRA report on 2019, shows that the road occupancy ratio increase from 13.5% (approx. 5,199 ha) in 2016 to 18% by March 2019, it is still below the 25% generally recommended for urban area.

The development of road networks and changes in land use and land cover (LULC) will lead to the conversion of natural environments to impervious surfaces, which will have substantial impacts on climate, hydrology, and urban ecosystems. Increased surface temperatures, changed carbon cycle, and decreased soil organic carbon density are the results of this change, which is mostly caused by urbanization. The equilibrium between increased air temperature induced by solar energy (heating process) and decreased air temperature owing to evaporation (cooling process) is affected by urbanization.

Increased impervious surfaces contribute to the urban heat island effect, raising surface temperatures by up to 3 K with a 50% increase in surface sealing. The warming is exacerbated by the heat retention of materials like concrete, which affects local air temperatures and boundary layer dynamics (Mohajerani et al., 2017). Impervious surfaces have an impact on the urban environment and are typically seen as a sign of the hydrology of urban watersheds (Wu et al., 2019).

Increased built-up area, road network development, natural landscape fragmentation, decrease drainage efficiency, increased stormwater runoff generation, increased flood frequency, water channelization into streams and other surface water bodies, decreased agricultural land, and altered regional microclimate are the main effects of urbanization (Shuster et al., 2005; Ladson et al., 2006; McGrane, 2016).

The Asphalt pavement and other dark surfaces in urban environments are the primary causes of the UHI (Calkins, 2012). The asphalt pavement absorbs the radiation of the sun rather than reflecting it, increasing the temperature of ambient air and pavement surfaces. The paved surfaces in urban and suburban areas are often warmer than the less-paved surfaces in rural areas. Pavement is usually comprised of materials with very low reflectivity (Dobos, 2003).

Over all, the study of urban roads is crucial for creating sustainable urban settings since it has an impact on the environment, livelihood and climate. In addition, this study can be utilized as a foundation for further researches and as a framework for city-wide in order to create sustainable urban corridor roadways.

1.3. Objectives of the Study

1.3.1. General Objective

The General objective of the research is to analyze the spatial and temporal variations in the Urban Heat Island (UHI) along the route from "Piassa" to "Megenagna" before and after corridor development.

1.3.2. Specific Objectives

- ☐ To analyze the variation in land surface temperature (LST) before and after corridor development along the roadway route from ‘Piassa’ to ‘Megenagna’.
- ☐ To assess trends in vegetation abundance using the Normalized difference vegetation index (NDVI) in the study area over the periods 2015, 2020, and 2024.
- ☐ To investigate the extent of built-up areas and their correlation with temperature increase using Normalized difference built-up index (NDBI)**.**
- ☐ To formulate and evaluate the combined impact of integrating LST, NDVI, and NDBI on UHII.

1.4. Research Questions

1. What is the variation between the Land Surface Temperature (LST) before and after corridor development along the road from "Piassa" to "Megenagna"?
2. What are the trends in vegetation abundance, and NDVI (Normalized difference vegetation index)?
3. What are the extents of built-up areas (NDBI) and the gradual increase in LST and UHII?
4. What is the combined impact of integrating LST, NDVI, and NDBI on Urban heat island intensity?

1.5 Scope of the Study

i. Spatial scope

The administrative level that the research aims to cover is at the ‘Arada’ and ‘Yeka’ sub-cities, Addis Ababa; on the road from ‘Piassa Jegol’ Square to ‘Megenagna Diaspora’ Square, which covers about 7.5 Km.

ii. Temporal scope

The research focus on a comparative temporal analysis of land surface temperature (LST),), Normalized Difference Vegetation Index (NDVI), Normalized Difference Built-up Index (NDBI), and Urban heat island intensity (UHII) for the years 2015, 2020 and 2024.

iii. Thematic scope

The study focuses on the intensity of the Urban Heat Island (UHI) using spatial and temporal variations in Land Surface Temperature (LST), Normalized Difference Vegetation Index (NDVI), and Normalized Difference Built-up Index (NDBI) along the route from "Piassa" to "Megenagna" before and after corridor development.

1.6 Significance of the Study

Urban roads have an array of effects on climate change, as a result, they are mainly susceptible to UHII, which aggravates the risk of global warming. Assessing the implications of urban roads on climate change is critical since the outcomes of the research will likely have a substantial impact on global environmental issues for developing sustainable urban environments. As urban roadways aggravate the urban heat island effect, research-based strategies must be implemented to mitigate these impacts and reduce their major contribution to global warming.

In general, the findings of this study paper may be used as a baseline document since the city is undergoing corridor development along road sides, which will provide prospective solutions for growth in other sections of the city and contribute to a sustainable urban environment at the city level. Furthermore, the document will be used as an input document for environmental advocates, future researchers, non-government organizations (NGOs), and policymakers, as it can serve as a blueprint for future projects by emphasizing the pros and cons of an inclusive research-based approach to the development of sustainable cities.

1.7 Research Limitations

As the research aims to insight the environmental impacts on the theme of UHII of corridor development from ‘Piassa’ to ‘Megenagna’ route from the first phase corridor development in which the project initially was securely processed; the research is thoroughly limited by data accessibility as the research needs maps that show before and after corridor development there is a variation on the corridor development proposal and implemented design due to political factors. And there was a lack of willingness to share data related to the project, mainly due to security concerns because of the sensitive nature of the project, and still ongoing process of corridor development in other areas of the city.

1.8 Organization of the paper

The first chapter presents introductions to the research including the Background of the Study, Statement of the Problem, Research Questions, Objectives of the Study, Objectives of the study, Scope of the Study, Significance of the Study, and Research Limitations. The second chapter presents theoretical and conceptual reviews of the kinds of literature. In chapter three, the materials and methods used in the research were discussed, including a description of the Study area, Data types and sources, Research Design, Method of data collection, Method of data analysis, Method of data presentation, Methodological framework, and reliability and validity of the data. The fourth chapter presents the results with specific discussions in each session on LST, NDVI, NDBI, and UHII. The Fifth chapter of the research describes the conclusion of the research, which includes the major findings of the research and recommends data-based possible scenarios for resolving the problem.

CHAPTER TWO: LITERATURE REVIEW

2.1. Definition of Terms

Convection

The process of convection is the movement of energy from a solid surface to a fluid, such as a liquid or gas. In UHIE, it is an energy transferred from the Earth's surface to the air above it. Corridor development /Roadside corridor development/ (Dimoudi, 2003).

Impervious surface area

The term "impervious surface area" describes surfaces, such as concrete, asphalt, and some types of roofing, that prevent water from penetrating the ground. These surfaces can increase runoff, which can cause flooding and water quality problems in adjacent bodies of water (Barnes, 2001).

Urparian

Explains the green spaces that surround walkways and roadways. The name was created by fusing the words "urban" and "riparian" (Raciti et al., 2006).

Streetscapes

Streetscapes are essential city organs that represent public life. A well-designed streetscape enhances quality of life and promotes community. Street furniture, walkways, and trees all promote social contact and pedestrian activity. Roads, greenery, people, buildings, animals, sidewalks, trees, street lights, and other components are all considered to be part of a streetscape. The streetscapes have an experience element and serve to portray the shape of the organically constructed environment. Additionally, streetscapes depict local inhabitants' public lives. There are several activities going on in these areas. The streetscape becomes the city's success criterion as it represents the culture of its residents (Rao, 2022).

2.2. Theoretical Review

2.2.1. The Complexity Theory

The Complexity Theory states that the metropolis is an ecosystem with intricate relationships across people, resources, material flows, and knowledge that affect one another. In Vienna at the beginning of the 20th century, Schmidt discovered these conditions (Schmidt, 1917). In the first half of the 20th century, research on heat islands in the US got underway (Mitchell, 1953).

2.2.2. Modernization theory

The study of modernization theory focuses on how societies evolve and change. It describes how civilizations evolve from traditional to contemporary states, particularly in light of social change, industrialization, and economic expansion. In the middle of the 20th century, especially following World War II, it became more well-known as researchers attempted to figure out how developing nations might catch up to the West in terms of development (Goorha, 2010). Theory of modernization aims to explain how and why societies develop, with a special emphasis on the shift from traditional to contemporary. Despite its influence, it is frequently criticized for being overly Western-centric and unsophisticated (Przeworski et al., 1997).

2.2.3. Urban system theory

Urban System Theory is a paradigm used in sociology, geography, and urban planning to comprehend how cities (urban areas) are structured, interact, and change over time as part of a larger economic and geographical system (Whebell, 1969s).

2.2.4. Urban Heat Island Theory

A British scientist Luke Howard's study provides a fundamental framework for comprehending the Urban Heat Island Effect in the 1810s on his observation in city of London is warmer than the nearby rural surroundings. He was the first to demonstrate that metropolitan air temperatures are frequently greater than those in the surrounding rural areas (Howard, 1833). According to Halder and Bandyopadhyay in 2021, the natural landscape is changed by urban expansion, which substitutes impermeable surfaces, greatly influencing the local climate and weather.

The intensity of the UHI is closely correlated with both internal city features (such as land-use pattern, building density, and city size) and external factors (such as climate, weather, and season) (Oke, 1982).

2.2.5. Urban Canopy

Multilayer buildings exist in an array of forms throughout metropolises. The heat radiated by a building is trapped by the adjacent higher building, resulting in the urban canopy. The creation of an urban canopy exacerbates UHI (Masson, 2006). Related to a concept of urban canopy, there is a concept termed as urban tree canopy; from an aerial perspective, the layer of leaves, branches, and stems covering the ground is known as the urban tree canopy (Raciti et al., 2006).

2.2.6. Wind Blocking

In urban and suburban regions, buildings serve as wind barriers, reducing wind speeds by as much as 60% (Landsberg, 1981). Wind speed is decreased by the presence of buildings that are situated close to one another. Consequently, the convectional cooling effect lowers. Thus, the impact is intensified since the heat that is stored is unable to released away (priyadarsini, 2008).

2.2.7. Urban rural Energy Balance

Featuring an emphasis on the variations in thermal absorption, retention, and the emission, it examines the distribution and transfer of energy between a metropolis and a nearby rural area. In a causal sense, disparities in energy balance and stability within urban and rural areas contribute to varying rates of warming and cooling near the surface. These distinctions generate distinct 15 periodic air temperature states, which at any one moment determine the extent of the UHI (Quart, 1982).

According to Chunhua in (2023), large tracts of low-permeable artificial surfaces took over high permeable natural underlying surfaces during this unprecedented urbanization, changing the energy balance and surface- water cycle and ultimately leading to the UHIE.

The energy balance equation is:

$$\text{Convection} + \text{Evaporation} + \text{Heat storage} = \text{Anthropogenic heat} + \text{Net radiation}$$

2.2.8. Urban evapotranspiration

The absence of vegetation in cities further affects the energy balance because it reduces evapotranspiration, which cools the surface naturally. Urbanization has an impact on the dynamics of the water cycle, denaturalizing the hydrological processes and increasing their complexity. Studies show that the expansion of impermeable surfaces in metropolitan areas can seriously disrupt the water balance by raising surface runoff and lowering evapotranspiration and groundwater recharge (Haase, 2009; Lee et al., 2010; Macdonald et al., 2021; Mejía et al., 2014; Wang et al., 2021).

Urban evapotranspiration from green infrastructure has received greater emphasis since it is acknowledged as a viable adaptation and mitigation approach for confronting the potential threat of urban heat stress resulting from urbanization and global climate change (Wang et al., 2021). As urban density rises, surface characteristics typically change as a result of less green space and more built-up areas (Oke, 1987).

Vegetation evapotranspiration also raises air humidity, and since humid air absorbs more heat, less heat builds up on the ground and building surfaces (Yan et al., 2023).

2.2.9. Spatial Analysis

The phrase "spatial analysis" is frequently used in the literature on Geographic Information Systems (GIS) and Geographic Information Science. In geography, the word "spatial analysis" has rooted that date at least to the 1950s, when it was first used to describe a summary of historical changes (Berry et al., 1968). Rearranging the spatial distribution of values or changing the spatial structure of the system being studied would affect the outcomes of any spatial study substantially (Chorley, 1972).

2.3. Conceptual review

According to Theeuwes in (2012), by weighting the effects of water basins and vegetation in metropolitan areas, they discovered that every 10% increase in vegetation lowers the temperature by 0.6K, and they highlighted that tree may significantly mitigate the impact. However, they 16 reached the conclusion that the presence of water bodies had the opposite effect of lowering the temperature.

2.3.1. Land surface temperature (LST)

Whereas vegetated regions and water bodies reduce LST, a larger percentage of impervious structures raises it (Dai et al., 2019). Variations in LST are influenced by the layout of these land covers (Li et al., 2016).

Thermal infrared (TIR) bands from satellites (like Landsat and MODIS) can be used to calculate LST. The following general formula (Planck’s law) is used to convert thermal infrared radiation to temperature:

$$LST = K2 / In ((K_1 / L\lambda) + 1)$$

Where:

- $L\lambda$ is the radiance at wavelength λ(lambda),
- K_1 and K_2 are calibration constants specific to the sensor,
- LST is the Land Surface Temperature in Kelvin.

2.3.2. Normalized difference vegetation index/NDVI/

The principle behind NDVI is that the presence of chlorophyll pigments causes "green" leaves to absorb light at red wavelengths, but their interior structure causes them to scatter light at near-infrared wavelengths (Farooq, 2012).

The NDVI, which is computed from the red and near-infrared bands of remote sensing data, is used to estimate vegetation cover. The following general formula is used to calculate NDVI:

$$NDVI = NIR - RED / NIR + RED$$

Where:

- NIR is the reflectance in the near-infrared band,
- RED is the reflectance in the red band,
- NDVI ranges from -1 to +1, where higher values indicate more vegetation.

Table 2.1: *NDVI value range description*

NDVI value range	Land cover type
High (0.5 to 1.0)	Dense and healthy vegetation
Moderate (0.3 to 0.5)	Sparse vegetation or lower-density vegetation
Low (0 to 0.3)	Barren land, urban areas, or minimal vegetation
Negative (-1 to o)	Non-vegetative surfaces(Water bodies, snow, clouds, bare soils)

Source: Atun et al., 2020

The formula for calculating the mean NDVI is:

$$Mean\ NDVI = \frac{NDVI\min + NDVI\max}{2}$$

Where:

- NDVImin - is the minimum NDVI value,
- NDVImax - is the maximum NDVI value.

The following formula is used for the standard deviation of two values:

$$SD = \sqrt{(Xmax-\mu)^2 + (Xmin-\mu)^2\ /2}$$

Where:

- X_{max} - is the maximum NDVI value,
- X_{min} - is the minimum NDVI value,
- μ - is the mean NDVI.

2.3.3. Normalized difference built-up index/NDBI/

Normalized Difference Built-Up Index Method, makes use of the middle infrared (SWIR 1) and near-infrared (NIR) channels. Studies that further highlight the density of urban buildings using the NDBI score. An efficient transformation for determining the appearance of an awakened area is NDBI (Danoedoro et al., 2018).

NDBI uses the short-wave infrared (SWIR) and near-infrared (NIR) bands to detect urban or built-up regions. The following general formula is used to calculate NDBI:

$$NDBI = SWIR - NIR\ /\ SWIR + NIR$$

Where:

- SWIR is the reflectance in the short-wave infrared band,
- NIR is the reflectance in the near-infrared band.
- NDBI values are typically positive for urban/built-up areas and negative for non-urban areas.

2.3.4. Urban heat island intensity

According to prior studies, rising temperatures in numerous cities globally have had a substantial effect on public health and well-being (Kotharkar et al., 2018). The UHIE is an inherent tendency of metropolitan regions to experience warmer outdoor temperatures (up to 12 K higher) than the surrounding rural area (Aleksandrowicz et al., 2017).

UHII measures how much the land surface temperature of the adjacent rural region varies from that of the urban area.

$$UHII = LST\ urban - LST\ rural$$

Where:

- LST urban is the land surface temperature of the urban area,
- LST rural is the land surface temperature of the rural or non-urban area.

Table 2.2: *UHI classification range*

UHI Class	*Formula*
Class 1 low	LST<mean-(2xSD)
Class 2 Sub-low	Mean-(2xSD)≤LST<mean-SD
Class 3 Moderate	Mean-SD≤LST<mean
Class 4 Sub-high	mean≤LST<mean+SD
Class 5 High	LST≥mean+SD

Source: Liu et al., 2021

The urban thermal field variance index (UTFVI)

There are several thermal comfort indices available to assess how the UHI affects urban life quality. In this work, the ecological assessment of UHI zones was conducted using the UTFVI by using the following equation (Zhang, 2006).

$$\mathrm{UTFVI} = \frac{(\mathrm{Ts} - \mathrm{Tmean})}{\mathrm{Tmean}}$$

Where:

UTFVI – Urban Thermal Field Variance Index

Ts – LST (°C)

Tmean – Mean LST (°C)

Table 2.3: *Threshold range of UTFVI*

UTFVI range	*Effect of Phenomenon*
< 0.005	Least significant heat island effect
0.005-0.015	Weak urban heat island effect

0.015-0.025	Moderate urban heat island effect
0.025-0.035	Strong urban heat island effect
UTFVI>0.035	Very strong urban heat island effect

Source: Waleed et al., 2023

2.3.5. Planning strategies and models

2.3.5.1. Urban Planning Strategies

According to Yamamoto in (2006), the Mitigation of the UHI effect can be greatly enhanced by an effective urban planning strategy. By logically orienting the buildings, a wind route is formed to allow cool airflow from the river into the metropolis. By reducing thermal accumulation, it is anticipated that in various types of urban areas, an adequate amount of open space and a wind channel will help to lessen the impact of the urban microclimate. In metropolitan spots, strategies such as creating wind corridors can improve ventilation and lessen heat buildup.

Road settings in urban areas are not exclusively intended for motor vehicle drivers and passengers, as well as for Vulnerable Road users, such as cyclists, pedestrians, those with disabilities, youngsters, and the elderly, who should receive a lot of care. As a result, a road infrastructure that is both acceptable and human-oriented should include the infrastructure necessary to meet their demands (Flores et al., 2021). As a result, segregated cycling infrastructure (bike lanes or tracks), walking infrastructure (wide, well-maintained sidewalks and pedestrianized areas), and infrastructure designed to make more accessible for people with disabilities to move around (such as curb ramps and tactile paving) create an important urban road principle (Macmillan et al., 2014; Oxley et al., 2010).

2.3.5.2. Permeable Pavements

Road and highway pavements made of high albedo materials might reflect more solar energy (Akbari et al., 2001). Cool paving lowers the temperature of the surface by 19.5°C (30°F) or more (Asaeda et al., 1996). The UHI impact can thus be lessened by choosing pavement materials carefully (Levinson et al., 2001).

In contrast to conventional pavements, permeable pavements have several benefits such as decreasing storm water runoff, ground water recharge, minimizing pollution discharges, enhancing air quality, and decreasing noise disturbances on roads and highways (Ferguson, 2005; Scholz et al., 2007).

According to Xu et al. in (2013), indicated that the impervious surface and land surface temperature had a substantial positive exponential connection. According to their findings, a 10% rise in imperviousness, when the impervious surface subsequently makes up over 70% of the land, may raise the land surface temperature by over 3.3 °C.

The two types of pavements that are most frequently constructed are Portland cement concrete, sometimes known as concrete, and asphalt cement concrete, also known as asphalt. When placed, asphalt is dark grey or black, and its initial solar reflectance ranges from 5 to 10%. Asphalt becomes lighter with time, and its solar reflectance rises to 10% to 20%. Heat from asphalt can reach 65°C (150°F) (Lisa, 2008). Laboratory testing of concrete that has been artificially brightened revealed solar reflectivity rates of up to 80% (Akbari, 2001).

Concrete pavements and light-colored asphalt

Concrete pavement is the most prevalent type of pavement which is light grey, with solar reflectance values usually between 35 and 40 percent when the pavements are new and reducing their solar reflectance to 25–35 percent over time due to the dirt in the pavement (Lisa, 2008).

Asphalt pavements can be lightened and cooled in various ways including adding Light pigment can be added to the asphalt mix or lighter-colored aggregates (rocks in the pavement mixture) or sand can be added and lighter aggregates to emulsion seal coats and chip seals that is used to top existing pavements during routine asphalt maintenance (Cartwright, 1998; Ting et al., 2001). These measures can increase the solar reflectance of the pavement by up to 30 percent (Lisa, 2008).

Lighter-colored aggregates and cement binders can further cool concrete pavements, since studies of particularly lightened concrete have demonstrated solar reflectance levels of up to 80% (Levinson et al., 2001).

2.3.5.3. Green Infrastructure

It is a systematic approach to land conservation that addresses the social and ecological effects of open space fragmentation and consumption (Benedict et al., 2006). UHIE can be effectively reduced through urban green spaces that are mostly made up of Vegetation and water features

(Chen et al., 2014). Reduced heat absorption (and consequently emission) by low albedo man-made urban surfaces results in lower temperatures brought on by both evapotranspiration and direct shadowing (Dimoudi et al., 2003).

By reviewing 75 research, the most prevalent characteristics that contribute to UHI were identified, including vegetation cover (44%), season (33%), built-up area (28%), day/night (25%), and population density (14%) (Deliami et al., 2018).

According to Goodman in 2018, rising temperatures impact human health, either directly through heat exposure or indirectly through heat-induced alterations to pollutants in the atmosphere. It has been shown that urban greenery has a significant ability to regulate urban temperatures (Qiu et al., 2013). The cooling effects of varying vegetation distributions can also be influenced by the spatial arrangement of vegetation (Li et al., 2012).

Trees and other vegetation cool their surroundings in two primary ways:

I. Evapotranspiration cools the air and vegetation by converting solar energy into vaporized water rather than heat, and
II. They shade surfaces from the sun's heat, which cools the surfaces and releases stored energy (Fadhil, 2023).

2.3.5.4. Concept of Green Roads

Green roads are an innovative approach to road construction and maintenance that emphasizes environmental friendliness and ecological sustainability. Green road construction's key goals are to minimize pollution in the natural environment and enhance sustainability in the transportation industry (Benedict, 2006).

2.3.5.5. Shading and Design

The shadow areas projected by buildings have recently become a novel indicator that was missing in earlier studies (Morrison et al., 2018; Dai et al., 2019) capturing ground shades cast by tall buildings through satellite images as one distinct type of land cover. Their results show that an increase of 1% in building shade area leads to LST decreases between 0.24% and 0.79%.

Shade trees, as defined by Sailor (2006), have a large canopy and may shield buildings and pedestrians from sunlight while keeping them relatively cool. Shade trees also contribute to lowering temperatures through evapotranspiration.

Akbari in (2001), stated that Shade trees are primarily responsible for keeping buildings relatively cool by blocking sunlight. It lessens the air temperature, reduces the building's air conditioning, and enhances the quality of the air. Also, Sailor in (2006), Trees that provide shade are also susceptible to severe storms that might endanger human life.

According to Liu in 2002, the green roof is limited to around 30°C (90°F), but the regular roof can achieve temperatures of 65°C (150°F).

2.3.6. Urban Road

2.3.6.1. Environmental impacts of Urban Road

Numerous studies demonstrate how urban roads affect the environment and climate change, including the effects of emissions and how road infrastructure exacerbates UHIE. The elevated temperatures in urban areas impact urban environmental quality and human well-being (Mohajerani et al., 2017).

2.3.6.2. Urbanization, Urban Road, and UHIE

Roads may occupy up to approximately 35% of the metropolitan landscape (Yang et al., 2021). Although urbanization has several advantages, it is also a key driver of concerns regarding the environment (Ünal et al., 2020). The surface energy balance is susceptible to severely affected by urbanization, leading to a decline in latent heat flow and a rise in sensible heat flux (Imran et al., 2019; Barnes et al., 2001). Urbanization, which fueled elements like road infrastructure, factories, building developments, etc., contributes considerably to climate change by warming the atmosphere and producing emissions linked to higher surface temperature termed as UHI (Muñoz et al., 2020).

Because of infrastructure and anthropogenic activity, cities have greater temperatures than their rural counterparts due to a phenomenon exacerbated by metropolitan roadways. Cities' temperatures rise as a result of more impermeable surfaces as well as reduced greenery (Wang et al., 2024).

Due to high population density, lack of green/open space areas, tall structures, and air pollution from industrial zones and transportation networks, urban regions are more susceptible to increased LST and UHI (Bijay et al., 2021).

2.3.6.3. Urban Road Expansion, corridor development and UHIE

Urban roads contribute to the UHI effect and change the microclimate at numerous scales (Millard, 2022; Mirabi et al., 2022).

The expansion of urban built-up regions results in the replacement of rural areas' undeveloped surfaces, which causes temperatures of the air and surface (Akbari et al., 2008; Gao et al., 2019).

Urban expansion could potentially have a substantial impact on the surface energy balance, leadi ng to a decrease in latent heat flow and a rise in sensible heat flux (Barnes et al., 2001). Urban expansion could increase urban air temperature and the surface temperatures by 0.75–2.80 ^{0}C and by 1.9–5.4 ^{0}C, respectively (Imran et al., 2019).

Road geometry will also alter wind patterns, direction, and solar radiation gains, leading to more concentrated heated and dirty air (Adiguzel & Cetin, 2023).

Table 2.4: *Variable classification in urban heat island*

Variables	*Type*	*Description*
Urban heat island effect (UHIE)	Dependent variable	UHII is DV whereas LST, NDBI, and NDVI are IV.
Land surface temperature (LST)	Dependent variable	Represents UHII and influenced by Land cover
Normalized difference built-up index (NDBI)	Independent variable	Indicated Built-up areas Increase in NDBI increases LST
Normalized difference vegetation index (NDVI)	Independent variable	Indicates vegetation cover; Increase in NDVI lowers LST

CHAPTER THREE: MATERIALS AND METHODS

3.1. Description of the Study Area

The study area is located in Addis Ababa, ‘Arada’, and ‘Yeka’ sub-city, particularly along the route from ‘Megenagna’ diaspora light, to ‘Piassa’ Jegol traffic light. It’s geographically located between 9°01'17.9"N to 9°01'57.4"N and 38°48'04.8"E to 38°45'14.7"E.

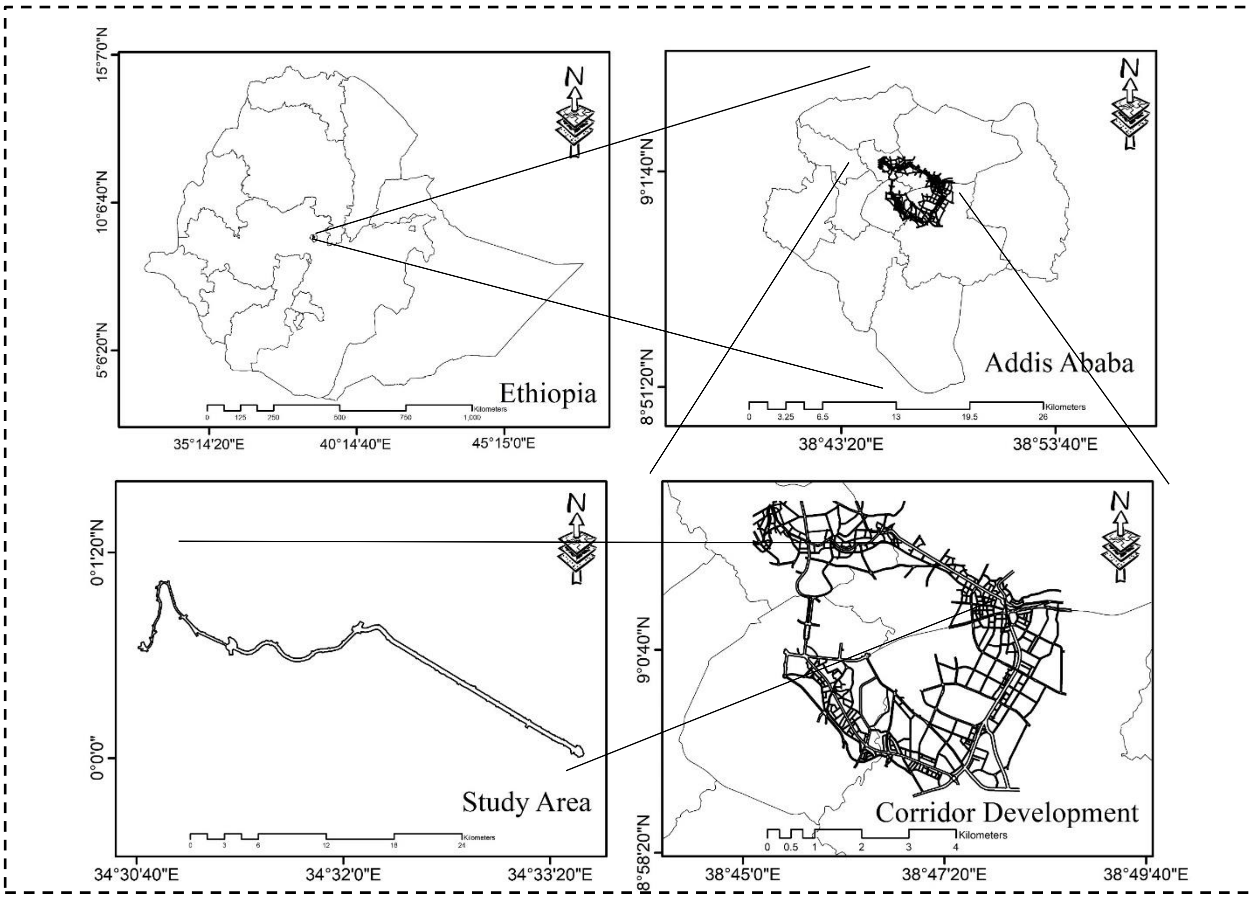

Figure 3.1. *Location map of the study area*

3.1.1. Site selection criteria

This study region was chosen among other areas because it was the first fully operational corridor that can be used for thoroughly analyze the environmental impact with regard to LST, NDVI, and NDBI. UHII In-depth analysis requires a close proximity to a rural or forest ecosystem, as it provides a baseline for studying correlations with the urban corridor, Therefore the study area has a nearby forest on the “Yeka” mountain which makes it suitable for the research.

The total study area is 7.5 kilometers along the roadside from ‘Megenagna’ to ‘Piassa corridor’. The study area /7.5Kilometer/ is selected as the total corridor length, i.e., from ‘Megenagna’ to ‘Piassa’ is 7.5 kilometers. The research is computed in the years 2015, 2020, and 2024 as the years clearly indicate periods before corridor development as a baseline and after corridor development i.e. 2024 indicating the post corridor condition.

3.2. Research design

The study employed both Descriptive and Exploratory research.

Descriptive method: This method is used for describing the temporal and spatial variations among the baseline status and the present circumstance before and after corridor development in terms of LST, NDVI, and NDBI to determine UHII. It is also used to describe various factors that contribute to the sustainable urban environment in the study area.

Exploratory method: This method is used to explore variations in LST, NDVI, and NDBI in order to determine whether the development of the corridor has altered the extent of vegetation and the environmental variables, particularly thermal environment, which are intimately linked to the intensity of urban heat islands.

3.3. Data types and sources

The study used a combination of both primary and secondary data to investigate urban heat island intensity (UHII) along the route from "Piassa" to "Megenagna" before and after corridor development.

Primary data: The major source of data for the study was direct field observation in the study area. Furthermore, information was obtained through interviews with administrations and other stakeholders pertaining to urban roads, environmental groups, and primarily corridor development projects in order to get opinions about the baseline condition and changes after corridor development.

Secondary data: The main sources of the secondary data include remote sensing data from the United States Geological Survey (USGS), Landsat 8 of the same dry season, and Google Earth Engine (GEE). Archives and published papers, as well as case studies of urban heat islands in urban areas, were also examined concerning sustainable urban road and design interventions.

Table 3.1: *Data source, Data set used, spatial resolution, and date of Acquisition*

Data Source	*Data set used*	*Spatial resolution*	*Date of Acquisition*
USGS Earth explorer	Landsat 8	30 Meters	2015 (01/01/15-31/12/15)
			2020 (01/01/20-31/12/20)
			2024 (01/01/24-31/12/24)

Satellite Imagery Data

The research's thematic focus is on UHII utilizing spatial and temporal deviations; hence, GEE was employed to track baseline conditions with post-corridor development, as well as remote sensing data, of Landsat 8 imagery from the USGS.

Table 3.2*: Satellite imagery description*

Source	*Level*	*Collection*	*Tier*	*Spatial resolution*	*Data set availability*
Landsat 8 (USGS)	02	02	01	30 Meters	2013/03/18 to 2025/03/08

Table 3.3: *Remote sensing data used in the study*

Remote sensing data description	*Band*	*Wavelength(πm)*	*Spectral Band resolution(m)*
LANDSAT 8 image and Thermal Infrared Sensor (TIRS)	Band 1 – Coastal aerosol	0.43-0.45	30
	Band 2 – Blue	0.45-0.51	30
	Band 3 – Green	0.53-0.59	30
	Band 4 – Red	0.64-0.67	30
	Band 5 – Near Infrared (NIR)	0.85-0.88	30
	Band 6 – SWIR I	1.57-1.65	30
	Band 7 – SWIR II	2.11-2.29	30
	Band 8 – Panchromatic	0.50-0.68	15
	Band 9 – Cirrus	1.36-1.38	30
	Band 10 – TIR I	10.60-11.19	100
	Band 11 – TIR II	11.50-12.51	100

Table 3.4: *Remote sensing data used in the study for surface reflectance*

Remote sensing data description	*Min*	*Max*	*Band*	*Scale*	*Offset*	*Wavelength (πm)*	*Spectral Band resolution(m)*
LANDSAT 8 Level 02, collection 02, Tier 01	1	65455	Band 1 – Coastal aerosol	2.75e-05	-0.2	0.435-0.451	30
			Band 2 – Blue			0.452-0.512	
			Band 3 – Green			0.533-0.590	
			Band 4 – Red			0.636-0.673	
			Band 5 – Near Infrared (NIR)			0.851-0.879	
			Band 6 – SWIR I			1.566-1.651	
			Band 7 – SWIR II			2.107-2.294	
			SR_QA_AEROSOL attributes				

Field Observation

To achieve the study's objective, a field survey was conducted to sort out the changes within the baseline condition and the present corridor development, which will include comprehensive observations on the corridor development road and landscape by focusing on urban road expansion with their heat retention character, extent of vegetation cover, and spread of built-up index and bare lands carried out to evaluate UHII deviation in the study area.

Key informant interview

A key informant interview were conducted with various governmental and private organizations to gather detailed and specific information relevant for the study. These organizations include Addis Ababa city land development and administration bureau, Addis Ababa city plan preparation and administration office, urban beautification and green development bureau, Addis Ababa city road authority (AACRA), Ethiopian metrological agency, Compass architectural and engineering consultancy plc. The individual’s interviews are selected by a purposive sampling method.

Table 3.5: *Key informant for the research interview*

R.no	*Institution*	*Title*	*Qty.(Person)*
1.	Addis Ababa city land development and administration bureau	General manager	1
2.	Addis Ababa city plan preparation and administration office		2
3.	Addis Ababa city land administration office	Office head	1
4.	Addis Ababa City Road Authority	Team leader	2

		Junior engineer	
5.	Urban Beautification and Green Development Bureau	Head of Design teams	1
6.	Ethiopian Metrological Agency	Office head	1
7.	Private consultancy organization	General manager	2
		Design head	
	Grand Total		10

3.4. Method of data analysis

The data was analyzed using a Geographic Information System (GIS) tool, employing a combination of quantitative and qualitative analytical approaches. Additionally, software tools such as SPSS, Python, and Microsoft Excel were used to support the data analysis. Non-measurable features, especially those related to quality, were described using qualitative methods.

3.4.1. Spatial analysis

This method is used to investigate the demographic deviations from the geographic environment by exploring patterns, spatial distribution, and spatial relationships, including the proximity between various elements, such as built-up area, roads, vegetation, etc. These were done by using the three primary elements (i.e. mathematical modeling, statistical methods, and cartographic modeling) in the Arc GIS by feeding the geospatial data.

According to Longley in (2015), since the outcomes of spatial analysis depend on the locations of the items under study, which was also applied for this research. The potential to investigate the spatial arrangements and interactions of points, lines, areas, and surfaces including adjacency, connectedness, distance, and directional linkages sets spatial analysis distinct from other data analysis (Unwin et al., 2002).

3.4.2. Temporal analysis

The temporal analysis method is used as a technique for creating an extensive timeline with multiple time points to compare the baseline, or pre-corridor development, and present, or post-corridor development, focuses on sequential trends in the temporal change in the study area over time. Various techniques, such as plotting to a histogram and change detection, are used to assess the shifts in the conditions in place. In order to analyze the changes in UHII, this technique enables a comprehensive investigation to discover the sequential trends in the research region throughout time, as well as temporal patterns directly related to roads, vegetation cover, and built-up index.

I. Temporal analysis of LST

The temporal analysis of LST can be done using the change detection method, where you compare LST at different time point's t1, t2, tnt_1, t_2, t_nt1, t2, tn:

$$\Delta LST\ (t) = LST\ (tn) - LST\ (t1)$$

Where:

- LST (tn) is the land surface temperature at time tn,
- LST(t1) is the land surface temperature at time t1,
- ΔLST (t) is the temporal change in LST between the two times.

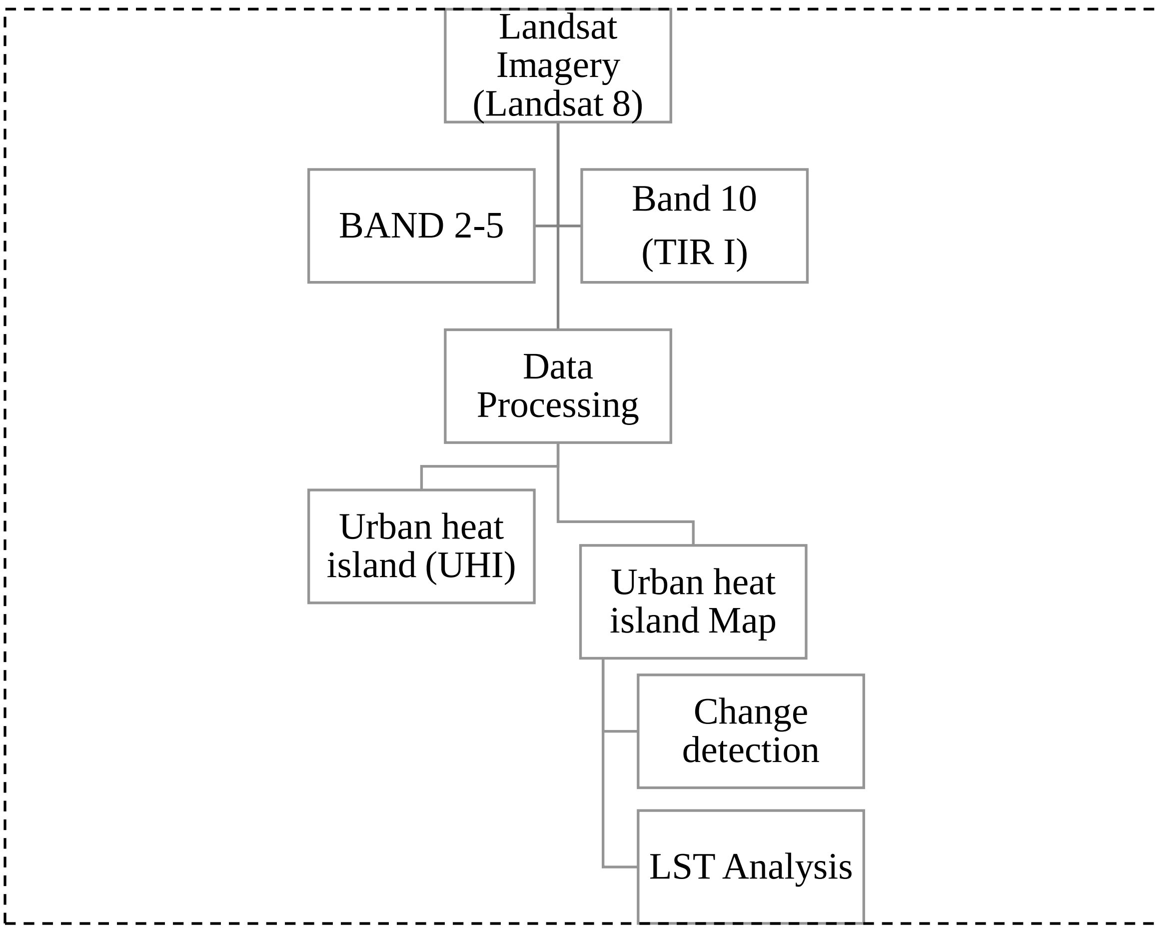

Figure 3.2. *LST Analysis workflow chart in Arc Gis*

II. Temporal analysis of NDVI

NDVI is utilized to track the dynamics of vegetation cover over time. Changes in vegetation over time can be examined with a method similar to LST. The temporal change in the NDVI can be computed as follows:

$$\Delta NDVI\ (t) = NDVI\ (tn) - NDVI\ (t1)$$

Where:

- NDVI (tn) is the NDVI at time tn,
- NDVI(t1) is the NDVI at time t1,
- ΔNDVI(t) is the temporal change in NDVI

III. Temporal analysis of NDBI

The NDBI evaluates the size of built-up or urban regions, and its temporal analysis aids in monitoring developments in urbanization. Like the other indices, the NDBI's temporal change can be calculated by comparing values across time:

$$\Delta NDBI\ (t) = NDBI\ (tn) - NDBI\ (t1)$$

Where:

- NDBI (tn) is the NDBI at time tn,
- NDBI(t1) is the NDBI at time t1,
- ΔNDBI(t) is the temporal change in NDBI

IV. Temporal analysis of UHII

For computing UHII, initially the temporal change in LST was computed for both urban and rural areas:

$$\Delta LST\ urban(t) = LST\ urban(tn) - LST\ urban(t1)$$

$$\Delta LST\ rural(t) = LST\ rural(tn) - LST\ rural(t1)$$

Then, the temporal change in UHII was calculated using the following equation:

$$\Delta UHII\ (t) = [LST\ urban(tn) - LST\ rural(tn)] - [LST\ urban(t1) - LST\ rural(t1)]$$

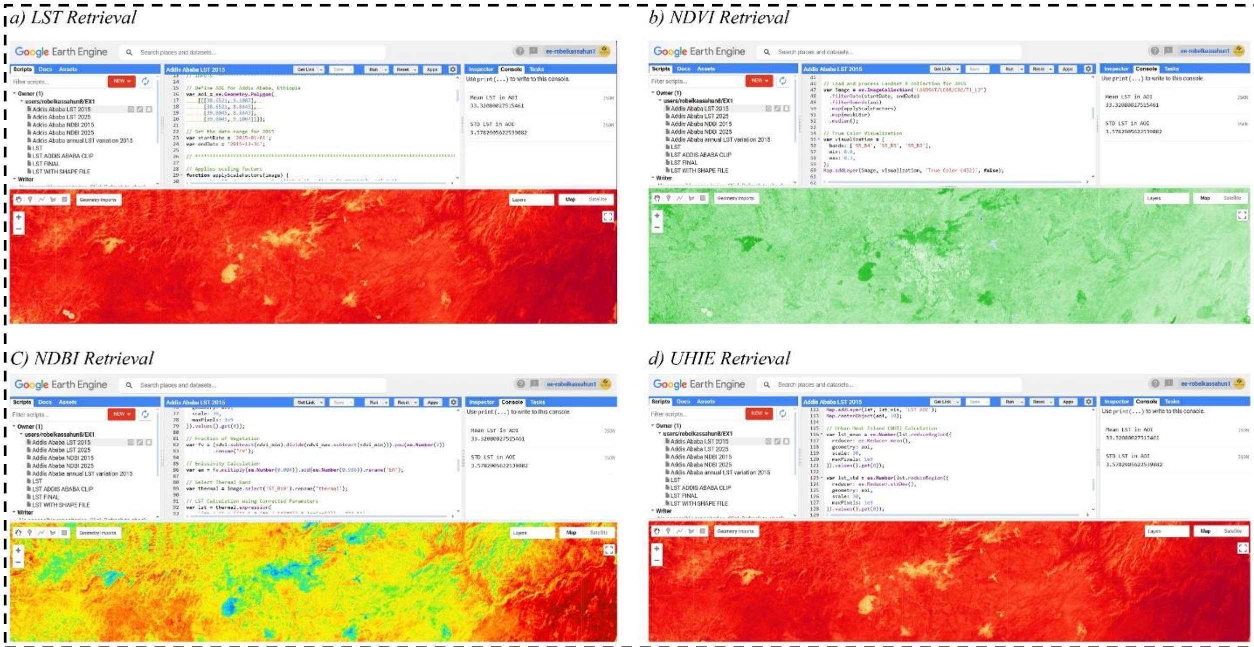

Figure 3.3. *Code script of a) LST, b) NDVI, c) NDBI, and d) UHIE retrieval*

3.4.3. Correlation analysis

Correlation is a statistical measure that demonstrates the degree to which two or more variables fluctuate. This approach is used to examine the negative and positive correlations or relationships that exist between the major variables, notably LST, NDVI, NDBI, and UHII, by analyzing how each variable relates to the one another. This study examines the correlation between LST and NDVI, LST and NDBI, LST and UHII, NDVI and NDBI, NDVI and UHII, and NDBI and UHII to investigate trends that influence UHII and identify factors contributing to the urban heat island effect, offering data-based findings to propose mitigating strategies.

Correlation is Positive or direct when the values increase together, and Negative when one value decreases as the other increases, and so-called inverse or contrary correlation.

Correlation can have a value:

- 1 is a perfect positive correlation
- 0 is no correlation (the values don't seem linked at all)

- -1 is a perfect negative correlation

For computing the correlation analysis; the most widely used technique is Pearson's correlation coefficient (r), which has the following equation:

$$r = \sum_{i=1}^{n} (xi - \bar{x})(yi - \bar{y}) \,/\, \sqrt{\sum_{i=1}^{n} (xi - \bar{x})^2 \sum_{i=1}^{n\,2} (yi - \bar{y})^2}$$

Where $\bar{x}$ is the mean of variable x values, and $\bar{y}$ is the mean of variable y values.

3.4.4. Regression analysis

The regression analysis method is used for computing and determining the relationship that exists between two or more variables which involves identifying and evaluating the relationship between a dependent variable and one or more independent variables, which are also called predictor or explanatory variables i.e. LST, NDVI, NDBI, and UHII statistically as it helps to recognize the trends of the correlation and how the changes in the dependent variable i.e. the variable we want to predict, is related to the independent variable i.e. the variable used to predict for providing valuable insight by quantifying the relationships between those variables.

Simple Regression Model

A simple linear regression analysis is one in which there is just one continuous dependent variable and one independent variable.

The following equation serves as a mathematical representation of the regression model:

$$\mathbf{y} = \beta 0 \pm \beta 1\, \boldsymbol{x}1 \pm \varepsilon 1$$

Where:

- x independent variable,
- y dependent variable,
- $\boldsymbol{n}$ Number of cases or individuals,
- $\sum \boldsymbol{x}\mathbf{y}$ Sum of the product of dependent and independent variables,
- $\beta 1$ The Slope of the regression line, /$\boldsymbol{\beta 1} = \boldsymbol{n} \sum \boldsymbol{x}\mathbf{y} - \sum \boldsymbol{x} \sum \mathbf{y} \,/\, \boldsymbol{n} \sum \boldsymbol{x}^{\mathbf{2}} - (\sum \boldsymbol{x})^2$/
- $\boldsymbol{\beta 0}$ the intercept points of the regression line and the y axis, /$\boldsymbol{\beta 0} = \mathbf{y} - \boldsymbol{\beta 1}\bar{\boldsymbol{x}}$/
- $\sum \boldsymbol{x}$ = Sum of independent variable,

- $\sum \mathbf{y}$ = Sum of dependent variable,
- $\sum \boldsymbol{x}\ \mathbf{2}$ = Sum of square independent variable,

Multiple Regression Model

The multiple regression model is an extension of simple linear regression. The purpose of multiple regression is to get a better understanding of the connection between a dependent or criterion variable and multiple independent or predictor variables (SESRIC, 2015).

The following equation represents the multiple regression model mathematically:

$$\boldsymbol{Y} = \boldsymbol{\beta 0} \pm \boldsymbol{\beta i}\ \boldsymbol{Xi} \ldots \ldots \ldots \ldots \pm \boldsymbol{\beta n}\ \boldsymbol{Xn} \pm \mathrm{u}$$

Where:

- $\boldsymbol{Xi}\ to\ \boldsymbol{Xn}$ Represent independent variables
- **Y** Dependent variable.
- $\beta 1$, the regression coefficient of variable $\boldsymbol{x1}$,

$$\boldsymbol{\beta 1} = (\sum \boldsymbol{x_1 y})\ (\sum) - (\sum \boldsymbol{x_2}\ \boldsymbol{y})\ (\sum \boldsymbol{x_1 x_2})\ /\ (\sum \boldsymbol{x_1}\ ^{\mathbf{2}})\ (\sum \boldsymbol{x_2}\ ^{\mathbf{2}}) - (\sum \boldsymbol{x_1 x_2})^2$$

- $\beta 2$ the regression coefficient of variable $\boldsymbol{x2}$,

$$\boldsymbol{\beta} 2 = (\sum \boldsymbol{x}_2 \boldsymbol{y})\ (\sum \boldsymbol{x}^{\mathbf{2}}{}_1) - (\sum \boldsymbol{x}_1\ \boldsymbol{y})\ (\sum \boldsymbol{x_1 x_2})\ /\ (\sum \boldsymbol{x_1}\ ^{\mathbf{2}})\ (\sum \boldsymbol{x_2}\ ^{\mathbf{2}}) - (\sum \boldsymbol{x_1 x_2})^2$$

- $\boldsymbol{\beta 0}$ the intercept points of the regression line and the y axis,

$$\boldsymbol{\beta 0} = \mathbf{y} - \boldsymbol{\beta 1}\overline{\overline{\boldsymbol{x}}\mathbf{1}} - \boldsymbol{\beta 2}\overline{\overline{\boldsymbol{x}}\mathbf{2}}\ /$$

3.5. Method of data presentation

Analytical and empirical results are presented in the form of: narrative, tabular, and graphical. A combination of text and illustrations are used to demonstrate the information gathered in a written form. Statistical data is presented using the tabular form. Additionally, maps and figures are presented in several graph and diagram forms.

3.6. Methodological Framework

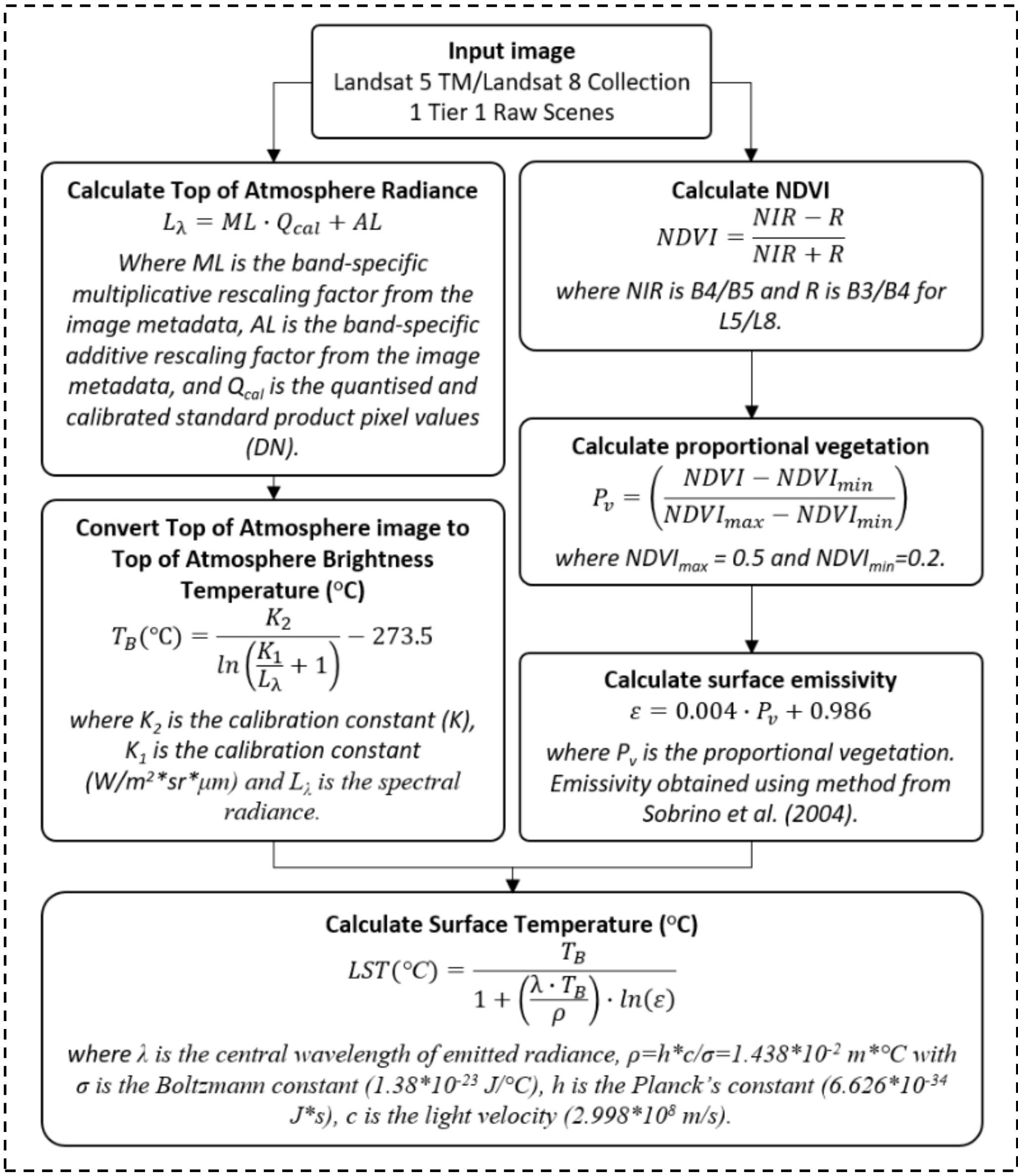

Figure 3.4. *Methodological workflow of the study*

3.7. Reliability and Validity

Research validity

UHII is directly influenced by factors LST, NDVI and NDBI. These influencing key variables are recognized as reliable indicators in various literatures and used in several of previous research. For the spatial and temporal variations study from a reliable source, i.e., Landsat 8 image from the United States Geological Survey (USGS) Earth Explorer. Furthermore, as an additional validation, the findings from the research were cross-checked with previous research and empirical data from a relatively similar area in the country.

Data and Method reliability

All remote sensing satellite imagery data are from a reliable source USGS Earth Explorer taken from a similar season across the study year to reduce seasonal variation. The results were cross-checked between each other, and their correlation is verified as expected. The NDVI, and NDBI data area was cross-checked with ground truth from google and further analyzed with the field observation data. The method used for the image processing and analysis is put in the methodological framework to justify that the research utilizes standardized procedures for data analysis.

Confusion (Error) matrices

Confusion matrices sometimes known as Error matrices, are the most common method of expressing classification accuracy (Lillesand et al., 2008), utilized in the research by creating 50 randomly taken sample reference points from the study area result and ground truth taken from Google images the accuracy was analyzed. The kappa coefficient, user accuracy, producer accuracy and overall accuracy were computed when the error matrix for both classifications is finalized.

According to Lillesand et al., (2008), the following formulas were utilized for the process

$$User\ Accuracy = \frac{number\ of\ coorrectly\ classified\ pixel}{total\ number\ of\ pixel}$$

$$Producers\ Accuracy = \frac{number\ of\ coorrectly\ classified\ pixel}{total\ number\ training\ set\ pixel}$$

The kappa coefficient (Khat) is a degree of convergence between two maps that account for every aspect of the confusion matrix.

$$\text{Overall accuracy} = \frac{\sum(\text{Sum of the diagonal elements })}{\text{Total number of accuracy sites(pixels)}} \times 100$$

$$\text{Khat} = \frac{\text{Obs} - \text{Exp}}{1 - \text{Exp}}$$

Where:

Khat - Kappa coefficient

Obs. - is Observed correct or overall accuracy (OAC)

Exp. - is it represents correct classification.

3.8. Ethical Consideration

For ensuring that the research is conducted responsibly, various ethical considerations were taken with respect to people, community, socio-cultural, and environment. While collecting primary data through mainly key informant interview the respondents have been clearly informed the purpose of the study and how their data will be utilized in the research so as to receive factual and more accurate information voluntarily.

CHAPTER FOUR: RESULT AND DISCUSSION

4.1. Results

4.1.1. Spatial and temporal patterns in LST

Spatial patterns on the road before and after corridor development

Due to the corridor development project in the study area region which covers a total length of 7.5Km of roadway, the core result from Figure 4.1 shows that there is an expansion of roads after the project implementation mainly due to the expansion of Pedestrian Street and the new concept of bicycle lane.

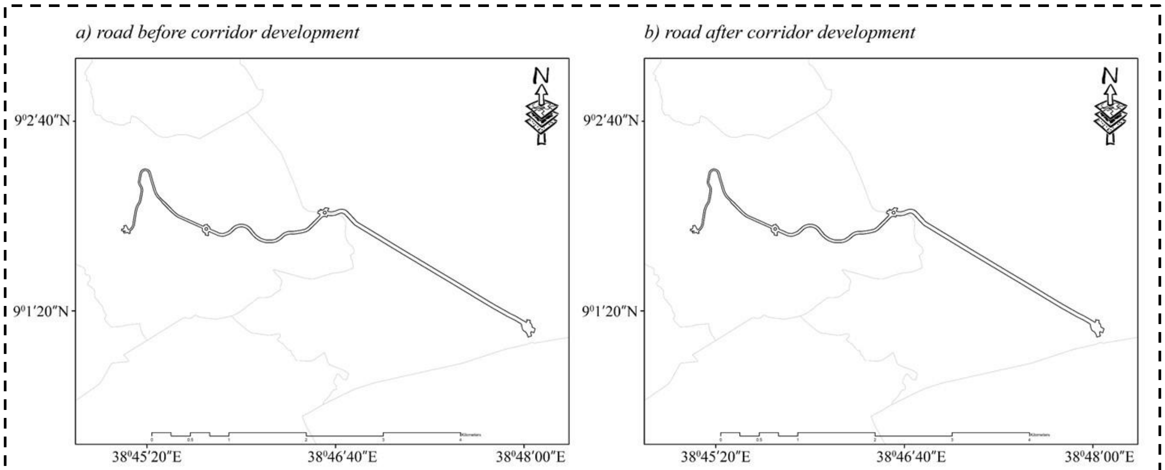

Project description	Year	Length(Km.)	Area(Sq.)	Variation
Before Corridor	2015	7.5Km	216111.149	111,447.608
After Corridor	2024		327558.757	

Figure 4.1. *Spatial patterns on the road before and after corridor Development*

The total area from the baseline condition before the corridor development from the result is 216111.149 Square meters (21.61Ha) of area which is expanded to 327558.757 Square meters (32.76Ha) (Figure 4.1). From the overall expansion of the road, the major parts of the expansion lie on grey infrastructure due to the expansion on vehicular road, Pedestrian Street, and bicycle lane.

Spatial and temporal patterns in Addis Ababa City LST

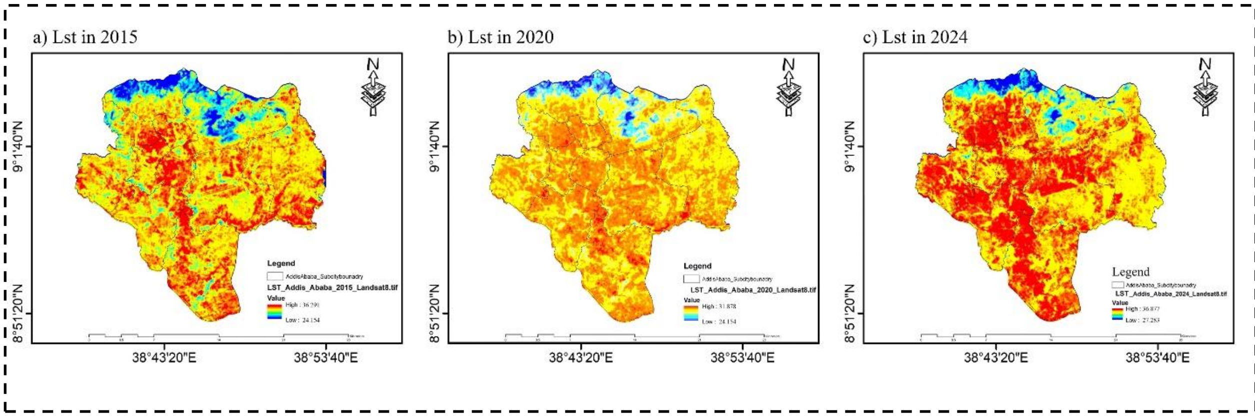

Figure 4.2. *Addis Ababa City: a) LST in 2015, b) LST in 2020, and c) LST in 2024*

Based on the statistical value on the above Figure 4.2, the temporal trends of the land surface temperature in Addis Ababa city show a moderate value in 2015, which decreases on the year 2020 and results in a high increasing trend on the year 2024. Based on this result, we can justify that the mean annual land surface temperature of Addis Ababa city shows an increasing trend.

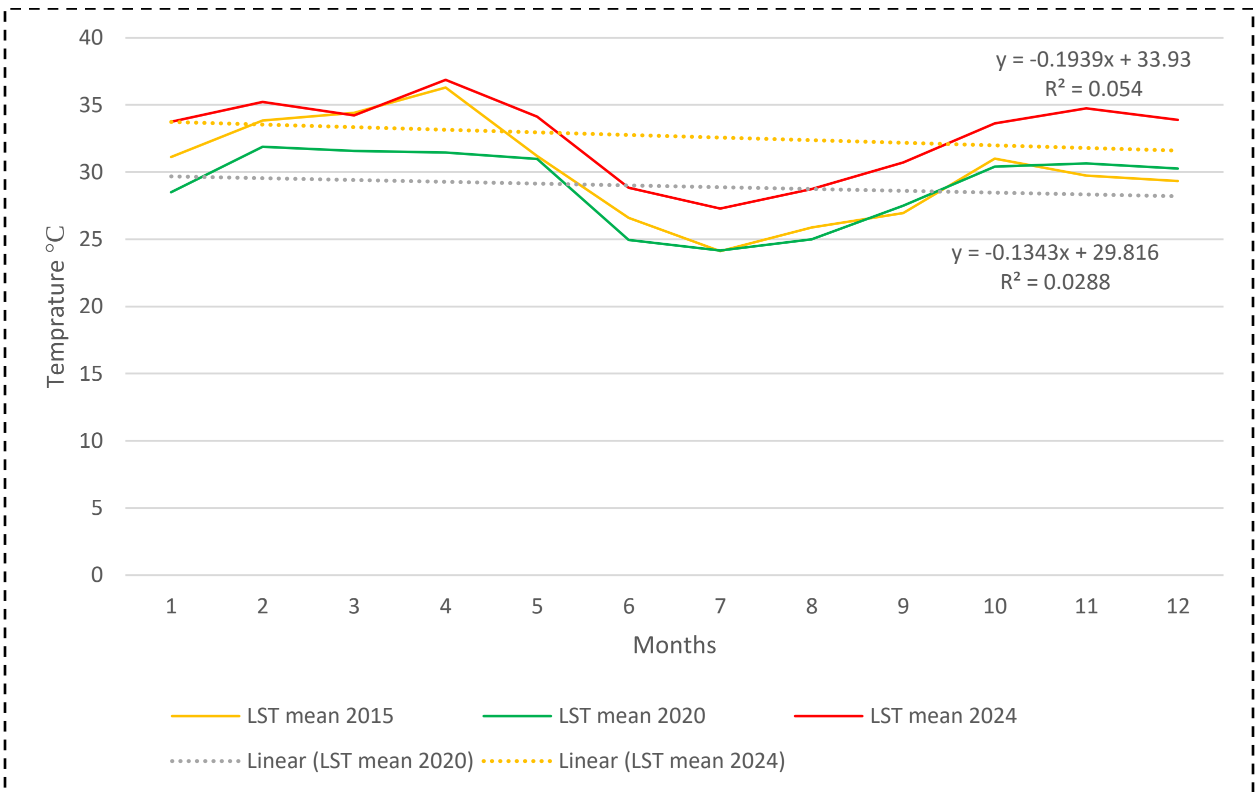

Figure 4.3. *Temporal Trend line in LST of Addis Ababa (2015, 2020, and 2024)*

As a cross reference, Temperature data from the Ethiopian Meteorological Institute (EMI) for the years 2015, 2020, and 2024 were investigated concerning Addis Ababa city temperature, specifically around the study area in their specific station point, i.e., Addis Ababa Bole Station, and Addis Ababa Obs Station results. The results from Figure 4.2, Figure 4.3, and annex 6 shows the core finding that the Land surface temperature trend in 2024 shows the highest value than 2020 as well as 2015 with LST mean value of 32.66975^{0}C higher with 3.72681^{0}C with the baseline of 2020 year with a LST mean value of 28.94294^{0}C and that of 2015 with LST mean value of 30.04213^{0}C.

Based on the slope of the trend line on Figure 4.3, the result shows an upper parabola, which implies Addis Ababa city LST shows a moderate result in the months January, February, March, September, and October. In comparison, relatively higher LST is experienced in November, April, and May. The lowest LST is around June, July, and August. In general, at the beginning and end of the year, the LST is relatively moderate, and around June and July, the LST in Addis Ababa lowers possibly due to seasonal change, which will increase rain and cloud cover in the area (Figure 4.3).

On the temperature result from Annex 6, the highest temperature data recorded in 2015 is in the month of April with the value 36.29118^{0}C, the highest temperature on 2020 is recorded on the month May with a value 31.87929^{0}C, and the highest temperature recorded on the year 2024 is on the month April with value 36.877^{0}C.

From the statistical result on figure 4.8, the extreme highest temperature recorded in 2024 is in the month of August with a value rated 31.80^{0}C. Addis Ababa city's extreme maximum temperature data for the year 2024 shows the highest temperature from the previous year’s taken, i.e., 2015 and 2020, which shows the city's average mean annual temperature shows an increasing trend from the previous year’s data.

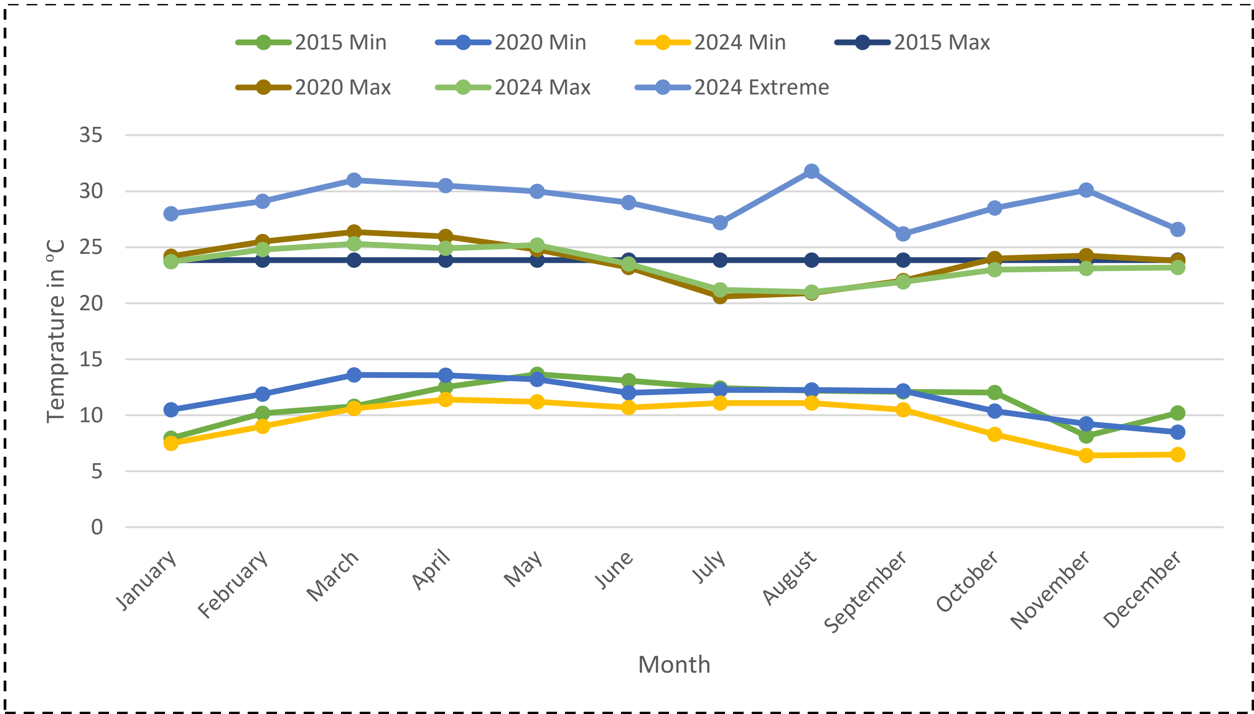

Figure 4.4. *Addis Ababa city minimum, mean, and maximum temperature line*

The annual mean minimum temperature on 2020 with the value 11.62^{0}C shows the highest from that of 11.27^{0}C in 2015 and the lowest 9.52^{0}C result on the year 2024 further more; As a city scale the average mean maximum temperature on 2024 is 23.4^{0}C which is the lowest value on that of 23.79^{0}C in 2020 and 23.84^{0}C on the year 2015 (figure 4.4). Even though the average mean temperature in 2024 is the lowest of all, the maximum mean annual temperature in the year is 29^{0}C, which shows more than 5.16^{0}C increase from the highest recorded mean value in 2015 (figure 4.4).

Spatial and temporal patterns in the study area LST

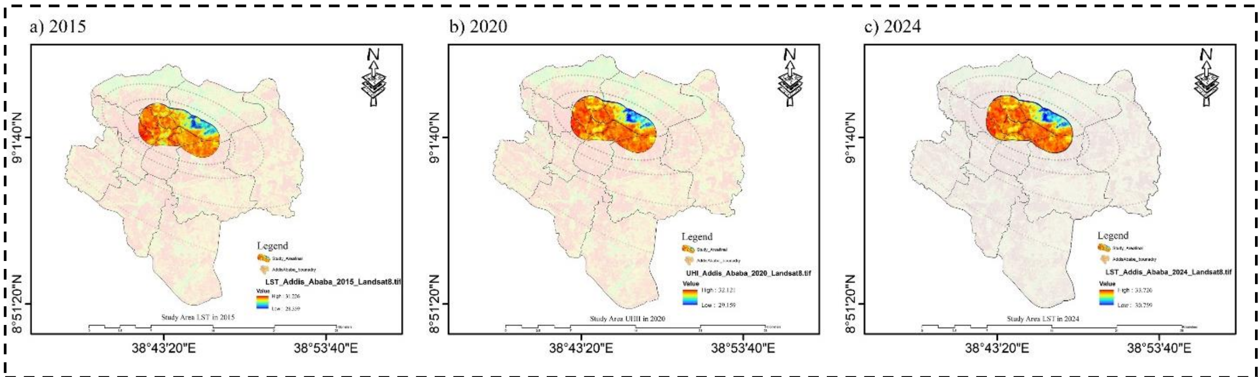

Figure 4.5. *Study Area LST, a) 2015, b) 2020, and c) 2024*

By computing the average LST in 2015, 2020, and 2024 comparatively the highest annual average LST from the years is recorded in 2024. In 2020, the mean annual average LST is relatively moderate, and in 2015, the lowest mean annual average LST is recorded. Based on these results, we can identify that the LST in the study area shows an increasing trend from 2015 to 2024 (Figure 4.5).

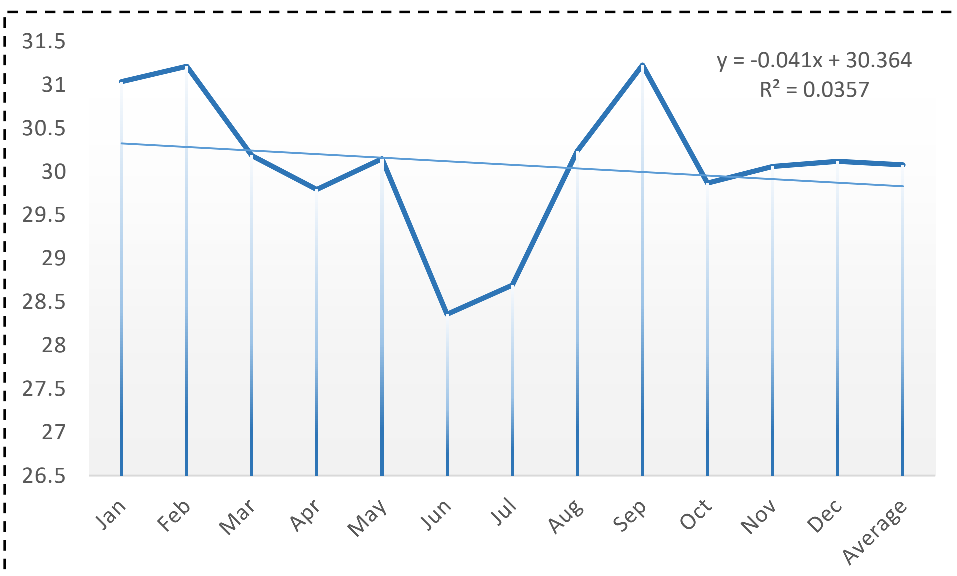

Figure 4.6. *Temporal Trend line in LST of the study area in 2015*

LST result for the year 2015 examined by taking the study corridor with a two kilometers (2KM.) buffer on both sides to analyze the urban-rural comparison shows a notable variation across different months. The lowest monthly average mean LST of 28.359^{0}C is recorded on the month

June which have cooler LST during this month possibly due to seasonal weather pattern of the study area such as rainfall and cloud cover and the highest monthly average mean LST value of 31.226^{0}C is recorded on the month March which directly implies that the area is significantly warmer during this month. Furthermore, the annual average mean LST of the year was calculated to be 30.077300 °C (Figure 4.6).

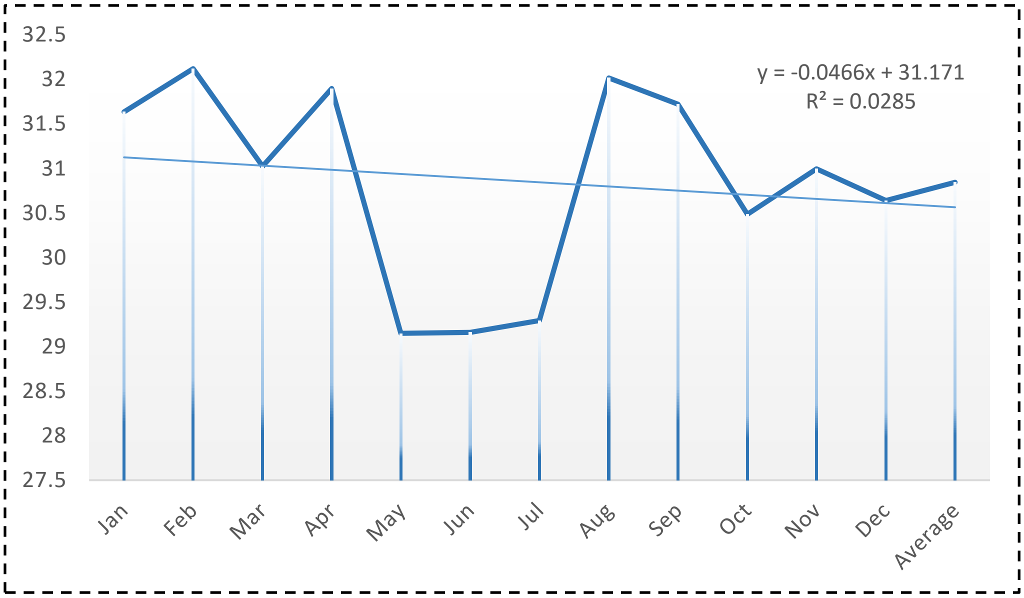

Figure 4.7. *Temporal Trend line in LST of the study area in 2020*

In the year 2020, the LST calculated by taking a two-kilometer (2KM.) buffer shows noticeable variation among the months. The average highest mean LST of 32.1210^{0}C is recorded in the month of February, which means that the surface temperature during the month was elevated. In contrast, the lowest mean average LST of 29.159^{0}C °C is recorded on the month June. The possible scenario for the decreasing factor of LST during this month could be seasonal shifts from warmer to winter months. The annual average mean LST on the year 2020 is recorded at 30.84431^{0}C which is taken as a baseline measurement before the implementation of the corridor development project in the study area (Figure 4.7).

Figure 4.8. *Temporal Trend line in LST of the study area in 2024*

Based on the statistical analysis on the year 2024; the lowest LST is recorded on the month June with monthly average mean LST of 30.759^{0}C which indicates that the LST of the study area is the coolest of the months and the maximum LST result of 33.726^{0}C is recorded on the month May which implies that the study area experiences the highest LST on this month. The calculated mean average annual LST is 32.82467^{0}C (Figure 4.8).

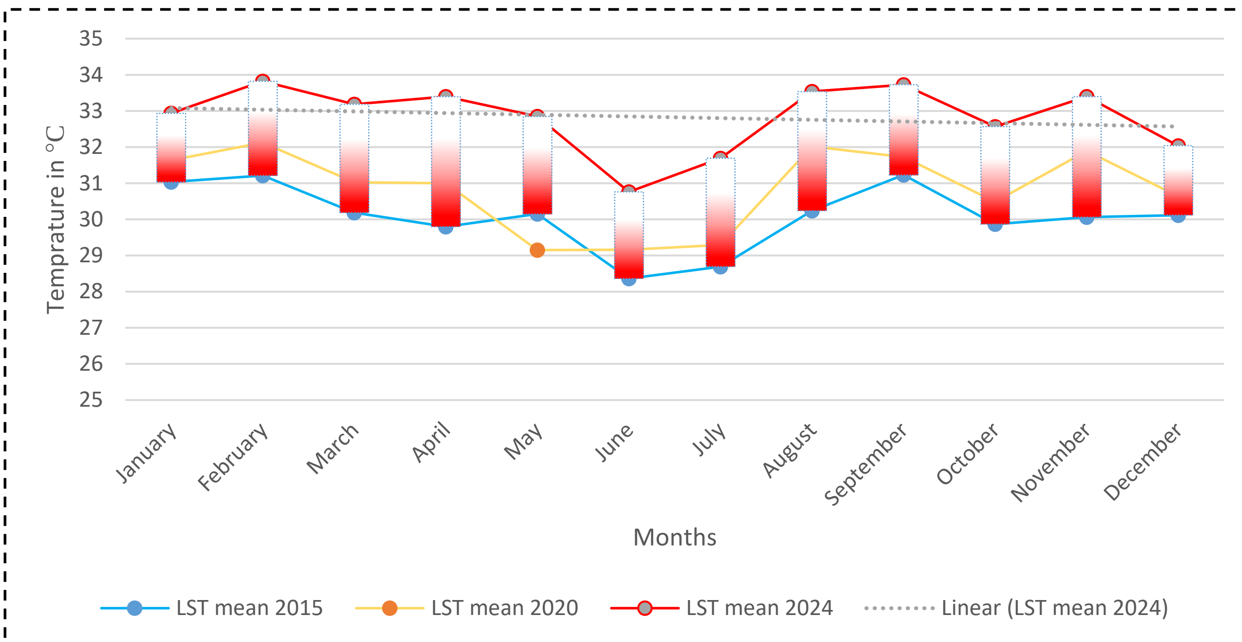

Figure 4.9. *Temporal Trend line in LST of study area (2015, 2020, and 2024)*

By comparing the average annual mean LST, in 2015 the mean value of 30.07733^{0}C shows the lowest than 2020 with an annual average mean LST of 30.84431^{0}C with an annual mean value of 0.76698^{0}C, and the highest annual mean average LST recorded in 2024 with a value of 32.82467^{0}C, which is the highest of all. The LST annual average mean LST in 20204 shows an increasing trend with a value of 2.74734^{0}C from 2015 and 1.98036^{0}C from the result in 2020 (Figure 4.9).

In general, the LST trend analyzed in the study is utilized to examine the trends of urban heat island intensity before and after corridor development in the study area. The results reveal an increasing trend over time as the results in 2024 show significantly higher LST values than the baseline taken before corridor development on the year 2020, as well as in 2015.

4.1.2. Spatial and temporal patterns in NDVI

Spatial and temporal patterns in Addis Ababa city NDVI

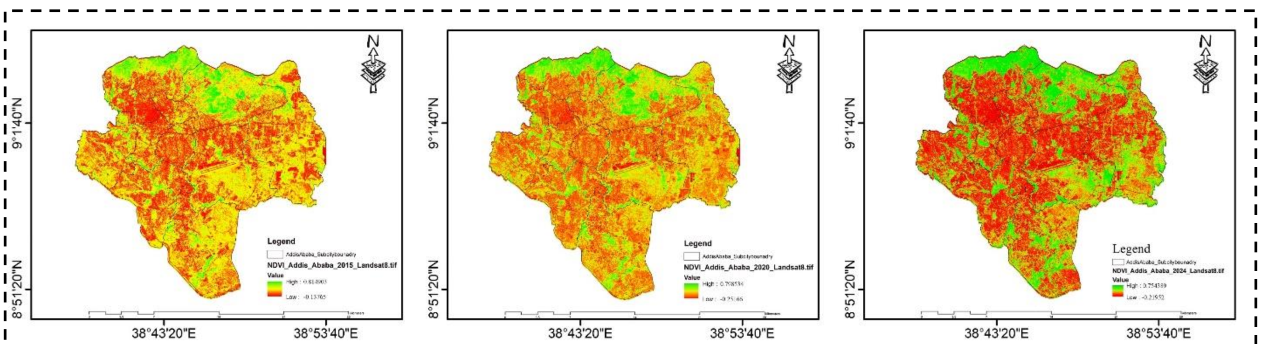

Figure 4.10. *Addis Ababa city NDVI in a) 2015, b) 2020, and c) 2024*

Recently, Addis Ababa city has undergone an inclusive transformation on environmental-related issues, which is reflected in the spatial pattern of NDVI in the city. Based on the result in the earlier years, the city vegetation cover was moderate in inner cities and high mainly in the highland areas and river sides. Due to unprecedented urbanization, the vegetation coverage shows a decreasing value, which indicates that the vegetation cover across the city is reducing. In 2024, due to the corridor development initiative in the city, the green coverage in the specific areas is resulting in a potential impact in enhancing vegetation cover across the city (Figure 4.10).

	NDVI_max	NDVI_mean	NDVI_min	NDVI_stdDev
2024	0.754388791	0.267435055	-0.219518681	0.486953736
2020	0.798534455	0.273436879	-0.251660697	0.525097576
2015	0.814903439	0.33862853	-0.137646379	0.476274909

Figure 4.11. *Temporal Trend bar in NDVI of Addis Ababa (2015, 2020, and 2024)*

The NDVI results in Addis Ababa city in the years 2015, 2020, and 2024 show a significant decreasing trend. In 2015, the NDVI maximum value recorded is 0.814903, which is higher by 0.016369 from the result in 2020, recorded value of 0.798534, and higher than the Maximum NDVI value in 2024, recorded 0.754389 by a value of 0.060514. The NDVI minimum results, which show negative values, indicate a minimum vegetation cover in the area. The highest mean NDVI result is recorded in 2015 with a value of 0.338629 in comparison with the moderate record with a value of 0.273437 in 2020, and the lowest record in 2024 is 0.267435. The results in the NDVI mean show a decreasing trend, which indicates the vegetation cover in the area is reducing (Figure 4.11).

Spatial and temporal patterns in the study area NDVI

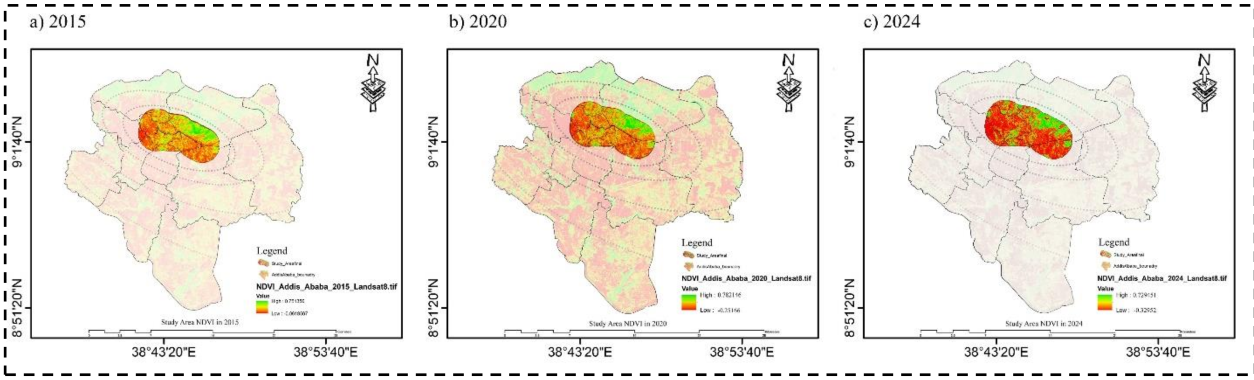

Figure 4.12. *Study Area NDVI in a) 2015, b) 2020, and c) 2024*

The result in NDVI of the year 2015 indicates various vegetation conditions in the study area. The maximum NDVI value recorded is 0.751356, which signifies that areas are having densely vegetated, i.e., 'Yeka' mountain forestry taken as a 'Rural' for the comparison, as the higher recorded value is computed by exhibiting a strong reflectance in the near infrared spectrum. The mean and minimum NDVI values are 0.34475 and -0.06186, respectively (Figure 4.12 and Table 4.1). The negative magnitude of the NDVI result indicates either that there is a low amount of vegetation in some part of the study area or some parts have no vegetation at all, i.e., the Study area corridor route /Road/ which is taken as an 'Urban' for the study.

Table 4.1: *Temporal Trends in NDVI of the Study Area (2015, 2020, and 2024)*

YEAR	NDVI_MAX	NDVI_MEAN	NDVI_MIN	NDVI_STDDEV
2015	0.751356	0.34475	-0.06186	0.529485
2020	0.782146	0.265243	-0.25166	0.529485
2024	0.729451	0.199966	-0.32952	0.529485

In the year 2020, the minimum annual average NDVI record value is -0.25166, the annual mean average NDVI is 0.265243, and the maximum annual average NDVI value is 0.782146 (Table 4.1). From the previous 2015 result we can identify that there is a noticeable decrease on both factors which indicates that there is a decrease on the densely vegetated area as the high value on 2015 reduces on 2020 and there is a decrease in NDVI minimum annual average value which implies that there is either of urban expansion, increased impervious surfaces, increased infrastructural change, environmental degradation, or vegetation loss over the past five year period.

In 2024, the average annual minimum NDVI result is -0.32952, the annual mean average NDVI is 0.199966, and the maximum average annual NDVI is 0.729451 (Table 4.1). While comparing these results in the year 2024 with those of 2020, which was previously considered as the data before corridor development, the result shows a significant reduction in both ‘rural’, the densely vegetated areas, and ‘urban’, the roadways and sparsely vegetated areas of the study area.

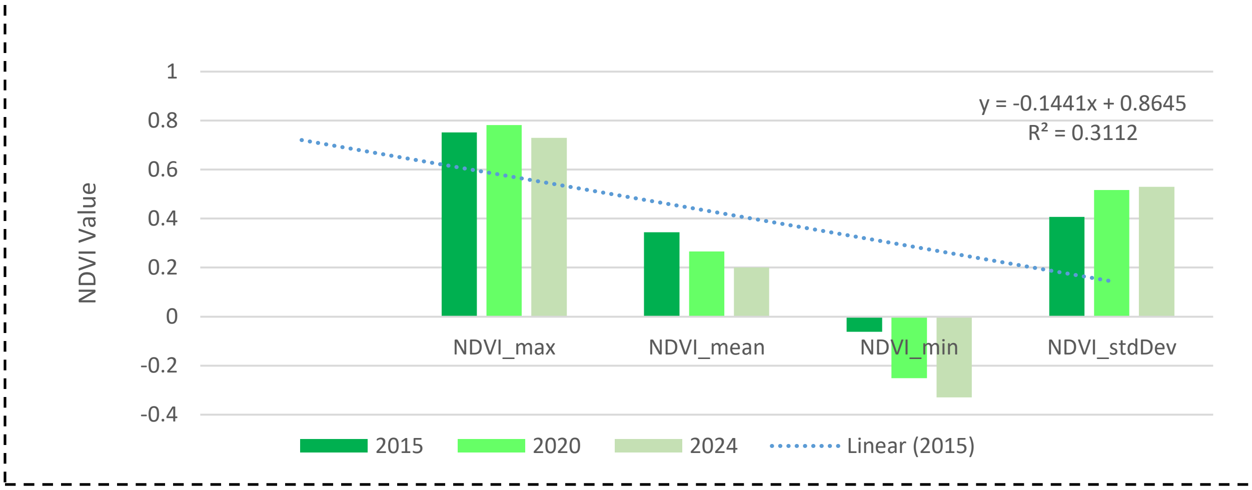

Figure 4.13. *Temporal Trend bar in NDVI of the Study Area (2015, 2020, and 2024)*

By comparing the average minimum annual NDVI on Figure 4.13 in the years 2015, 2020, and 2024, the recorded values are -0.06186, -0.25166, and -0.32952 respectively. The result shows an increase in the negative value of the NDVI minimum value indicating that there is a reduction of vegetation over time (Figure 4.13).

The maximum NDVI annual average result in 2015 is 0.751356 which indicates there is a high vegetation density in the study area i.e. ‘Yeka’ mountain taken as a ‘Rural’ for the study comparison. In 2020 the recorded result 0.782146 shows slight improvement from 2015 but again in 2024 the value reduced to 0.729451 indicates the vegetation cover in the study area is reduced (Figure 4.13).

By investigating the activities in the study area, the main reason for the increase in vegetation cover around 2020 is the conservation effort in the period and mainly the green initiative at that time. In the results of 2024, the potential reasons for the decrease of vegetation cover are mainly related to anthropogenic activity in the area, including environmental impact due to infrastructure development including urban road expansion on the corridor development. In general, the overall results from NDVI show a noticeable decrease over time which implies that there is a reduction in vegetation cover in the study area.

4.1.3. Spatial and temporal patterns in NDBI

Spatial and temporal patterns in Addis Ababa city NDBI

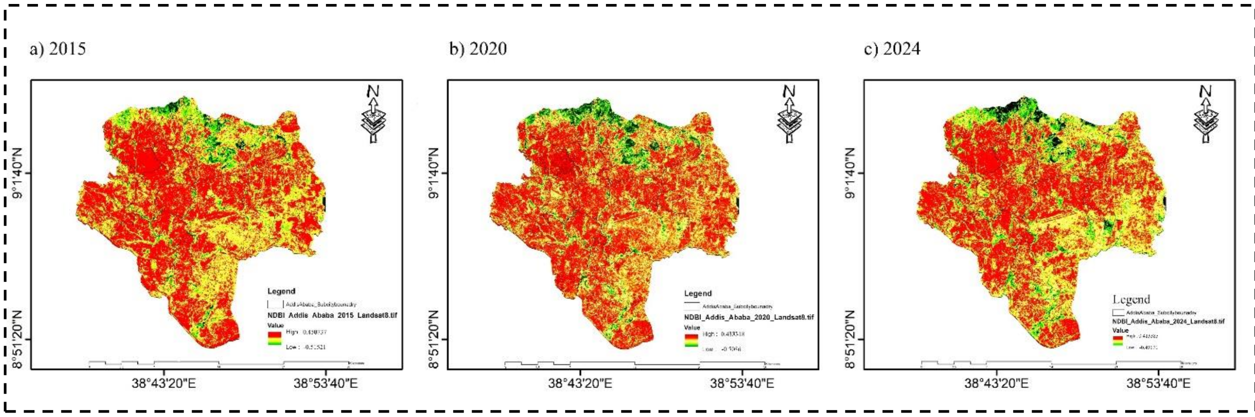

Figure 4.14 *Addis Ababa city NDBI in a) 2015, b) 2020, and c) 2024*

Addis Ababa city has undergone unprecedented urbanization over the past years, which has led to noticeable changes in the NDBI of the city. Based on the results of the investigation at the city scale, there is a significant change in the built-up areas from the year 2015 to 2020, possibly due to urbanization and urban sprawl (Figure 4.14). In 2024, the trend shows a decreasing effect with reduced built-up areas. By checking different literature and investigating the baseline condition, the possible reason for the decreased built-up index in 2024 is due to the inclusive urban corridor and redevelopment sites, which seek the demolition of dense low-rise residential areas.

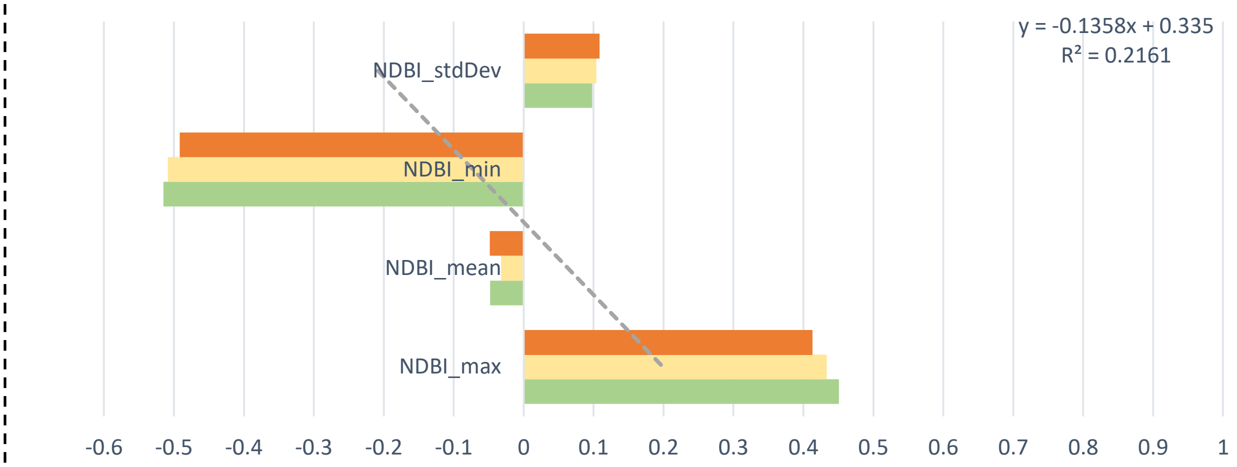

	NDBI_max	NDBI_mean	NDBI_min	NDBI_stdDev
2024	0.413382626	-0.04831	-0.49171	0.108532
2020	0.433317513	-0.03238	-0.5086	0.103988
2015	0.450737043	-0.04792	-0.51521	0.098139

NDBI Value

2024 2020 2015 Linear (2024)

Figure 4.15. *Temporal Trend bar in NDBI of Addis Ababa (2015, 2020, and 2024)*

The NDBI result for Addis Ababa city from 2015 to 2020 shows a significantly increasing trend, which implies that there is a substantial expansion of built-up areas during the period. The mean average annual NDBI recorded in 2015 is -0.04792, which is higher than that of 2020 with a value of -0.03238, which implies that there is a noticeable change in built-up areas over the five-year period. In 2024, the result became -0.04831, showing a decreasing trend from the previous 2020 (Figure 4.15.).

Spatial and temporal patterns in the study area NDBI

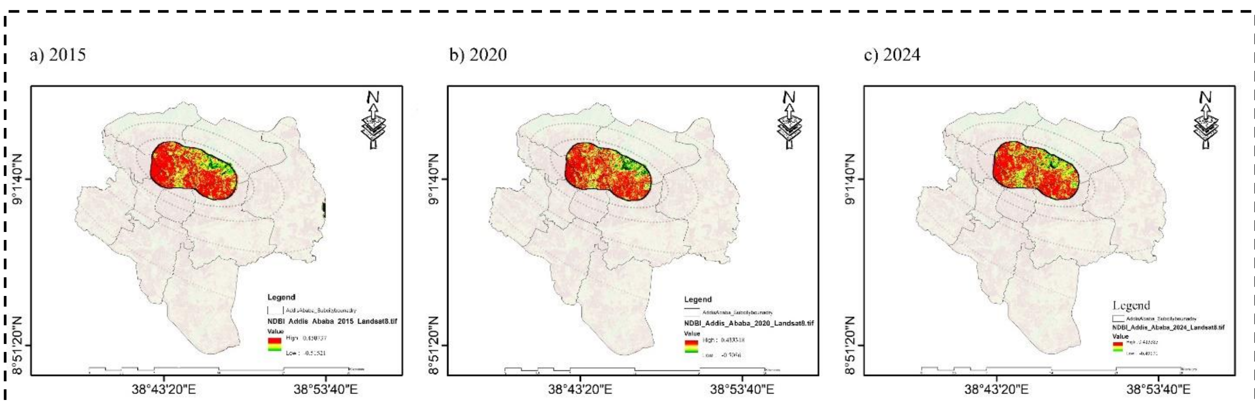

Figure 4.16. Spatial and temporal patterns of NDBI in the study area, a) 2015, b) 2020, and c) 2024

Based on the results of NDBI, the study area clearly shows that the trends of built-up index on 2015 was relatively moderate and in 2020 the built-up value shows an increasing effect which implies that the area is exhibiting urban expansion, in 2024 this value extensively increase along the road way which means that built-up areas in the study area are showing increasing effect and the green spaces are reduced as investigated by an in depth analysis which indicates there is an increasing trend in NDBI over time (Figure 4.16).

Figure 57. *Temporal Trend bar in NDBI of Study Area (2015, 2020, and 2024)*

The results of NDBI in 2015 indicate that there is a high built-up density compared to other years in the study. The average annual maximum built-up index value is 0.25323 which indicates the concentrated built-up areas including infrastructure, roads, and buildings. The average minimum NDBI value is -0.41486, which shows that there is a densely vegetated area, i.e. 'Yeka' mountain, given that green spaces have weak reflectance in the near infrared spectrum (Figure 4.17).

In 2020, the average annual maximum NDBI recorded 0.490157 which have significant increase from 2015 which clearly indicates there is a high built-up area expansion on the period. The average annual minimum NDBI value is -0.70388 (Figure 4.17).

In 2024, the minimum annual average NDBI value is -0.41639 shows that there are green spaces with low built-up density specifically ‘Yeka’ mountain which is taken as a ‘Rural’ for comparison, and the maximum annual average NDBI value is 0.300674 which indicates the roads, buildings and other impervious surfaces which are taken as an ‘urban’ for the study (Figure 4.17).

4.1.4. Combined result of variations on UHIE

Spatial and temporal patterns in Addis Ababa city UHIE

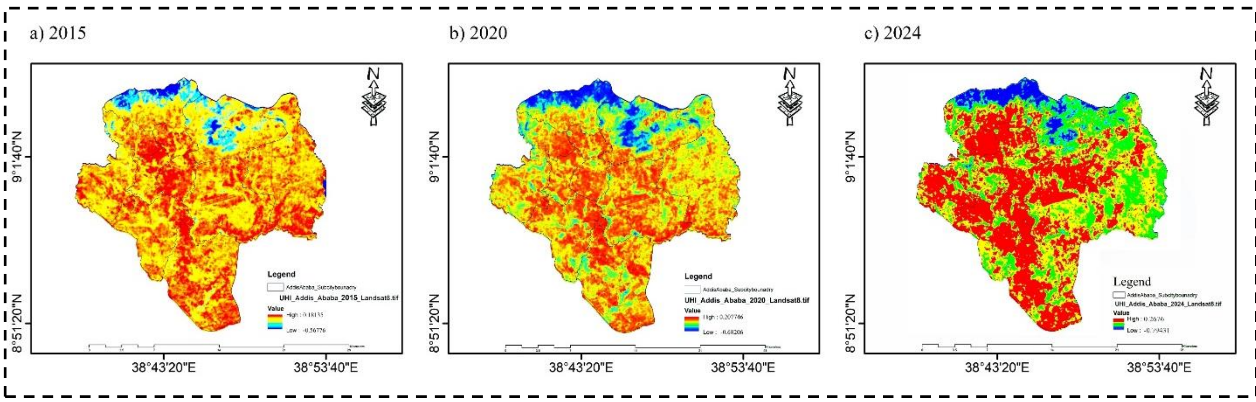

Figure 4.18. *Addis Ababa city UHIE in 2015, 2020, and 2024*

Addis Ababa city is experiencing significant changes in the trends of UHII due to several driving factors. Various reports, literature, and studies documented that the city temperature increases over time due to different reasons, i.e., urbanization, infrastructure development, urban expansion, environmental degradation, etc. (Figure 4.18).

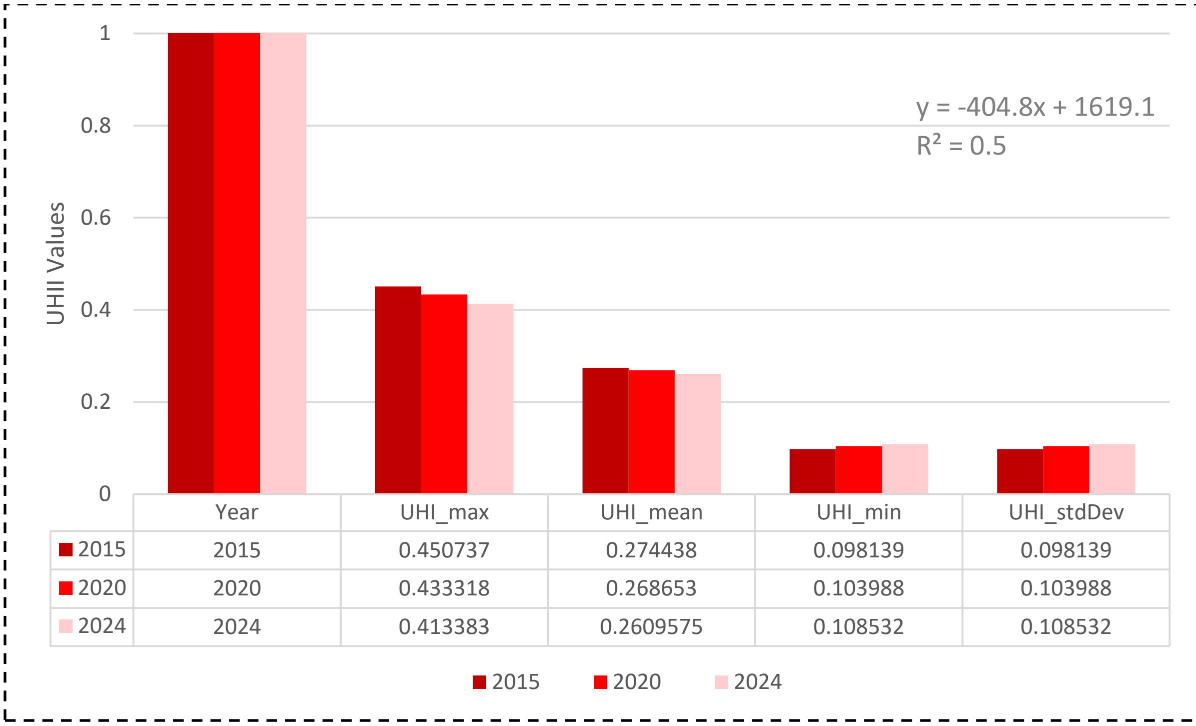

	Year	UHI_max	UHI_mean	UHI_min	UHI_stdDev
2015	2015	0.450737	0.274438	0.098139	0.098139
2020	2020	0.433318	0.268653	0.103988	0.103988
2024	2024	0.413383	0.2609575	0.108532	0.108532

Figure 4.19. *Temporal Trend bar chart in UHIE of Addis Ababa (2015, 2020, and 2024)*

Based on the result on Figure 4.19 from the three UHII mean values the most negative which indicates the least UHII is recorded in 2015 with the value -0.193205, the second most negative value is recorded in 2020 as -0.237157 whereas the least negative value which describes relatively higher UHII is recorded in 2024 with the value -0.263355. From the trend analysis, the major finding of this mean result clearly shows that there has been a gradual increase in UHII of Addis Ababa city over time (Figure 4.19).

Spatial and temporal patterns in the study area UHIE

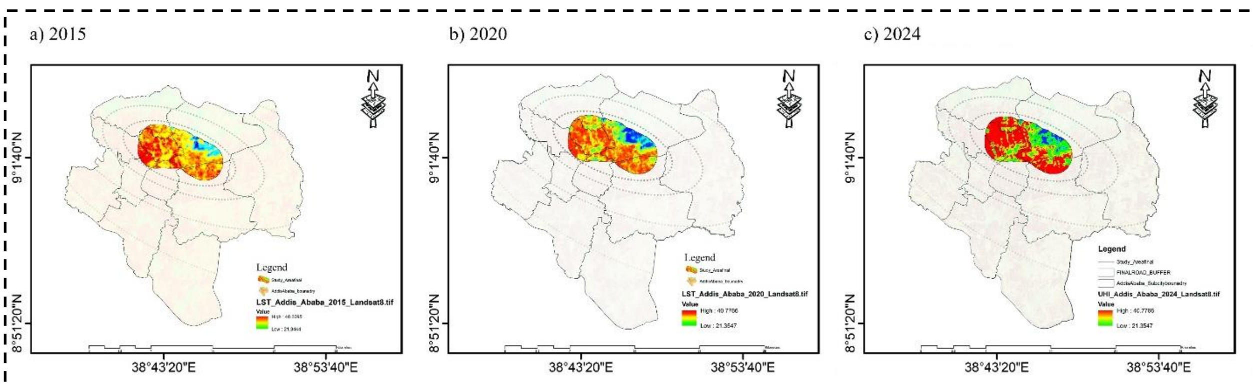

Figure 6.20. *Study Area UHII in a) 2015, b) 2020, and c) 2024*

Based on the combined results in 2015 from LST, NDBI, and NDVI, the UHII for 2015 is analyzed within the study area by taking an area of Two kilometers (2KM.) buffer from ‘Megenagna’ to ‘Piassa’ corridor road.

The average annual minimum UHII value is -0.6951 with a negative value which indicates that the vegetation cover in the area majorly ‘Yeka’ mountain taken as a ‘rural’ counterbalanced the urban heat generated from the built-up areas mainly the road from ‘Megenagna’ to ‘Piassa’ taken as an ‘Urban’ for comparison. The average annual maximum UHII value is 0.201162, which indicates the ‘Urban’ areas, i.e. road from ‘Megenagna’ to ‘Piassa’ in the study region, have relatively higher temperature as compared to the surrounding ‘Rural’ area, i.e., ‘Yeka’ mountain (Figure 4.20).

The average annual maximum UHII value in 2020 is 0.217746, which means that the ‘Urban’ areas in the study region are experiencing substantial urban heat than their surrounding ‘Rural’ area, mainly the densely vegetated area ‘Yeka’ mountain. In this year, the average annual minimum UHII value is -0.73206, which indicates that the densely vegetated area i.e., ‘Yeka’ mountain and other green infrastructure in the study area, counterbalanced the urban heat generated from the built-up areas (Figure 4.20).

In the year 2024, the annual average minimum UHII value recorded is -0.79431, which means that the vegetation cover in the study area including the densely vegetated ‘Yeka’ mountain counterbalanced the urban heat generated from the built-up areas. The average annual maximum UHII value recorded in the year is 0.2476, which implies that the ‘Urban’ areas in the study region are experiencing substantially higher temperature as compared to the surrounding ‘Rural’ area mainly ‘Yeka’ mountain.

Based on the above results in the study from the years 2015, 2020, and 2024, it is justified that the urban temporal trends of UHII in the study areas clearly show an increasing trend over time. The major finding of this result intensifies the UHIE is increasing, which means that urban areas in the study region, i.e. ‘Megenagna’ to ‘Piassa’ road, is experiencing warmer temperatures as compared to the surrounding ‘Rural’ areas mainly the densely vegetated ‘Yeka’ mountain.

	Year	UHI_max	UHI_mean	UHI_min	UHI_stdDev
2015	2015	0.201162	-0.246969	-0.6951	0.448131
2020	2020	0.217746	-0.257157	-0.73206	0.474903
2024	2024	0.2476	-0.273355	-0.79431	0.520955

2015 2020 2024

Figure 4.21. *Temporal Trend bar chart in UHII of the study area (2015, 2020, and 2024)*

From the result on figure 4.21 the most negative UHII mean value from the three years is recorded in 2015 with value of -0.246969 which indicates the least UHII with relatively high cooling effect, in 2020 the recorded value increased to -0.257157 which indicates moderate UHII and the least negative value recorded is in the year 2024 with the value -0.273355 which indicates relatively Higher UHII than the result in 2020 as well as 2015 (Figure 4.21).

By analyzing the results of the annual average mean UHII value, the UHII value is showing a consistent increase over time. The shifts in the temporal trend of UHII shows the growing impacts of the corridor development i.e. anthropogenic intervention as it encompasses urban expansion and urbanization for the execution of the project, on the micro climate of the road side taken as an ‘Urban’ area for the study which emphasizes the need for incorporating mitigating strategies including sustainable urban planning strategies to mitigate the UHIE in the study area.

4.2 Discussions

4.2.1. Spatial and temporal patterns in LST

Recently, Addis Ababa city's inner urban areas have been experiencing relatively higher temperatures as compared to their surrounding 'Rural' areas a resulting in LST showing a substantial increase over time. As UTFVI is directly correlated with LST, it is the most commonly used index for the ecological assessment of the urban environment (Alfraihat et al., 2016; Li et al., 2013). The trends of LST in Addis Ababa city investigated by UTFVI result in 2015 shows a mean value of 30.04213^{0}C which is slightly higher with 1.09919^{0}C from 2020 and this value extensively increased to 3.72681^{0}C on 2024 with a mean annual average value of 32.66975^{0}C which shows a clear substantial increase of LST in the city (Figure 4.3).

Urban settings are dominating over green and open spaces which resulting in an increase in UHIE in different areas of the city, which is making the city warmer (Mathias et al., 2016). There are various contributing factors for these phenomena are mainly driven by city-wide rapid urbanization and urban expansion, which leads to an increase in road infrastructure, including pedestrian, bicycle lanes, and impervious surfaces, which absorb more heat than greenery.

The LST on the study area, i.e. corridor development road from 'Megenagna' to 'Piassa' route, shows an increasing trend over time (Figure 4.5). The LST is computed by taking the 'Yeka' mountain and other vegetation cover mainly on road roadside with a catchment area of a Two-kilometer buffer (2Km.) as a 'Rural' and the road as an 'Urban' result that the urban areas are experiencing relatively higher LST than the 'rural'.

Before the corridor development, the study area's total road coverage was 216111.149 square meters (21.61 hectares), and it increased to 327558.757 square meters (32.76 hectares) following the corridor development. The majority of the expansion is on grey infrastructure because of the expansion of the bicycle lane, Pedestrian Street, and vehicle road. Based on previous researchers finding, there was a substantial positive linear correlation among impervious surface and LST; a 10% increase in imperviousness might result in around 3.3°C increase in land surface temperature when the impervious surface eventually accounts for more than seventy percent /70%/ of the land (Xu et al., 2013,). An expansion in urban areas could raise LST by approximately 1.9–5.4 ^{0}C and the urban air temperature around 0.75–2.80 ^{0}C (Imran et al., 2019), which implies that an increase in the study areas road coverage with over fifty percent /50%/ ratio will increase the areas LST evidentially on a high rate.

The anthropogenic intervention in the study area impacts the LST and leads to increasing UHIE as Infrastructures, including roads, buildings, pedestrians, and other constructions, minimize urban vegetation cover (Siti et al., 2013).

According to the study area LST result; the ‘Rural’ i.e. vegetation cover including street side greeneries relatively balanced the ‘Urban’ i.e. Buildings, roads, and other infrastructures area heat by provisioning cooling effect mainly through balancing Incoming solar energy from sun light and outgoing radiation from surfaces to the environment to manage excessive heating by regulating temperature (Ries, 2002; Baccini et al., 2008).

Land surface temperature has an extensive impact on microclimate change and vegetation growth (Shahid, 2014). Therefore, as the trends on LST of the area increase, the microclimate also increases, which will directly impact the surrounding area’s livelihood and roadside activities, including minimizing walkability for pedestrians.

The primary contributing factor of urban heat islands in cities is a rise in LST (Qaid et al., 2016; Vasenev et al., 2021). Due to anthropogenic activities and alterations to the natural environment through various infrastructures such as roads having low thermal albedo materials that do not reflect sunlight effectively, will lead to an increase in LST, which is directly proportional to UHI.

Urban built-up areas expansion, which incorporates urban road expansion, results decline of vegetation cover, which contributes to an increase in LST and intensifies UHI (Warkaye et al., 2018; Teferi et al., 2017). Because green spaces absorb heat mostly during the dry season, which lowers LST, reducing them due to urban growth will have a major detrimental impact on the environment (Samson et al., 2018).

Material selection in urban infrastructure plays a crucial role in mitigating UHIE (Voogt et al., 2003), as the main causes of UHIE are the high heat-absorbing characteristics of pavements, concrete structures, and other various impervious surfaces to rising surface temperature in urban areas, which leads to an increase in UHIE of the area. Higher albedo lowers pavement surface temperatures (Yang et al., 2015).

4.2.2. Spatial and temporal patterns in NDVI

The most popular technique for analyzing the amount of vegetative coverage in an area using remote sensing images is the NDVI (Angadi et al., 2020; Ghosh et al., 2020). The NDVI is widely recognized effective indicator for LST (Weng et al., 2004) with a strong negative correlation, i.e. Increase in vegetation index decreases LST; accordingly, the decreasing trend in the result of the study shows an increasing trend in the SUHI.

Due to unprecedented urbanization and urban expansion, Addis Ababa city vegetation cover trend shows a substantial decrease, even though recently there has been a focus given to environmental protection and green development by establishing an urban beautification and green development bureau as a governmental institution.

In remote sensing, NDVI is a useful measure of vegetation cover (Mackey et al., 2012). Even though considerable focus has been given to environmental protection, results show a potential improvement in enhancing vegetation cover in the city, the vegetation cover on a city scale still shows a decreasing trend, as the result in Map 4, indicating the extent of green coverage within the city over time.

The Addis Ababa city NDVI results in the years 2015, 2020, and 2024 is a justification for the visible decreasing trend (Figure 4.10). In 2015, the NDVI maximum value recorded is 0.814903 which is higher than the result in 2020 recorded value of 0.798534 and higher than the Maximum NDVI value in 2024 recorded 0.754389 (Figure 4.11); This progressive decreasing result in NDVI means that the vegetation density as a city scale is reducing over time which will have direct impact on increasing LST as their correlation is negative and an increase trend in NDBI which will results in an increasing trend the cities UHIE and urban air temperature; As Vegetation cover is the main contributing factor of UHI, accounting for around 44% of the total (Deliami et al., 2018).

NDVI value ranges from -1 to +1; values near or trending towards -1 indicate bareland, an open space, or a water body, while values near or trending towards 1 imply vegetative cover. According to th study area NDVI result, the average minimum annual NDVI for 2015, 2020, and 2024 is -0.06186, -0.25166, and -0.32952, respectively. The outcome demonstrates that a decrease in vegetation over time is indicated by an increase in the negative value of the NDVI minimum value. This decreasing trend in urban green spaces impacts the study areas UHIE as these green spaces have better cooling effect (Kong et al., 2014).

Land cover in urban environment plays significant role in providing ecosystem services (Bradley, 1995; Bastian et al., 2002), including regulating service by controlling local temperature through absorbing and storing carbon dioxide majorly by vegetation cover; therefore the decreasing trend in the study areas NDVI (Table 4.1) showing a reduction in green coverage which implies that the vegetation cover including densely vegetated 'Yeka' mountain, street side greeneries … etc. in the study area is incapable of provisioning ecosystem service in the area majorly regulating service.

Change in Land use Land cover (LULC) by the conversion of green spaces into impermeable surfaces has led to extensive environmental problems, including UHIE (Weng et al., 2001). As vegetation cover helps to mitigate UHIE through processes such as evapotranspiration and cooling the environment through shading, enhancement of green coverage by fostering sustainable green infrastructure should be prioritized to enhance green coverage in the study area. Having a linear correlation, a ten percent (10%) increase in vegetation coverage would cool the air by 0.23^0C (Wong et al., 2005)

The ecology will be significantly impacted since vegetative cover is replaced by impermeable surfaces. An Increase in impervious surface i.e., asphalt roads, concrete pedestrian etc., will linearly increase the LST in the area, while green infrastructures decrease it (Dai et al., 2019; Li et al., 2016); areas with more green infrastructure show less tendency of having the highest LST.

According to Kong el al., in 2014; urban green areas including densely vegetated areas, street side green areas, green open spaces… etc. have a better cooling effect than urban water bodies (Kong et al., 2014) due to several reason mainly by the process of evapotranspiration as which they release moisture in to the air that will minimize the surface temperature and providing shading that can minimize the direct contact of sunlight to surface by absorbing solar radiation.

Changes in LULC primarily impact the surface temperature of the urban area and its surrounding environments by replacing vegetated areas and open spaces with impermeable surfaces (Balew et al., 2020; Sisay et al., 2019) by exposing the urban areas to direct solar radiation which increases the Surface urban heat island (SUHI). Therefore, the decreasing trends in NDVI of the study area, which means the loss of vegetation cover in the area, will increase SUHI along the roadside corridor, which will have a direct impact on walkability.

4.2.3. Spatial and temporal patterns in NDBI

The NDBI algorithm is used to detect changes over time in the built-up environment by analyzing the built-up area using the NIR and Red bands (Varshney, 2013; Xu, 2007). Using this method; Due to unprecedented urbanization Addis Ababa city is undergoing a noticeable changes in NDBI studied on the years in 2015, 2020 and 2024 overtime (Figure 4.10) Confirmed by Regassa et al., in 2020 by the calculated result of the city NDBI as in 1990 it was only 125.1km2 (23.7%), which was increased to 132.8km2 (25.2%) in 2003 and expanded to 208.3km2 (39.5%) in 2020 (Figure 4.15).

In the city, urban built-up areas expansion is becoming common (Kassa et al., 2015), with highly expanding mainly over green areas, urban forests, and grasslands (Regassa et al., 2020), which will lead to an extensive decrease in the NDVI of the city that linearly impacts the UHIE.

In the study area, the NDBI trend shows an increasing trend from 2015 to 2020 with an implication of elevated built-up areas through urban expansion (Figure 4.17), surprisingly, this result shows a unexpected gradual decrease from 2020 to 2024 (Figure 4.17) due to the major reason investigated through historical imagery over time and key informant interview on the areas that low rise dense residences were demolished and relocated by corridor development project on road sides including buildings without proper setbacks and the other by ‘Chaka’ project for Future expansion.

The value of the NDBI indicator varies from -1 to +1; the highest values represent the constructed area, while the lowest values represent the lack of construction for the given area. Based on this, the result shows that from 2015 to 2020 shows that there is a reduction in the mean NDBI value from -0.0808 to -0.1069, which suggests that there is a reduction in Built-up area.

Through further investigation in the area through field observation and compiling the results with key informants’ information, the mean result from NDBI is from the increased vegetation from the government initiative in the period. From the year 2020 to 2024, the mean NDBI result shows a noticeable increase, which indicates there is a rise in built-up area which is directly linked mainly to the urban road expansion, as it’s one of the major components in the study.

Based on the spatial scope of the study the expansion on the road i.e. ‘Megenagna’ to ‘Piassa’ road; which leads an increase in Built-up density and impervious surfaces alters urban landscapes to have a faster absorption rate and smaller thermal capacity (Bornstein, 1968; Rosenfeld et al., 1995; Song, 2004) which will increase the LST and linearly elevates UHIE in the area.

LULC changes induced by rapid urbanization are one of the biggest environmental concerns (Weng et al., 2001; Regassa et al., 2020) as the changes in LULC are mainly related to the expansion of built-up areas, which directly alter the natural environment which increasing the vulnerability of the area to environmental issues such as an increase in LST and an increase in SUHI.

The study area NDBI result, which was computed by comparing the road before and after corridor development, primarily focuses on the road's extension from "Megenagna" to "Piassa" as a result of the corridor development, which intends to establish a new bicycle lane and extend the pedestrian line. According to field observation findings, a concrete pavement technology was used to create the bike and pedestrian lanes. Lighter-colored aggregates and cement binders can further cool concrete pavements, since studies of particularly lightened concrete have demonstrated solar reflectance levels of up to Eighty percent /80%/ (Levinson, 2001).

Additionally, various studies have explored strategies to enhance concrete pavement performance. Concrete pavement can be renovated by using a technique called white topping, which uses fiber reinforcement to strengthen the pavement, keeping additional layers thinner and reducing the curing time (Lisa, 2008; Hurd, 1997).

The enhancement of concrete pavements is significant due to their higher solar reflectance compared to conventional asphalt pavements. The concrete pavement with forty-five percent (45%) solar reflectance, which is higher than asphalt pavement, has ten percent (10%) solar reflectance (Lisa, 2008).

Various Previous studies on UHI have concentrated on assessing the relationship between LST and land cover composition (Chen et al., 2014; Weng et al., 2004) this implication and the result from studies indicates that an increase in NDBI which is an effective indicator on identifying impervious surfaces in an area increases the Built-up land cover substantially rises the UHII.

4.2.4. Trends on urban heat island intensity (UHII)

Due to an increasing trend in LST (Figure 4.3), increasing trend in NDBI (Figure 4.15) and decreasing trend in NDVI (Figure 4.11) which impacts the value of UHII; the combined UHII result of Addis Ababa city (Figure 4.19) shows an increasing trend and the city is experiencing significant changes on the trends of UHII due to several driving factors including urban road expansion.

From the three years of the study i.e. 2015, 2020, and 2024 in Addis Ababa, the most negative value of average mean UHII is recorded in 2015 with the value -0.193205 (Figure 4.20), the second most negative value is recorded in 2020 as -0.237157, and the least negative value which describes relatively higher UHII is recorded in 2024 with the value -0.263355 (Figure 4.21).

According to the study area's results, the lowest UHII was recorded in 2015 with a mean value of -0.246969; this value increased to -0.257157 in 2020, and by 2024, the value of -0.273355 rises drastically, indicating a comparatively higher UHII than the results in 2020 and 2015 (Figure 4.21). This result should be seriously considered, as UHI adversely affects population health and intensifies the effects of heatwaves, which have resulted in illnesses and death worldwide (Li et al., 2013; Stone, 2012).

As a result of NDVI shows a continuous decreasing trend (Table 4.1). Investigating the impact of UHI and SUHI, using remote sensing to track shifts in LULC types and patterns of landscape provides essential information for the evaluation and analysis of SUHI (Korme et al., 2019) to statistically analyze the shifts mainly in NDVI, as Vegetation cover is the main driving factor of UHI (Deliami et al., 2018).

By understanding the relationship, specifically the correlation and regression between LST, NDVI, and NDBI (Isufi et al., 2021), the observed increasing dynamics in LST of the study area over time that have a strong linear correlation with NDBI with an increased value, and a decreasing trend in NDVI imply that the area is experiencing an increasing trend on the aspects of UHIE.

CHAPTER 5: CONCLUSION AND RECOMMENDATIONS

5.1. Conclusion

The findings reveal a substantial increase in UHI over the study period, as it is conducted to analyze the study areas' spatial and temporal variations in the UHI trends over time before and after corridor development. UHII is a critical phenomenon extensively influenced by factors, specifically LST, NDVI, and NDBI, which shows the variations through interaction among the natural landscape and urban environment. From the major findings of the research illustrated, we can conclude that the substantial increase in the UHII of the study area resulted from an intensification of built-up areas and a reduction in the amount and density of vegetation cover, leading to an upward trend in LST, which linearly increases the UHII.

LST, NDVI, and NDBI have an interconnected role in which LST is a dependent variable over NDVI and NDBI. The finding of the research on the Primary objective on LST shows a noticeable increase on the study period over time with an increasing trend on NDBI which have positive correlation with NDBI. Based on the finding we can conclude that an expansion in impervious surfaces and decrease in NDVI due to a decrease in the density and amount of vegetation cover which minimizes the shading purposes of vegetation to the impervious surfaces that will minimize the solar radiation and reduction in vegetation cover reduces the evapotranspiration that contributes to the substantial increase in UHII which reflects the root causes and impacts of urbanization and urban expansion on the environment which will have substantial implication on the urban resilience, environmental sustainability which gradually affects public health.

The investigation aimed to attain the second objective of the study on NDVI, which shows a downward trend which have a linearly negative correlation with UHII, implying an extensive increasing trend on LST as the cooling effect from the vegetation is prominently reduced. Based on these findings it's possible to conclude that urban green infrastructure can mitigate UHII naturally. Additionally, reduction in vegetation cover will impact the thermal dynamics of urban areas by increasing their vulnerability to heat retention which results increase in LST and at the same time increases the susceptibility of the areas to higher UHII. Therefore, enhancing green infrastructure with a proper scientifically based approach considering various environmental factors and their purpose, i.e., Shading, ornamental, perennial vegetation's can mitigate UHII.

From the results of NDBI based on the third objective of the study, an extensive increasing trend in NDBI value is observed that is linearly correlated with LST, which will increase the UHII in the study area. This increasing trend in NDBI resulted from the road expansion due to corridor development in the study area that leading to an increase in the impervious surfaces by altering the natural environment, which is positively correlated with LST and UHII. The rise in urban infrastructure and impervious surfaces directly alters the natural environment, which exacerbates the UHII which suggesting inclusive urban planning strategies for balancing both the urban environment and natural landscape to a sustainable urban environment.

By utilizing remote sensing data, the research emphasized the interconnection among the main factors of UHII i.e. LST, NDVI and NDBI, to insight the major finding of this research resulted from combined impacts of reducing vegetation cover and rise in built-up area density implying an elevated UHII along roadway from 'Megenagna' to 'Piassa' corridor development which implies urban area expansion in the study area specifically road expansion including pedestrian and Bike lane leads the area to micro climate change by exposing to higher thermal retention and increase in LST which simultaneously rises the UHI and SUHI/.

On the other hand, finding from key informants and detail investigation by comparing road before corridor development plan on structural plan 9, structural plan 10, and the road map before corridor development from AACRA with corridor development proposal and After corridor development road on the route from 'Megenagna' to 'Piassa' section which shows a result with more than Fifty percent /50%/ road expansion. This road expansion highly increases the impervious surfaces in the study area, which exacerbates the urban-rural temperature difference.

As the study utilizes remote sensing, Google Earth Engine, and Geographic Information System (GIS), it enhances how these systems can be effectively used for analyzing the spatial and temporal dynamics of urban areas UHII by investigating the LST, NDVI, and NDBI through the variation in vegetation cover and built-up density, which will influence the surface temperature linearly with UHII.

5.2. Recommendation

- As an initial management recommendation, Addis Ababa city municipality should implement urban management strategies which focus on enhancing vegetation coverage, waste management, and sustainable urban drainage systems.
- It is highly recommended for Addis Ababa city municipality to develop and implement urban heat island action plan, integrating mitigating strategies, sustainable building codes and standards.
- Additionally, Policy makers are expected to propose and implement a proactive inclusive policy, rules and enforcing regulations to minimize the adverse impacts of UHII on the environment to achieve a sustainable, resilient environment in urban areas.
- To evaluate the corridor development project's implications on UHII, the main recommendation based on the research findings emphasizes the significance of a comprehensive environmental impact assessment.
- It is strongly recommended to apply the concept of wind blocking by green infrastructure mainly in the areas with a high building density for enhancing the cooling effect by designing urban spaces that avoid the accumulation of urban heat, which is linearly correlated with LST and UHII.

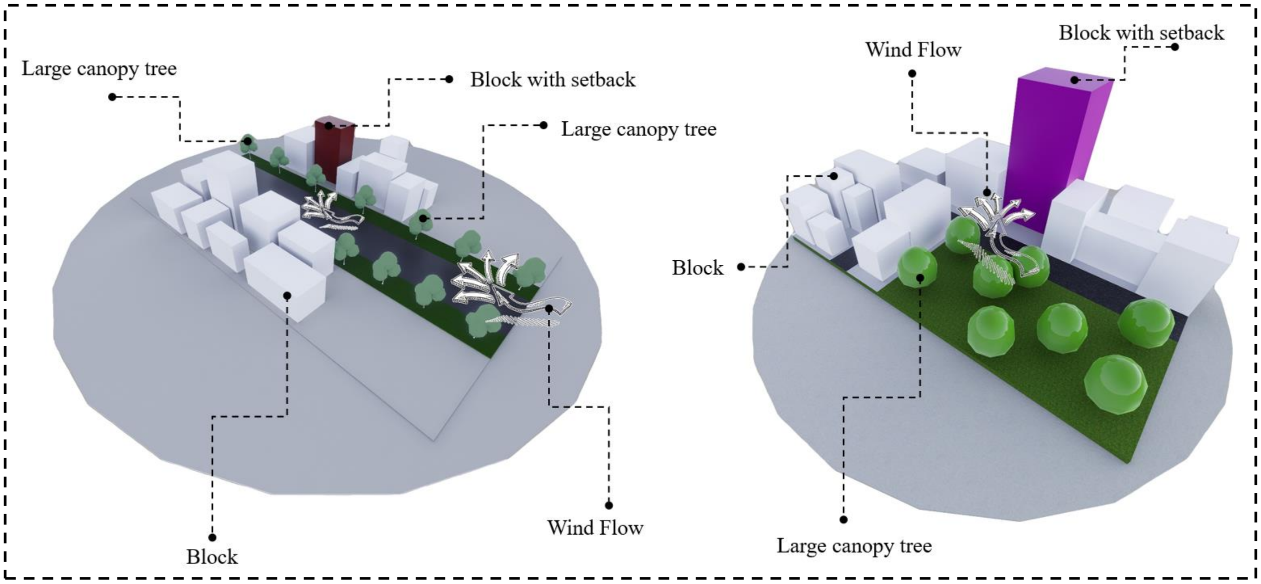

Figure 5.1. *Green infrastructure, and wind blocking conceptual model*

- ☐ Providing an urban street canopy method is highly recommend proactive method and nature- based solution which reduce the LST by providing shading for the area which linearly minimizes the UHII in the area, enhance air quality, reduces noise pollution as trees can be used as a sound barrier, increase aesthetical value; which increase the urban resilience of the area.

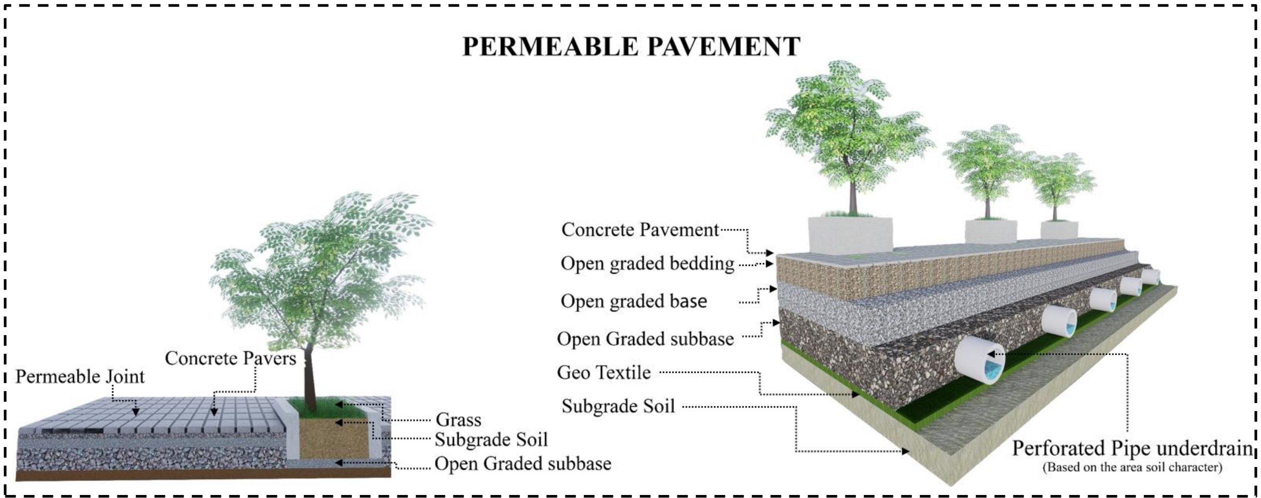

Figure 5.2. *Proposed Permeable pavement strategy*

- ☐ As there is a high rate of streetscapes and roadway expansion in the study area projected for enhancing non-motorized transport, parking facilities, and adding bicycle lanes, the rate of impervious surface increased as the construction employs reinforced concrete pavement technology, which needs to promote permeable pavement strategies.
- ☐ It's extensively recommended to adopt Permeable pavement strategies with a proper material selection and construction technique as the sample model in Figure 27 as permeable pavements minimize overheating, reduce surface runoff, and increase ground water, which will help to achieve urban resilience and a sustainable urban environment.
- ☐ It's recommended to integrate biophysical parameters such as Humidity, precipitation, soil type, plant species listed on Annex 10, focusing more on indigenous, surface albedo rate, Material characters, surrounding building radiation rates, etc., in future research for a holistic evaluation to increase the result effectiveness.
- ☐ While planting trees, it's thoroughly recommended to consider species variety as a preliminary criterion for various reasons, including diversity in aesthetic value, and the

major reason to protect damage to the plant from rapidly spreading plant disease, which will attack the natural environment due to uniformity in species.

Figure 5.3. *Shades, Nature-based solutions, and case study*

- ☐ Priority should be given to enhance green infrastructure through adaptive urban planning strategies to ensure a sustainable and resilient urban environment by integrating the natural ecosystem with the urban environment.
- ☐ Enhancing Nature-based solutions for mitigating UHII should be promoted such as enhancing purpose-based plantations like shaded plants as shown on Annex 10 that reduce direct solar radiation.
- ☐ Priority should be given to climate adaptive strategy on the theme of UHII including enhancing blue-green infrastructure, encouraging natural ecosystem preservation and conservation mechanisms, promoting permeable pavement etc.

- ☐ An adaptive urban green strategy should be promoted for provisioning the most efficient and effective species type as specified in Annex 10 that can regulate micro temperature by reducing the surface temperature in the area by cooling the environment.

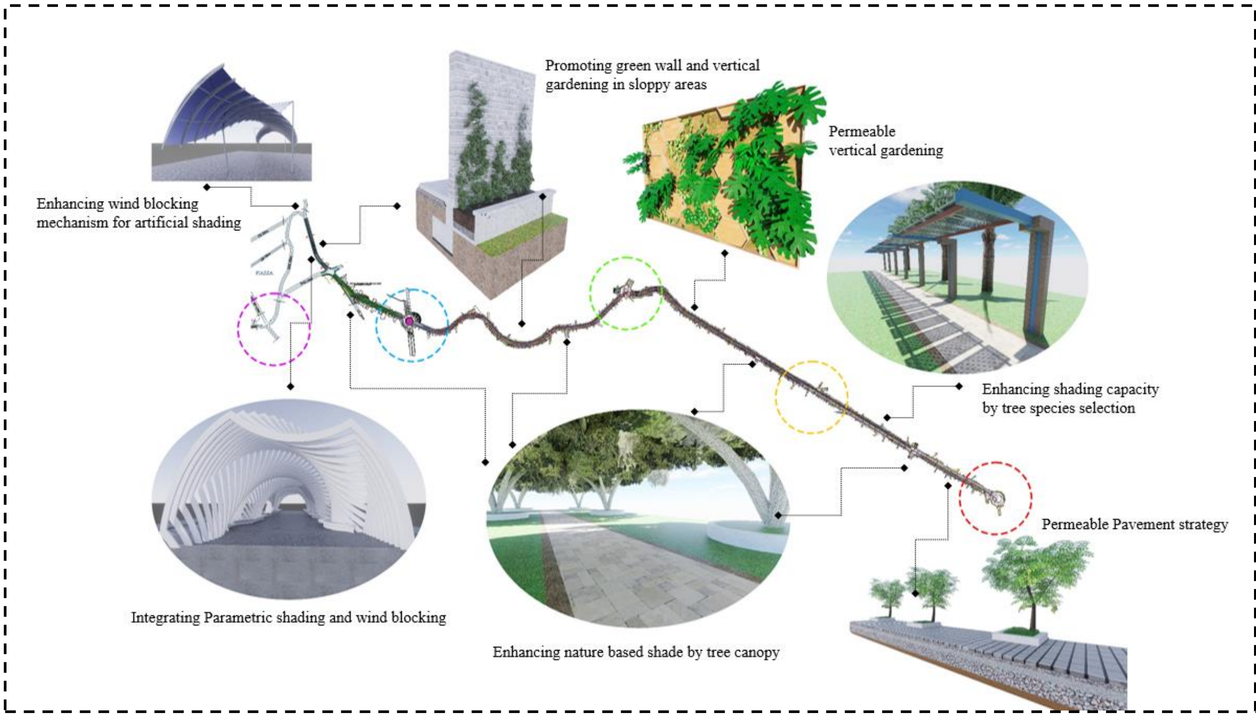

Figure 5.4. *Proposed strategies with corridor development road*

- ☐ Cross-sectoral and multi-disciplinary approach should be enhanced to ensure comprehensive inclusive solution with experts' integration to achieve effective and sustainable intervention to mitigate the increasing impacts of UHII.
- ☐ It's recommended to further study the spatial and temporal dynamics of UHII using methods i.e. and advanced technique to increase the accuracy of the result,
- ☐ As the study demonstrates that Google Earth Engine with remote sensing and GIS is effective in analyzing UHII dynamics of urban areas, it is strongly recommended that using GEE future research using GEE will help to improve the efficiency and accuracy of the result.
- ☐ Future studies should explore in-depth analysis through adaptive advanced approaches by integrating satellite imagery data with the Baseline situation (ground truth) for the accuracy and spatially detailed result to develop effective mitigation strategy.

Reference

Addis Ababa City Roads Authority, 2019. The preparatory survey report for the project for upgrading road maintenance equipment in Addis Ababa City.

Aleksandrowicz, Vuckovic, M., Kiesel, K., Mahdavi, A., 2017. Current trends in urban heat island mitigation research: observations based on a comprehensive research repository, urban climate.

Alfraihat, R., Mulugeta, G., & Gala, T., 2016. Ecological evaluation of urban heat island in Chicago city, USA. Journal of atmospheric pollution. 4 (1), 23–29.

Akbari, H., Bell, R., Brazel, T., Cole, D., Estes, M., Heisler, G., 2008. Reducing Urban Heat Islands: Compendium of Strategies; United States Environmental Protection Agency (USEPA): Washington DC, USA.

Akbari, H., Pomerantz, M., Taha, H., 2001. Cool surfaces and shade trees to reduce energy use and improve air quality in urban areas, solar energy. 70 (3), 295-310. https://doi.org/10.1016/s0038-092x (00)00089-x.

Asaeda, T., Ca, T., Wake, A., 1996. 'Heat storage of pavement and its effect on the lower atmosphere'. Atmospheric environment. 30 (3), 413–427.

Atun, R.; Kalkan, K., Gürsoy, Ö., 2020. Determining the forest fire risk with sentinel 2 images. 1 (1), 22-26.

Baccini, M., Biggeri, A., Accetta, G., Kosatsky, T., Katsouyanni, K., Analitis, A., Anderson, H., Bisanti, L., D'Ippoliti, D., Danova, J., Forsberg, B., Medina, S., Paldy, A., Rabczenko, D., Chindler, C., Michelozzi, 2008. Heat effects on mortality in 15 european cities. Epidemiology. 1 (19), 711-719. https://doi: 10.1097/ede.0b013e318176bfcd.

Balew, A., Korme, T., 2020. Monitoring land surface temperature in Bahir Dar city and its sur rounding using Landsat images. The Egyptian journal of remote sensing and space science. 23, 371–386. https://doi.org/10.1016/j.ejrs.2020.02.001.

Balmford, A., Green, R., Phalan, B., Proc, R., 2012.What conservationists need to know about farming. 279, 2714–2724.

Barnes, K., Morgan, J., Roberge, M., 2001. Impervious surfaces and the quality of natural and built environments; department of geography and environmental planning, Towson University: Towson, MD, USA.

Benedict, M., McMahon, E., 2006. Green infrastructure: smart conservation for the 21st century. Renewable resources journal. Green infrastructure: linking landscapes and communities. Island press, washington. 12-17.

Berry, B., Marble, D., Englewood C., Prentice N., Bertin, J., 1968. Semiology of graphics: diagrams, networks, maps. Madison, university of Wisconsin press.

Bijay et al., 2021. Monitoring the effect of urban development on urban heat island based on remote sensing and geo-spatial approach in Kolkata and adjacent area.

Bornstein, R., 1968. Observations of the urban heat island effect in New York City. Journal of applied meteorology. 4 (7), 575-582.

Bradley, G., 1995. Urban forestry landscapes: integrating multi-disciplinary perspectives. Seattle: University of Washington press.

Calkins, M., 2012. The sustainable sites handbook: a complete guide to the principles, strategies, and best practices for sustainable landscapes. New Jersey, USA.

Cartwright, P., 1998. ‘Blue diamond materials and excel paving provide colored asphalt for union station project’.

Central Statistical Agency, 2010. "The 2007 Population and Housing Census".

Central Statistical Agency, 2012. "Urban Employment Unemployment Survey (UEUS)." 2003, 2004, 2006, 2009, 2010, 2011, 2012.

Cetin, M., Adiguzel, F., Cetin, Ilknur Z., 2023. Determination of the effect of urban forest and other green areas on surface temperature in Antalya. In: concepts and applications of remote sensing in forestry. 319-336.

Chen A., Yao X., Sun R., 2014. Effect of urban green patterns on surface urban cool islands and its seasonal variations. Urban forestry & urban greening. 13(4): 646 654. http://doi: 10.1016/j.ufug.2014.07.006

Chen, F., 2011. Impact of upstream urbanization on the urban heat island effects along the Washington Baltimore corridor.

Chen, F., Yang, X., Zhu, W., 2014. WRF simulations of urban heat island under hot-weather synoptic conditions: the case study of Hangzhou city, china, atmospheric research. 138, 364-377. https://doi.org/10.1016/j.atmosres.2013.12.005.

Chorley, R., 1972. Spatial analysis in geomorphology. London: Methuen.

Dai, Z., Guldmann, J., Hu, Y., 2019. Thermal impacts of greenery, water, and impervious structures in Beijing's Olympic area: A spatial regression approach, Ecological Indicators. 97, 77-88. https://doi.org/10.1016/j.ecolind.2018.09.041.

Dararat, K., 2020. Time series analysis of land use and land cover changes related to urban heat island intensity: case of Bangkok metropolitan area in Thailand.

Das, S., Angadi, D., 2020. Land use-land cover (LULC) transformation and its relation with land surface temperature changes: a case study of Barrackpore Subdivision, West Bengal, India.

Deilami, K.; Kamruzzaman, M., Liu, Y, 2018. Urban heat island effect: a systematic review of spatio-temporal factors, data, methods, and mitigation measures. 1 (67), 30–42.

Desa, 2018. World Urbanization Prospects: The 2018 Revision (ST/ESA/SER.A/420); United Nations: New York, NY, USA.

Dimoudi, A., Nikolopoulou, M., 2003. Vegetation in the urban environment: microclimatic analysis and benefits, energy and buildings. 35 (1), 69-76. https://doi.org/10.1016/s0378-7788(02)00081-6.

Dobos, E., Albedo, M., Dekker, I., Miskolc, Hungary G., 2012. Heat islands: understanding and mitigating heat in urban areas. Earth scan, London, UK.

Fadhil, M., Hamoodi, A., Ziboon, 2023. Mitigating urban heat island effects in urban environments: strategies and tools. http://doi:10.1088/1755-1315/1129/1/012025.

Farooq A., Qurat, F., 2012. Phonologically-tuned Modis Ndvi-based time series (2000-2012) for monitoring of vegetation and climate change in north-eastern punjab, pakistan. http://creativecommons. org/licenses/by-nc/3.0/).

Ferguson, B., 2005. Porous Pavements (First edition). Crc Press. https://doi.org/10.1201/9781420038439

Flores, V., Cristina, L., Parapinski, C., Saldeño, Y., 2021. A proposal to compare urban infrastructure using multi-criteria analysis, Land Use Policy. https://doi.org/10.1016/j.landusepol.2020.105173.

Gao, Z., Hou, Y., Chen, W., 2019. Enhanced sensitivity of the urban heat island effect to summer temperatures induced by urban expansion.

Goergen, M., Al-Hawamdeh, A., Chiu, I., Mallin, C., Mitleton, E., 2010. Corporate governance and complexity theory; edward elgar publishing ltd.: cheltenham, uk.

Goodman, J., Hurwitz, M., Park, J., Smith, J., 2018. Heat and learning. National bureau of economic research.

Goorha, Prateek. (2010). Modernization Theory.

Haase, Dagmar, 2009. Effects of urbanization on the water balance. A long-term trajectory. Environmental impact assessment review.

Halder, B., Bandyopadhyay J., 2021. Evaluating the impact of climate change on urban environment using geospatial technologies in the planning area of Bilaspur, India environ. 5 (10).

Howard, L., 1833. The climate of London: deduced from meteorological observations made in the metropolis and at various places around it.

Hurd, M., 1997. ‘Ultra-thin white topping’. Concrete construction.

Imran, H., Kala, J., Ng, A., Muthu Kumaran, S., 2019. Impacts of future urban expansion on urban heat island effects during heatwave events in the city of Melbourne in southeast Australia.

Isufi, F., Berila, A., Bulliqi, S., 2021. Measuring UHI using Landsat 8 oli and tirs data with Ndvi and Ndbi in municipality of Prishtina. 3(14), 25-36.

Iswari, N., Suharyadi, R., Danoedoro, P., 2018. Developing an extraction method of urban built-up area based on remote sensing imagery transformation index.

Kasa, L., Zeleke, G., Alemu, D., Hagos, F., Heinimann, A., 2015. Impact of urbanization of Addis Ababa city on peri-urban environment and livelihoods. https:// www. resea rchga te. net/ publi cation/ 26780 2706

Kong, F., Yin, H., James, P., Hutyra, R., He, H., 2014. Effects of spatial pattern of greenspace on urban cooling in a large metropolitan area of eastern China Landscape and Urban Planning.

Kotharkar, R., Ramesh, A., Bagade, 2018. Urban Heat Island studies in South Asia: A critical review, Urban Climate. https://doi.org/10.1016/j.uclim.2017.12.006.

Ladson A., Walsh C., Fletcher T., 2006. Improving stream health in urban areas by reducing runoff frequency from impervious surfaces. 10 (1), 23-33.

Laurance, F., Goosem, M., Laurance, S., 2009. Impacts of roads and linear clearings on tropical forests. 24 (12), 659–669.

Lee, J., Pak, G., Yoo, Chulsang, Kim, S., Yoon, J., 2010. Effects of land use change and water reuse options on urban water cycle. Journal of environmental sciences (China).

Levinson, R., Akbari, H., 2001. Effects of composition and exposure on the solar reflectance of portland cement concrete.

Li, D., Bou-Zeid, E., 2013. Synergistic interactions between urban heat islands and heat waves: the impact in cities is larger than the sum of its parts. Journal of applied meteorology and climatology. 52, 2051–2064.

Li, X., Song C., Cao L., 2011. Impacts of landscape structure on surface urban heat islands: a case study of Shanghai, China. Remote Sensing of Environment. 115(12), 3249-3263. http://doi: 10.1016/j.rse.2011.07.008

Lillesand, T., Kiefer, R., Chipman, J., 2008. Remote sensing and image interpretation. 6th ed. New York: Wiley.

Lisa, G., 2008. Heat islands: understanding and mitigating heat in urban areas

Liu, J., Schlünzen, K., Frisius, T., Tian, Z., 2021. Effects of urbanization on precipitation in Beijing.

Liu, K., 2002. 'A National Research Council Canada study evaluates green roof systems' thermal performances', Professional Roofing.

Liu, K., 2002. Energy efficiency and environmental benefits of rooftop gardens, Construction Canada. 44 (2), 20-23.

Liu, Q., Xie, M., Wu, R., Xue, Q., Chen, B., Li, Z., Li, X., 2021. From expanding areas to stable areas: Identification, classification and determinants of multiple frequency urban heat islands.

Li, X., Li, W., Middel, A., Harlan, L., Brazel, A., Turner, I., 2016. Remote sensing of the surface urban heat island and land architecture in Phoenix, Arizona: Combined effects of land composition and configuration and cadastral-demographic-economic factors. Remote Sensing of Environment. 174, 233-243.

Li, X., Zhou, W., Ouyang, Z., 2012. Spatial pattern of greenspace affects land surface temperature: evidence from the heavily urbanized Beijing metropolitan area, China. **27**, 887–898. https://doi.org/10.1007/s10980-012-9731-6.

Longley, Paul, A., Michael, F., Goodchild, David, J., Maguire, David, W., Rhind, 2015. Geographic Information Science and Systems. New York, NY: Wiley.

Lütz, M., Bastian, O., 2002. Implementation of landscape planning and nature conservation in the agricultural landscape-A case study from Saxony. Agriculture, Ecosystems and Environment. 92(3), 159–170.

Macdonald, N., Miller, J., 2021. Understanding the impact of the built environment mosaic on rainfall-runoff behavior. Journal of Hydrology.

Mackey, W., Lee, X., Smith, R., 2012. Remotely sensing the cooling effects of city scale efforts to reduce urban heat island. Building and Environment. 49, 348-358.

Macmillan, A., Connor, J., Witten, K., Kearns, R., Rees, D., Woodward A., 2014. The societal costs and benefits of commuter bicycling: simulating the effects of specific policies using system dynamics modeling. 22, 335–344; https://doi.org/10.1289/ehp.1307250

Masson, V., 2006. Urban surface modeling and the meso scale impact of cities. Theoretical and applied climatology. 84(3), 35-45.

Mathias, T., Tebarek L., 2016. The city of Addis Ababa from 'forest city' to 'urban heat island': assessment of urban green space dynamics. 10 (2), 254-262.

Ma, Q., Wu, J., He, C., Hu, G., 2019. Reprint of Spatial scaling of urban impervious surfaces across evolving landscapes: From cities to urban regions. 187, 132-144.

McGrane S., 2016. Impacts of urbanization on hydrological and water quality dynamics, and urban water management: A review. 61(13), 2295-2311.

Mejia, Alfonso, D., Edoardo, R., Florian, J., Tijana, G., 2014. A stochastic model of streamflow for urbanized basins. Water Resources Research.

Miklas, S., Grabowiecki, P., 2007. Review of permeable pavement systems, Building and Environment. 42(11), 3830-3836. https://doi.org/10.1016/j.buildenv.2006.11.016.

Mirabi, e., Davies, P., 2022. A ststematic review investigating linear infrastructure effects on urban heat island and its interaction with urban heat island typologies. http://doi.org/10.1016/j.uclim/2022.201261.

Mishra, P., Rai, A., Rai, S., 2020. Land use and land cover change detection using geospatial techniques in the Sikkim Himalaya, India. The Egyptian Journal of Remote Sensing and Space Sci ence. 23(2), 133–143.

Mitchell, J., 1953. 'On the causes of instrumentally observed secular temperature trends'. Journal of Meteorology. 10, 244–261.

Mitchell, J., 1961. 'The temperature of cities'. Weatherwise. 14, 224–229.

Mlambo, A., 1994. From Dirt Tracks to Modern Highways: Towards a History of Roads and Road Transportation in Colonial Zimbabwe, 1890 to World War II. Zambezia. 21(2), 147–166. https://www.africabib.org/rec.php?RID=14201837

Mohajerani, A. Bakaric, J. and Jeffrey-Bailey, T. 2017, 'The urban heat island effect, it's cause, and mitigation, with reference to thermal properties of asphalt concrete', journal of environment management, Elsevier, United kingdom, vol. 197, pp. 522-538 ISSN: 0301-4797 https://researchbank.rmit.edu.au/view/rmit:43518

Morrison, W., Kotthaus, S., Grimmond, C., Inagaki, A., Yin, T., Gastellu, E., Kanda, M., Christopher, J., 2018. A novel method to obtain three-dimensional urban surface temperature from ground-based thermography, Remote Sensing of Environment.15, 268-283. https://doi.org/10.1016/j.rse.2018.05.004.

Muñoz, P., Zwick, S., Mirzabaev, A., 2020. The impact of urbanization on Austria's carbon footprint.

Oke, T., 1981. Canyon geometry and the nocturnal urban heat island: Comparison of scale model and field observations. 237–254.

Oke, T., 1982. The energetic basis of the urban heat island. 108, 1-24 https://doi.org/10.1002/qj.49710845502

Oke, T., 1987. Boundary Layer Climates, 2nd ed.; Routledge, Taylor and Francis Group: Cambridge, UK.

Oxley, J., Langford, A., Charlton, J., 2010. The safe mobility of older drivers: a challenge for urban road designers, Journal of Transport Geography. 18 (5), 642-648. https://doi.org/10.1016/j.jtrangeo.2010.04.005.

Piyoosh, A., Ghosh, S., 2020. Analysis of land use land cover change using a new and existing spectral indices and its impact on normalized land surface temperature. 1 (9), 1–23.

Priyadarsini, R., Hien, W., David, C., 2008. Microclimatic modeling of the urban thermal environment of Singapore to mitigate urban heat island. 82(8), 727-745.

Przeworski, A., and Limongi, F. (1997) Modernization: Theories and Facts. World Politics 49 (2), 155–83.

Qaid, A., Lamit, H., Ossen, D., Shahminan, R., 2016. Urban heat island and thermal comfort conditions at micro-climate scale in a tropical planned city. Energy and Buildings. 133, 577–595.

Qiu, G., Zhang, Q., Wan, C., Liang, X., Li, X., 2013. Effects of evapotranspiration on mitigation of urban temperature by vegetation and urban agriculture. Journal of Integrative Agriculture. 12, 1307-1315.

Qiu, G., Yan, C., Liu, Y., 2023. urban evapotranspiration and its effects on water budget and energy balance: Review and perspectives. Earth-Science Reviews. 246. 104577. 10.1016/j.earscirev.2023.104577.

Raciti, S., Galvin, M., Grove, J., Neil D., Todd, A., Clagett, S., 2006. Urban Tree Canopy Goal Setting.

Rao, Anzal. (2022). Urban Streetscapes. 10.13140/RG.2.2.12934.86085.

Regassa, B., Kassaw, M., Bagyaraj, M., 2020. Analysis of urban expansion and modeling of LULC changes using geospatial techniques: the case of Adama City. Remote Sensing of Land. 4(2), 40-58 https://doi.org/10.21523/gcj1.20040104.

Reinhard, M., Yasin, S., 2011. Sustainable Cities and Society. 1 (91), 45-53.

Ries, C.; Pillmann, W., Kellner, K., Stadler, P., 2002. Urban Green Space Management Information -Processing and Use of Remote Sensing Images and Scanner Data. Proceedings of Environmental Informatics.

Rosenfeld, A., Akbari, H., Bretz, S., Fishman, L., Kurn, M., Sailor, D., 1995. Mitigation of urban heat islands: Materials, utility programs, updates.

Saghir, J., Santoro, J., 2018. Urbanisation in Sub-Saharan Africa: Meeting Challenges by Bridging Stakeholders Center for Strategic and International Studies (CSIS). https://www.csis.org/analysis/urbanization-sub-saharan-africa

Sailor, D., 2006. Mitigation of urban heat island recent progress and future prospects. Paper presented at the Paper presented on American meteorological society 6th symposium on the urban environment and forum on managing our physical and natural resources.

Samson w., Suryabhagavan K., Satishkumar, B., 2018. Urban green areas to mitigate urban heat island effect: the case of Addis Ababa, Ethiopia. 44 (4), 353-367.

Schmidt, J., 1917. Racial Investigations. I. Zoarces viviparous L. and Local Races of the same. Comptes Rendus des Travaux du Laboratoire Carlsberg. 13, 279-396.

Shahid, M., 2014. Land Surface Temperature Retrieval of Landsat 8 Data Using Split Window Algorithm- A Case Study of Ranchi District. International Journal of Engineering Development and Research. 2 (4), 3840-3849.

Shuster, W., Bonta, J., Thurston, H., Warnemuende, E., Smith, D., 2005. Impacts of impervious surface on watershed hydrology: A review. Urban Water. 2 (4), 263-275.

Sisay, C., Korme, T., oda, 2019. Understanding land surface temperature on rift areas to examine the spatial variation of urban heat island: the case of Hawassa, southern Ethiopia. Geo Journal. https://doi.org/ 10.1007/s10708-019-10110-5.

Siti, N., Afzan, B., Naim, W., Alamah, M., 2013. Green Spaces Growth Impact on the Urban Microclimate. Procedia–Social and Behavioral Sciences. 105, 547-557.

Song, Y., 2004. Influence of new town development on the urban heat island-the case of the Bundang area. Journal of Environmental Sciences (China). 17, 641-645.

Stone, B., 2012. The city and the coming climate: Climate change in the places we live. Cambridge University Press

Subhanil, G., Himanshu G., Anindita, D., Neetu, G., 2018. Analytical study of land surface temperature with NDVI and NDBI using Landsat 8 OLI and TIRS data in Florence and Naples city, Italy, European Journal of Remote Sensing. 51 (1), 667-678. http://DOI: 10.1080/22797254.2018.1474494

Sullivan, O., David J., 2002. Geographic Information Analysis. New York, NY: Wiley.

Teferi, E., Abraha, H., 2017. Urban heat island effect of Addis Ababa City: Implications of urban green spaces for climate change adaptation. In Climate change adaptation in Africa (pp. 539–552). Springer, Cham.

Theeuwes, N., Steeneveld, G., Ronda, R., Heusinkveld, B., Holtslag, A., 2012. Mitigation of the urban heat island effect using vegetation and water bodies.

The Statistical, Economic and Social Research and Training Centre for Islamic Countries (SESRIC) 2015.

Ting, M., Koomey, J., Pomerantz, M., 2001. Preliminary Evaluation of the Lifecycle Costs and Market Barriers of Reflective Pavements.

Ünal, S., Sonuç, Y., Incecik, S., 2020. Investigating urban heat island intensity in Istanbul. 139, 175–190. https://doi.org/10.1007/s00704-019-02953-2

Varshney, A., 2013. Improved NDBI differencing algorithm for built up regions change detection from remote-sensing data: An automated approach. Remote Sensing Letters. 4 (5), 504-512.

Vasenev, V., Varentsov, M., Konstantinov, P., Romzaykina, O., Kanareykina, I., Dvornikov, Y., Manukyan, V., 2021. Projecting urban heat island effect on the spatial-temporal variation of microbial respiration in urban soils of Moscow megalopolis. Science of the Total Environment.

Voogt, J., Oke, T., 2003. Thermal remote sensing of urban climates. Remote Sensing of Environment. 86, 370–384.

Waleed, M., Sajjad, M., Acheampong, O., Alam, M., 2023. Towards Sustainable and Livable Cities: Leveraging Remote Sensing, Machine Learning, and Geo-Information

Modelling to Explore and Predict Thermal Field Variance in Response to Urban Growth. Sustainability (Switzerland). https://doi.org/10.3390/su15021416.

Wang, A., Zhang, M., Chen, E., Zhang, C., Han, Y., 2024. Impact of seasonal global land surface temperature (lst) change on Gross Primary Production in the early 21st century, sustainable cities, and society. 101, (21), 1-26. https://doi.org/10.1016/j.uclim.2017.04.002.

Wang, K., Onodera, S., Saito, M., Shimizu, Y., 2021. Long-Term Variations in Water Balance by Increase in Percent Imperviousness of Urban Regions. Journal of Hydrology.

Wang, W., He, J., Wang, X., 2024. Quantitatively comparing the morphological influences on the cool island effect in urban waterfront blue-green spaces across six cities near 30°N, Urban Climate. https://doi.org/10.1016/j.uclim.2024.102076.

Warkaye, S., Suryabhagwan, K., Satishkumar, B., 2018. Urban green areas to mitigate urban heat island effect: The case of Addis Ababa. Ethiopia International Journal of Ecology. 44, 353–367.

Weng, Q., Lo, C., 2001. Spatial analysis of urban growth impacts on vegetative greenness with Landsat TM data. Geocarto International. 16(4), 17–25.

Weng, Q., Dengsheng, L., Schubring, J., 2004. Estimation of land surface temperature–vegetation abundance relationship for urban heat island studies. Remote Sensing of Environment. 89, 467–483.

Whebell, C. F. J. (1969). Corridors: A Theory of urban Systems. Annals of the Association of American Geographers, 59(1), 1–26. https://doi.org/10.1111/j.1467-8306.1969.tb00655.x

Wong, H., Yu, C., 2005. Study of green areas and urban heat island in a tropical city. Habitat International. 29, 547-558.

Xu, H., 2007. Extraction of urban built-up land features from Landsat imagery using a Thematic-oriented Index Combination technique. Photogrammetric Engineering & Remote Sensing. 73 (12), 1381–1391.

Xu, Hanqiu, L., Dongfeng, Tang, Fei, 2013. The impact of impervious surface development on land surface temperature in a subtropical city: Xiamen, China. International Journal of Climatology. 33 (8),1873.

Yamamoto, Y., 2006. Measures to mitigate urban heat islands. Science and Technology Trends Quarterly Review. 18 (1), 65- 83.

Yang, J., 2021. Observing the impact of urban morphology and building geometry on thermal environment by high spatial resolution thermal images.

Yang, J., Wang, H., Kaloush, E., 2015. Environmental impacts of reflective materials: Is high albedo a 'silver bullet' for mitigating urban heat island? 47 (0), 830 – 843.

Yiran, A., Stringer, L., 2017. Adaptation to Climatic Hazards in the Savannah Ecosystem: Improving Adaptation Policy and Action. Environmental Management. 60 (4), 665-678.

Zhang, L., Shou, Y., Dickerson, R., 2009. Upstream urbanization exacerbates urban heat island effects. http://doi: 10.1029/2009GL041082

Annex 1 Publishable Manuscript

Comparative analysis of urban heat island effect before and after corridor development of ‘Piassa’ to ‘Megenagna’ route, Addis Ababa, Ethiopia

Robel Kassahun and Aramde Fetene

Department of Urban and Regional Planning, College of Technology and Built Environment, Addis Ababa University, Ethiopia

June, 2025

Addis Ababa, Ethiopia

Abstract

Urban expansion and unprecedented urbanization in cities like Addis Ababa are increasing the vulnerability of the areas to urban heat island intensity (UHII) phenomena with an increasing trend in urban thermal dynamics. This research analyzed the spatial and temporal variations in the Urban Heat Island (UHI) along the route from "Piassa" to "Megenagna" before and after corridor development through field observation, using a combination of remote sensing data, and Landsat 8 imagery by the tools Google Earth Engine, and ArcMap. The results demonstrate an increasing trend in LST 30.08° in 2015 to 32.82467^{0}C in 2024. Concurrently, the NDVI result shows a decreasing trend over time 0.34475 in 2015, to 0.265243 in 2020, and further dropped to 0.199966 in 2024. The mean annual NDBI in 2015 was -0.03495, increased to 0.001339 in 2020 indicating built-up area expansion, but dropped to -0.02705 in 2024 due to the demolished residence in the area. The overall UHII value shows an increasing trend over time with the most negative UHII annual mean average value in 2015 is 0.246969, increased to -0.257157 in 2020 and further increased to -0.273355 in 2024. The findings reveal a significant inverse relationship between NDVI and LST, highlighting the role of sustainable corridor design and Green infrastructure for mitigating the impact of UHII. Furthermore, Future studies should explore in depth analysis through adaptive advanced approaches by integrating satellite imagery data with the Baseline situation (ground truth) for the accuracy and spatially detailed result to develop effective mitigation strategy.

Key Words: Corridor development, impervious surfaces, Streetscape, and Urban heat island effect

1. Introduction

Roads are spreading all across the world due to major factors, including rising populations and improved connectivity. According to the World Bank, urban populations are growing at an annual rate of approximately 1.8%; Sub-Saharan Africa (SSA) has the highest urban growth rate, at around 3.6% per year (Yiral et al., 2020; Bocquier, 2005). It is widely recognized as the world's fastest-urbanizing area, with an urban population of around 472 million, which is expected to double within the next 25 years (Saghir & Santoro, 2018).

In Ethiopia, roadways serve as the principal infrastructure that has developed drastically, accounting for more than 95% of both passenger and freight transportation (AACRA, 2009). The Ethiopian government emphasizes the need to develop high-quality infrastructure to support the country's rapid urban expansion, as well as the significance of building organizational frameworks to ensure infrastructure sustainability.

The metropolis of Addis Ababa, which has been the driving force behind the robust 8 economic growth, is rapidly urbanizing and constructing several roadways. Furthermore, the city of Addis Ababa encourages the building and upgrading of city roadways as part of its long term development strategy presented on the Addis Ababa City Structure Plan (AACRA, 2009).

Urbanization has led to a rapid expansion in road construction and extension. Due to this growth, metropolitan road networks require expansion and modifications to handle rising traffic loads and a variety of transportation requirements. The development and operation of these routes also greatly contribute to climate change by altering the natural environment. Urbanization can alter local climate and form an urban heat island (Landsberg, 1981). Metropolitan regions are now grappling with two severe environmental problems: flooding and a rise in the urban Heat Island effect (UHI) under the favorable influence of larger-scale flow Therefore, a smaller city with upstream urbanization can have a larger UHI than a larger city with no upstream urbanization (Zhang et al., 2009).

The development of road networks and change in land use and land cover (LULC) will lead the conversion of natural environments to impervious surfaces has substantial impacts on climate, hydrology, and urban ecosystems. Increased built-up area, road network development, natural landscape fragmentation decreased drainage efficiency, increased storm water runoff generation, increased flood frequency, water channelization into streams and other surface water bodies, decresed agricultural land, and altered regional microclimate are the main effct of urbanization (Shuster et al., 2005; Ladson et al., 2006, and McGrane, 2016). With the right planning and placement, they can benefit the environment rather than damaging it (Laurance et al., 2009, and Balmford et al., 2012).

Assessing the implications of urban roads on climate change is critical since the outcomes of the research will likely have a substantial impact on global environmental issues for developing sustainable urban environments. Hence, this research aimed to enhance urban resilience through sustainable urban planning by developing a research-based alternative strategic approach on the theme of urban roads and further providing a recommendation to mitigate the imposed impacts.

2. Materials and methods

2.1. Area

The study area is located in Addis Ababa, ‘Arada’, and ‘Yeka’ sub-city, particularly along the route from ‘Megenagna’ diaspora light to ‘Piassa’ Jegol traffic light. It’s geographically located between 9°01'17.9"N 38°48'04.8"E and 9°01'57.4"N 38°45'14.7"E.

This study region was chosen from among other areas because it was the first fully operational corridor that could be used to thoroughly analyze the environmental impact of LST, NDVI, and NDBI. For in-depth analysis of UHII, there should be a close proximity to a rural or forest ecosystem, which provides a baseline for studying correlations with the urban corridor, Therefore, the study area has a nearby forest ecosystem, “Yeka” mountain, which makes it suitable for the research.

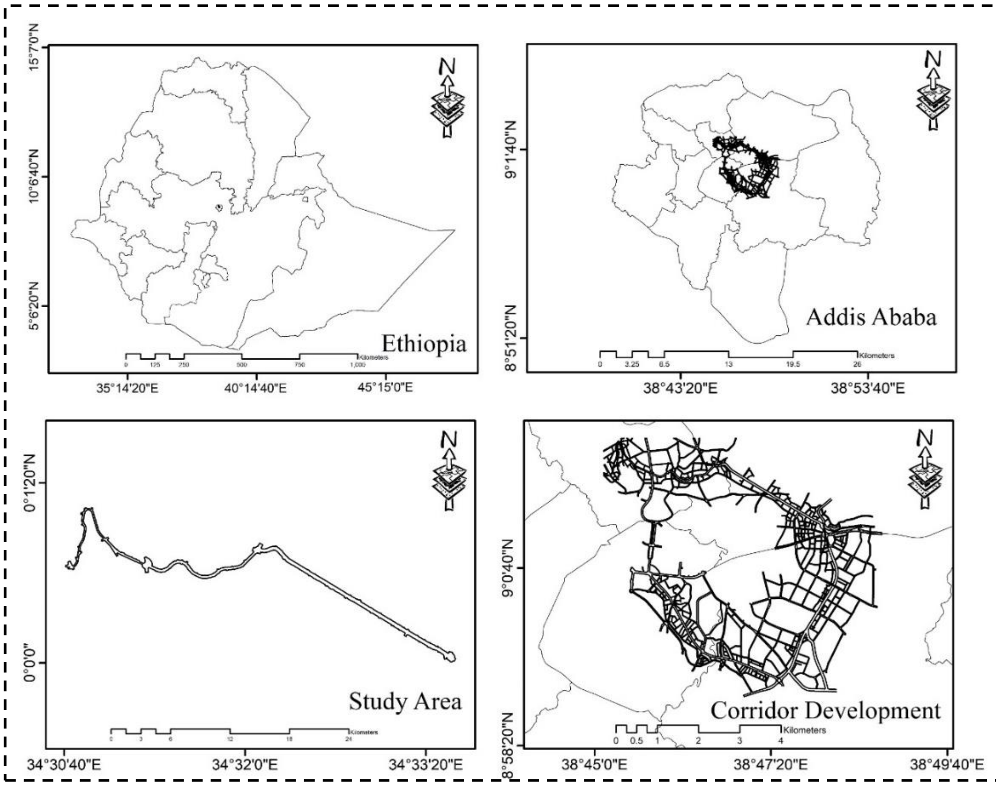

Figure 1: Location map of the study area

2.2. Type and source of data

The study utilizes both primary and secondary data sources. The primary data were gathered through direct field observation and key informant interviews with stakeholders involved in corridor development Phase I. Secondary data were remote sensing satellite images, i.e., Landsat 8, collected from USGS Earth Explorer and Google Earth Engine.

Table 1: Data source, Data set used, spatial resolution and date of Acquisition

Data Source	*Data set used*	*Spatial resolution (M)*	*Date of Acquisition*
USGS Earth explorer	Landsat 8	30	2015 (01/01/15-31/12/15)
			2020 (01/01/15-31/12/15)
			2024 (01/01/15-31/12/15)

The research's thematic focus is on resolving UHII utilizing spatial and temporal deviations; hence, GEE was employed to track baseline conditions with post-corridor development, as well as remote sensing data, and Landsat 8, imagery from the USGS.

Table 2: Remote sensing data used in the study

Remote sensing data description	*Band*	*Wavelength (πm)*	*Spectral Band resolution(m)*
LANDSAT 8 image and Thermal infrared sensor (TIRS)	Band 1 – Coastal aerosol	0.43-0.45	30
	Band 2 – Blue	0.45-0.51	
	Band 3 – Green	0.53-0.59	
	Band 4 – Red	0.64-0.67	
	Band 5 – Near Infrared (NIR)	0.85-0.88	
	Band 6 – SWIR I	1.57-1.65	
	Band 7 – SWIR II	2.11-2.29	
	Band 8 – Panchromatic	0.50-0.68	15
	Band 9 – Cirrus	1.36-1.38	30
	Band 10 – TIR I	10.60-11.19	100
	Band 11 – TIR II	11.50-12.51	

2.3. Method of data analysis

Data gathered and analyzed using a tool Global information system (GIS) is examined using a combined approach of quantitative and qualitative analysis methodologies. Additionally, analytical tools such as SPSS, Python, and Microsoft Excel have been utilized for the data analysis. Non-measurable features, particularly those associated with quality, are also given a qualitative description.

Spatial analysis

Is Utilized to investigate the demographic deviations from the geographic environment by exploring patterns, spatial distribution, and spatial relationships, including the proximity between various elements, such as built-up area, roads, vegetation, etc. Using three primary elements i.e. mathematical modeling, statistical methods, and cartographic modeling using ArcMap by inputting the gathered geospatial data.

Temporal analysis

Is used for creating an extensive timeline with multiple time points to compare the baseline, or pre-corridor development, and present, or post-corridor development, focuses on sequential trends in the temporal change in the study area over time. Various techniques, such as plotting to a histogram and change detection, are used to assess the shifts in the conditions in place. In order to analyze the changes in UHII, this technique enables comprehensive investigation to discover the sequential trends in the research region throughout time, as well as temporal patterns directly related to roads, vegetation cover, and built-up index.

The temporal analysis of LST, NDVI, and NDBI can be done using the **change detection** method where you compare LST at different time point's t1, t2, tnt_1, t_2, t_nt1, t2, tn:

$$\Delta \mathbf{LST\ (t) = LST\ (tn) - LST\ (t1)}$$

Where:

- LST (tn) is the land surface temperature at time tn,
- LST(t1) is the land surface temperature at time t1,
- ΔLST (t) is the temporal change in LST between the two times.

N.B. NDVI, and NDBI can be executed by replacing them on LST.

For computing UHII, initially we compute the temporal change in LST for both urban and rural areas:

$$\Delta \mathbf{LST\ urban(t) = LST\ urban(tn) - LST\ urban(t1)}$$

$$\Delta \mathbf{LST\ rural(t) = LST\ rural(tn) - LST\ rural(t1)}$$

Then, we will calculate the temporal change in **UHII**:

$$\Delta \mathbf{UHII\ (t) = [LST\ urban(tn) - LST\ rural(tn)] - [LST\ urban(t1) - LST\ rural(t1)]}$$

Correlation analysis

This approach is used to examine the negative and positive correlations or relationships that exist between the major variables, notably LST, NDVI, NDBI, and UHII, by analyzing how each variable relates to the one another in order to investigate trends that influence UHII and identify factors contributing to the urban heat island effect.

Correlation value ranges from 1 to -1. 1 is a perfect positive correlation, 0 is no correlation (the values don't seem linked at all), and 1 is a perfect negative correlation.

For computing the correlation analysis; the most widely used technique is Pearson's correlation coefficient (r), has the following the following equation:

$$r = \sum^{n}_{i=1} (xi - \bar{x})\ (yi - \bar{y})\ /\ \sqrt{\sum^{n}_{i=1} (xi - \bar{x})^{2} \sum^{n}_{i=1}{}^{2} (yi - \bar{y})\ 2}$$

Where: $\bar{x}$ is the mean of variable x values, and $\bar{y}$ is the mean of variable y values.

Regression analysis

The regression analysis method is utilized for computing and determining the relationship that exists between two or more variables which involves identifying and evaluating the relationship between a dependent variable and one or more independent variables, which are also called predictor or explanatory variables i.e. LST, NDVI, NDBI, and UHII.

The following equation serves as a mathematical representation of the regression model:

$$\mathbf{y} = \boldsymbol{\beta 0} \pm \boldsymbol{\beta 1}\ \boldsymbol{x 1} \pm \boldsymbol{\varepsilon 1}$$

Where:

x independent variable, y dependent variable, $\boldsymbol{n}$ Number of cases or individuals, $\beta 1$ the Slope of the regression line, $\boldsymbol{\beta 0}$ the intercept points of the regression line and the y axis.

2.4. Methodological Framework

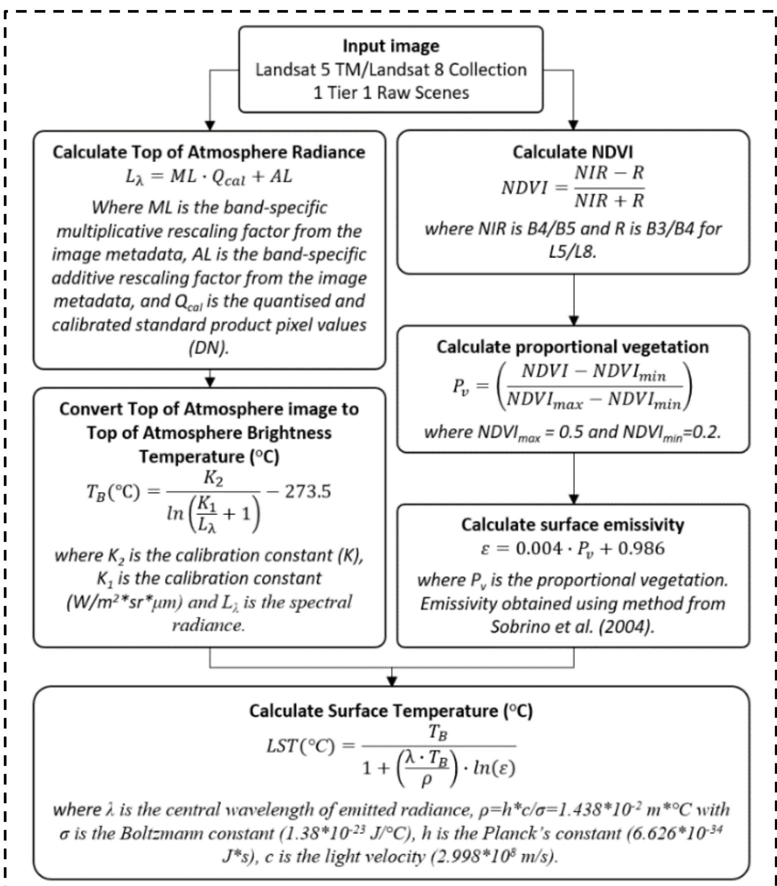

Figure 2 Methodological workflow of the study

3. Result and Discussion

3.1. Results

3.1.1. Spatial and temporal patterns in LST

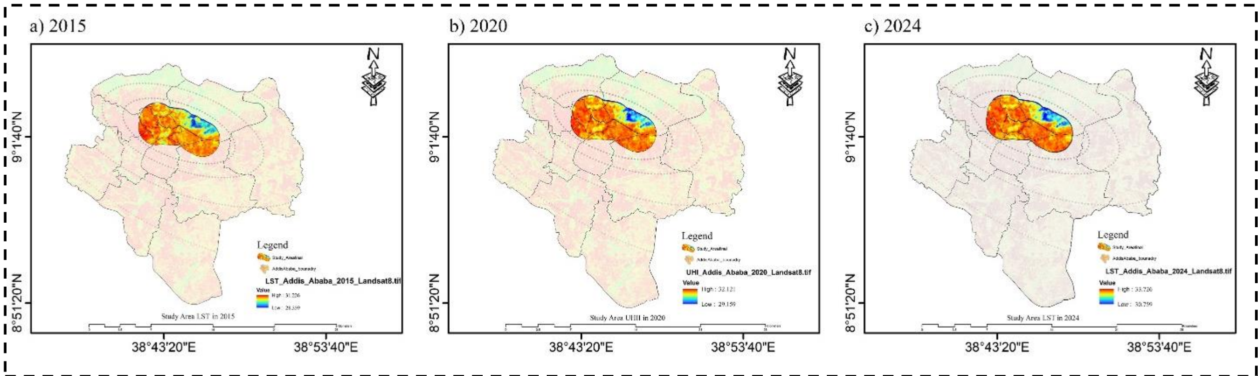

Figure 3 Study Area LST a) 2015, b) 2020, and c) 2024

By computing the average LST in 2015, 2020, and 2024 comparatively the highest annual average LST from the years is recorded in 2024. In 2020, the mean annual average LST is relatively moderate, and in 2015, the lowest mean annual average LST is recorded. Based on these results, we can identify that the LST in the study area shows an increasing trend from 2015 to 2024.

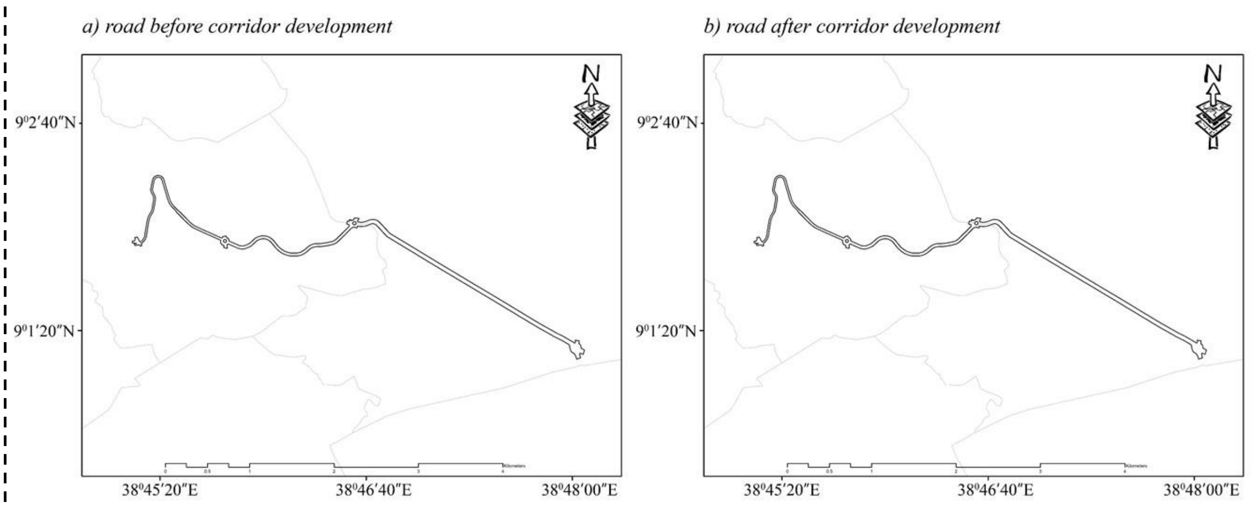

Project description	Year	Length(Km.)	Area(Sq.)	Variation
Before Corridor	2015	7.5Km	216111.149	111,447.608
After Corridor	2024		327558.757	

Figure 4 Spatial patterns on road before and after corridor Development

Due to the corridor development project in the study area region which covers a total length of 7.5Km range roadway, the core result from Figure 4 shows that there is an expansion of roads after the project implementation, mainly due to the expansion of Pedestrian Street and a new concept of bicycle lane. The total area from the baseline condition before the corridor development from the result is 216111.149 Square meters (21.61Ha) of area, which is expanded to 327558.757 Square meters (32.76Ha) (Figure 5). From the overall expansion of the road, the major parts of the expansion lie on grey infrastructure due to the expansion of vehicular roads, Pedestrian streets, and bicycle lanes.

LST result for the year 2015, examined by taking the study corridor with a two-kilometer (2KM.) buffer on every side to analyze the urban-rural comparison, shows a notable variation across different months. The lowest monthly average mean LST of 28.359^{0}C is recorded on the month June which have cooler LST during this month possibly due to seasonal weather pattern of the study area such as rainfall and cloud cover and the highest monthly average mean LST value of 31.226^{0}C is recorded on the month March which directly implies that the area is significantly warmer during this month. Furthermore, the annual average mean LST of the year was calculated to be 30.0773^{0}C °C (Figure 4).

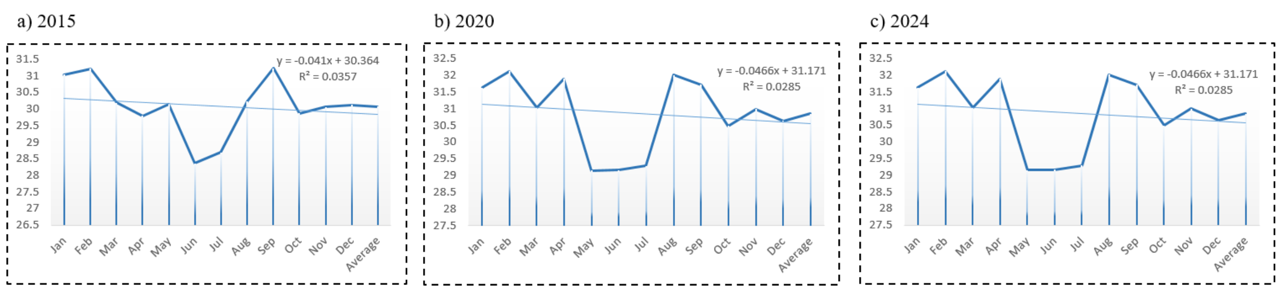

Figure 5 Temporal Trend line chart in LST of study area a) 2015, b) 2020, and c) 2024 in ^{0}C

In the year 2020 the LST calculated by taking Two two-kilometer (2KM.) buffer shows noticeable variation among the months. The average highest mean LST of 32.121^{0}C is recorded on the month February which means that the surface temperature during the month was elevated high. In contrast, the lowest mean average LST of 29.159^{0}C is recorded on the month June. The possible scenario to the decreasing factor of LST during this month could be seasonal shifts from warmer to winter months. The annual average mean LST on the year 2020 is recorded at 30.84431^{0}C which is taken as a baseline measurement before the implementation of corridor development project in the study area.

Based on the statistical analysis on the year 2024; the lowest LST is recorded on the month June with monthly average mean LST of 30.759^{0}C which indicates that the LST of the study area is the coolest of the months and the maximum LST result of 33.726^{0}C is recorded on the month May which implies that the study area experiences the highest LST on this month. The calculated mean average annual LST is 32.82467^{0}C (Figure 5).

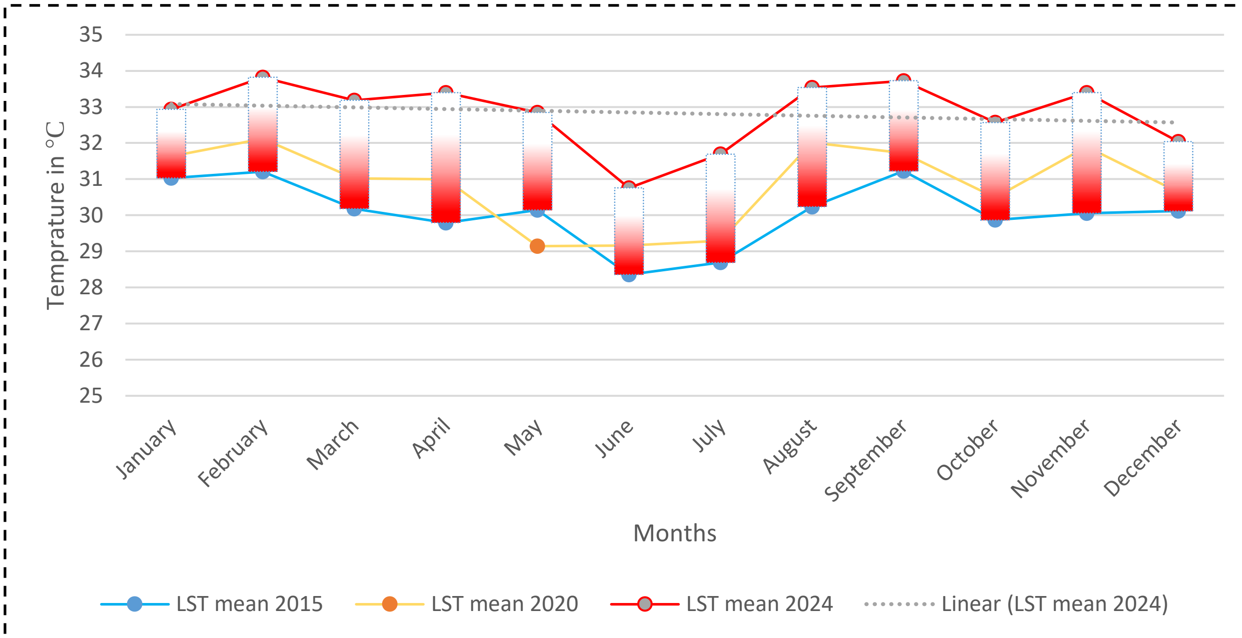

Figure 6 Temporal Trend line chart in LST of study area (2015, 2020, and 2024)

By comparing the average annual mean LST; in 2015 the mean value of 30.07733^{0}C shows the lowest than 2020 with annual average mean LST of 30.84431^{0}C with annual mean value of 0.76698^{0}C and the highest annual mean average LST recorded in 2024 with a value 32.82467^{0}C which is the highest of All. The LST annual average mean LST in 20204 shows an increasing trend with a value of 2.74734^{0}C from 2015 and 1.98036^{0}C from the result in 2020.

In general, the LST trend analyzed in the study is utilized to examine the trends of urban heat island intensity before and after corridor development in the study area. The results reveals an increasing trend over time as the results in 2024 shows significantly higher LST value than the baseline taken before corridor development on the year 2020 as well as in 2015.

3.1.2. Spatial and temporal patterns in NDVI

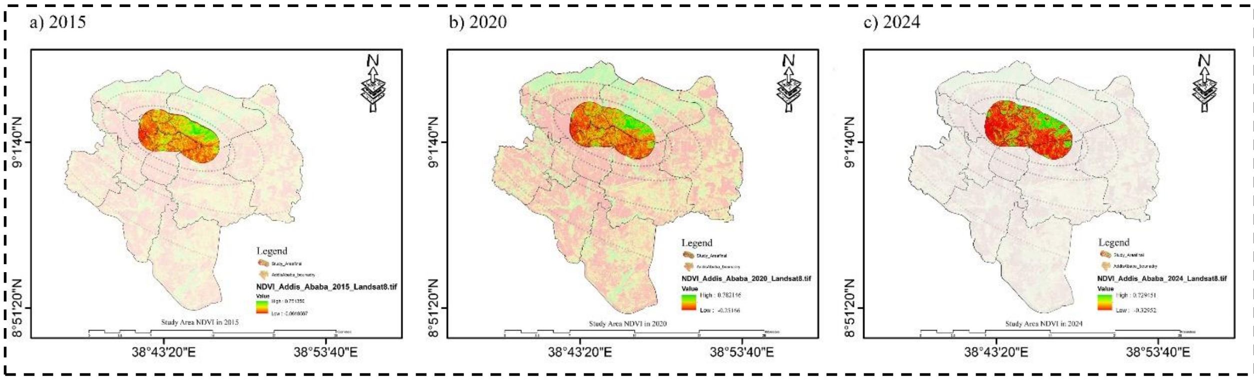

Figure 7 Study Area NDVI in a) 2015, b) 2020, and c) 2024

The result in NDVI of the year 2015 indicates various vegetation condition in the study area. The maximum NDVI value recorded is 0.751356 which signifies that there are areas having densely vegetated i.e. 'Yeka' mountain forestry taken as a 'Rural' for the comparison; as the higher recorded value is computed by exhibiting a strong reflectance in the near infrared spectrum. The mean and minimum NDVI value is 0.34475, and -0.06186 respectively (Figure 7).

The negative magnitude of the NDVI result indicates either there is a lowest amount of vegetation in some part of the study area or there are some parts having No vegetation at all i.e. Study area corridor route /Road/ which is taken as an 'Urban' for the study.

In the year 2020, the minimum annual average NDVI record value is -0.25166, the annual mean average NDVI is 0.265243, and the maximum annual average NDVI value is 0.782146 (Figure 8). From the previous 2015 result we can identify that there is a noticeable decrease on both factors which indicates that there is a decrease on the densely vegetated area as the high value on 2015 reduces on 2020 and there is a decrease in NDVI minimum annual average value which implies that there is either of urban expansion, increased impervious surfaces, increased infrastructural change, environmental degradation, or vegetation loss over the past five year period.

In 2024, the average annual minimum NDVI result is -0.32952, the annual mean average NDVI is 0.199966 and the maximum average

Annual NDVI is 0.729451 (Figure 8). While comparing this results in the year 2024 with that of 2020 which is previously considered as the data before corridor development the result shows significant reduction on both ‘rural’ the densely vegetated areas and ‘urban’ the road ways and sparsely vegetated areas of the study area.

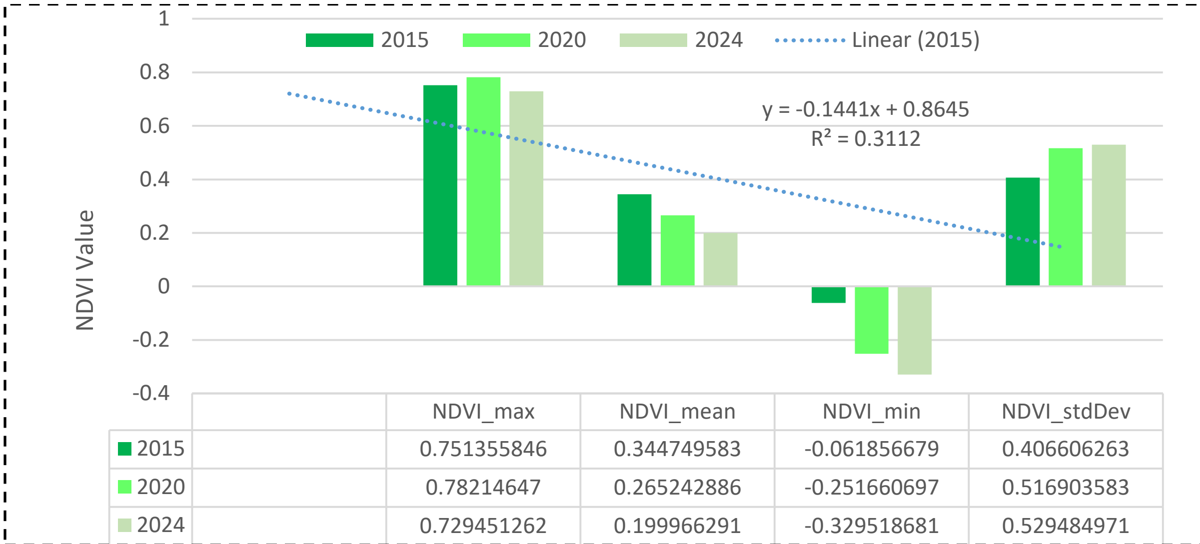

Figure 8 Temporal Trend bar chart in NDVI of Study Area (2015, 2020, and 2024)

By comparing the average minimum annual NDVI on figure 8 in the years 2015, 2020 and 2024 the recorded value is -0.06186, -0.25166, and -0.32952 respectively. The result shows an increase in the negative value of NDVI minimum value indicates that there is a reduction of vegetation over time.

The maximum NDVI annual average result in 2015 is 0.751356 which indicates there is a high vegetation density in the study area i.e. ‘Yeka’ mountain taken as a ‘Rural’ for the study comparison. In 2020 the recorded result 0.782146 shows slight improvement from 2015 but again in 2024 the value reduced to 0.729451 indicates the vegetation cover in the study area is reduced (Figure 8).

By investigating the activities in the study area the main reason for the increase in vegetation cover around 2020 is the conservation effort in the period and mainly the green initiative at that time. In the results of 2024 the potentials reasons for the decreasing of vegetation cover is mainly related to anthropogenic activity in the area including environmental impact due to infrastructure development including urban road expansion on the corridor development. In general, the overall results from NDVI shows a noticeable decrease over time which implies that there is a reduction in vegetation cover in the study area.

3.1.3. Spatial and temporal patterns in NDBI

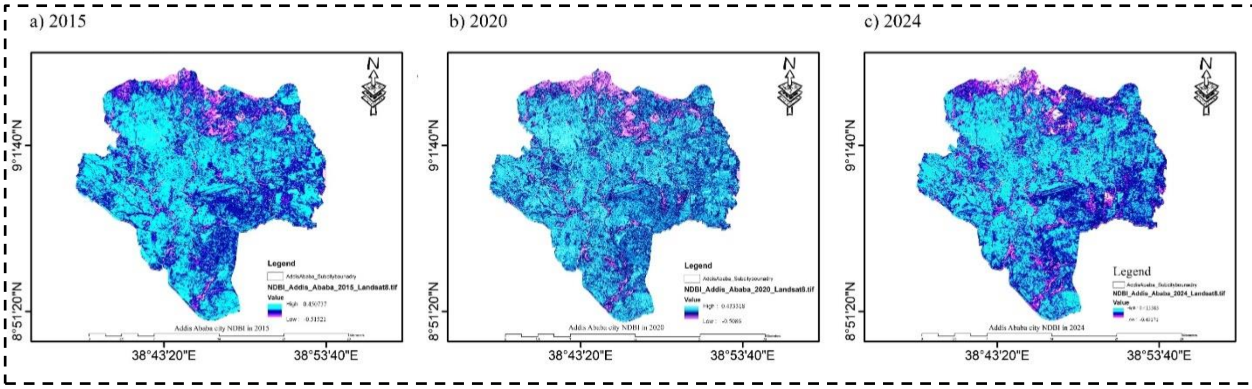

Figure 9 Study Area NDBI in a) 2015, b) 2020, and c) 2024

Based on the results of NDBI, the study area clearly shows that the trends of built-up index on 2015 was relatively moderate and in 2020 the built-up value shows an increasing effect which implies that the area is exhibiting urban expansion, in 2024 this value extensively increase along the road way which means that built-up areas in the study area are showing increasing effect and the green spaces are reduced as investigated by an in depth analysis which clearly indicates there is an increasing trend in NDBI over time.

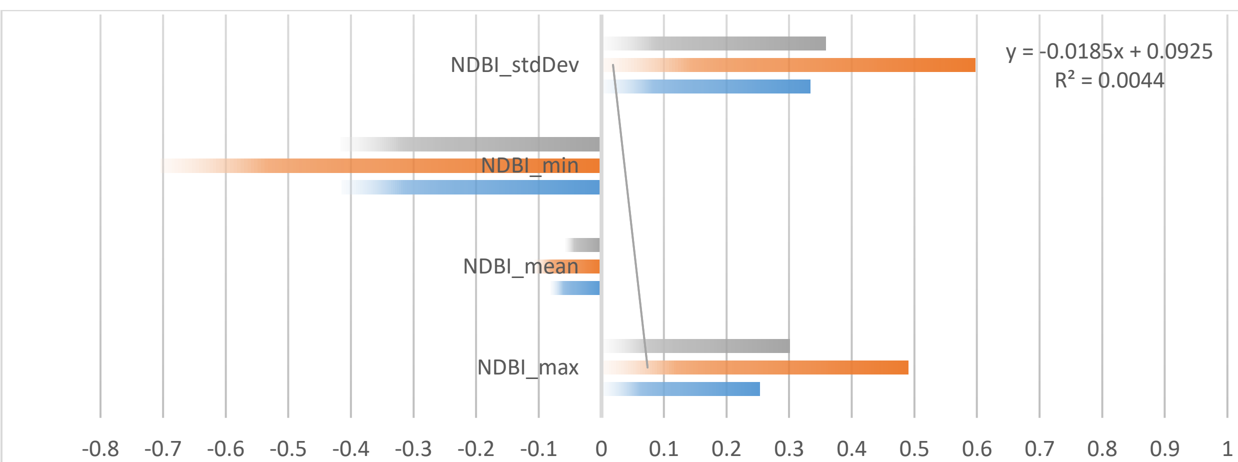

	NDBI_max	NDBI_mean	NDBI_min	NDBI_stdDev
2024	0.300674136	-0.057856068	-0.416386272	0.358530204
2020	0.490156865	-0.106862001	-0.703880866	0.597018866
2015	0.253229775	-0.080812888	-0.41485555	0.334042662

NDVI VALUE

2024 2020 2015 Linear (2024) Linear (2024)

Figure 10 Temporal Trend bar chart in NDBI of Study Area (2015, 2020, and 2024)

The results of NDBI in 2015 indicates that there is a high built-up density compared to other years in the study. The average annual maximum built-up index value is 0.25323 which indicates the concentrated built-up areas including infrastructure, roads, and buildings. The average minimum NDBI value is -0.41486 which shows that there is a densely vegetated area i.e. ‘Yeka’ mountain given that green spaces have weak reflectance in the near infrared spectrum (Figure 10).

In 2020 the average annual maximum NDBI recorded 0.490157 which have significant increase from 2015 which clearly indicates there is a high built-up area expansion on the period. The average annual minimum NDBI value is -0.70388 (Figure 10).

In 2024, the minimum annual average NDBI value is -0.41639 shows that there are green spaces with low built-up density specifically ‘Yeka’ mountain which is taken as a ‘Rural’ for comparison and the maximum annual average NDBI value is 0.300674 which indicates the roads, buildings and other impervious surfaces which are taken as an ‘urban’ for the study (Figure 10).

3.1.4. Combined result of variations on UHIE

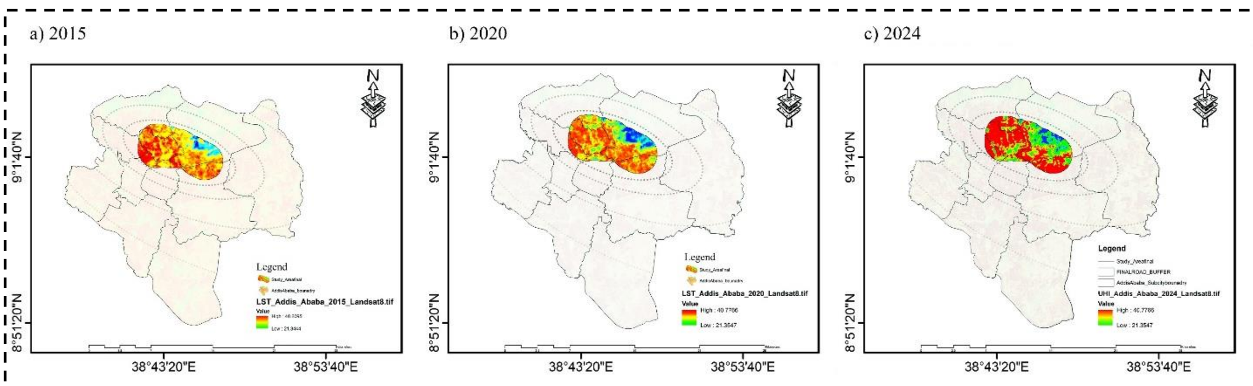

Figure 11 Study Area UHII in a) 2015, b) 2020, and c) 2024

Based on the combined results in 2015 from LST, NDBI and NDVI, the UHII for 2015 is analyzed within the study area by taking an area of Two kilometers (2KM.) buffer from ‘Megenagna’ to ‘Piassa’ corridor road.

The average annual minimum UHII value is -0.6951 with a negative value which indicates that the vegetation cover in the area majorly ‘Yeka’ mountain taken as a ‘rural’ counter balanced the urban heat generated from the built-up areas mainly the road from ‘Megenagna’ to ‘Piassa’ taken as an ‘Urban’ for comparison. The average annual maximum UHII value is 0.201162 which indicates the

‘Urban’ areas i.e. road from ‘Megenagna’ to ‘Piassa’ in the study region have relatively higher temperature as compared to the surrounding ‘Rural’ area i.e. ‘Yeka’ mountain (Figure 11).

The average annual maximum UHII value in 2020 is 0.217746 which means that the ‘Urban’ areas in the study region is experiencing substantial urban heat than their surrounding ‘Rural’ area mainly the densely vegetated area ‘Yeka’ mountain. In this year, the average annual minimum UHII value is -0.73206 which indicates that the densely vegetated area i.e. ‘Yeka’ mountain and other green infrastructure in the study area counter balanced the urban heat generated from the built-up areas (Figure 11).

In the year 2024, the annual average minimum UHII value recorded is -0.79431 which means that the vegetation cover in the study area including the densely vegetated ‘Yeka’ mountain counter balanced the urban heat generated from the built-up areas. The average annual maximum UHII value recorded in the year is 0.2476 which implies that the ‘Urban’ areas in the study region is experiencing substantially higher temperature as compared to the surrounding ‘Rural’ area majorly ‘Yeka’ mountain.

Based on the above results in the study from the years 2015, 2020, and 2024, it is justified that the urban the temporal trends of UHII on the study areas clearly shows an increasing trend over time. The major finding of this result intensifies the UHIE is increasing which means that urban areas in the study region i.e. ‘Megenagna’ to ‘Piassa’ road is experiencing warmer temperature as compared to the surrounding ‘Rural’ areas majorly the densely vegetated ‘Yeka’ mountain.

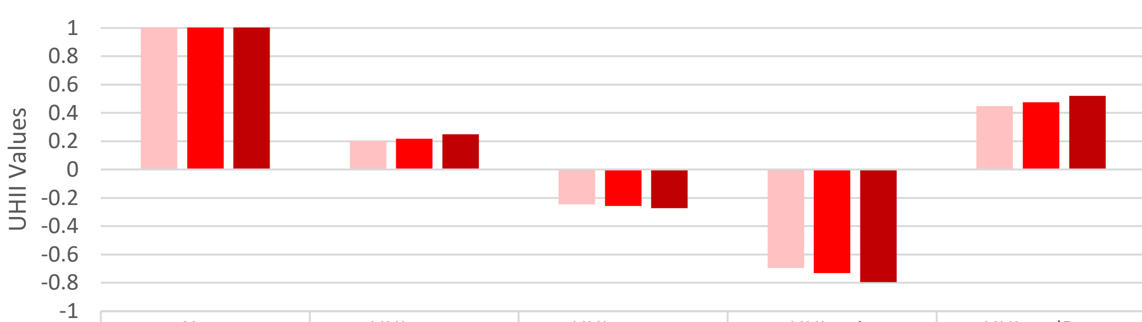

	Year	UHI_max	UHI_mean	UHI_min	UHI_stdDev
2015	2015	0.201162	-0.246969	-0.6951	0.448131
2020	2020	0.217746	-0.257157	-0.73206	0.474903
2024	2024	0.2476	-0.273355	-0.79431	0.520955

2015 2020 2024

Figure 12 Temporal Trend bar chart in UHII of study area (2015, 2020, and 2024)

From the result on figure 4.21 the most negative UHII mean value from the three years is recorded in 2015 with value of -0.246969 which indicates the least UHII with relatively high cooling effect, in 2020 the recorded value increased to -0.257157 which indicates moderate UHII and the least negative value recorded is in the year 2024 with the value -0.273355 which indicates relatively Higher UHII than the result in 2020 as well as 2015.

By analyzing the results of the annual average mean UHII value, the UHII value is showing a consistent increase over time. The shifts in the temporal trend of UHII shows the growing impacts of the corridor development i.e. anthropogenic intervention as it encompasses urban expansion and urbanization for the execution of the project, on the micro climate of the road side taken as an 'Urban' area for the study which emphasizes the need for incorporating mitigating strategies including sustainable urban planning strategies to mitigate the UHIE in the study area.

3.2 Discussions

3.2.1. LST Dynamics

Urban settings are dominating over green and open spaces which results increasing UHIE in different areas of the city which is making the city warmer (Mathias et al., 2016). There are various contributing factors for this phenomena mainly driven by city wise rapid urbanization and urban expansion which leads to an increase in road infrastructure including pedestrian, bicycle lane, and impervious surfaces which absorb more heat than greeneries.

The LST on the study area i.e. corridor development road from 'Megenagna' to 'Piassa' route shows an increasing trend over time (Figure 5). The LST is computed by taking the 'Yeka' mountain and other vegetation cover mainly on road side with a catchment area of Two kilometer buffer (2Km.) as a 'Rural' and the road as an 'Urban' results that the urban areas are experiencing relatively higher LST than the 'rural'.

Before the corridor development, the study area's total road coverage was 216111.149 square meters (21.61 hectares) and it was increased to 327558.757 square meters (32.76 hectares) following the corridor development. The majority of the expansion is on grey infrastructure because of the expansion of the bicycle lane, Pedestrian Street, and vehicle road. Based on previous researchers finding, there was a substantial positive linear correlation among impervious surface and LST; a 10%

increase in imperviousness might result in around 3.3°C increase in land surface temperature when the impervious surface eventually accounts for more than seventy percent /70%/ of the land (Xu et al. in 2013,). An expansion in urban areas could raise LST by approximately 1.9–5.4 ^{0}C and the urban air temperature around 0.75–2.80 ^{0}C (Imran et al., 2019), which implies that an increase in the study areas road coverage with over fifty percent /50%/ ratio will increase the areas LST evidentially on a high rate.

The primary contributing factor of urban heat islands in cities is a rise in LST (Qaid et al., 2016; Vasenev et al., 2021). Due to anthropogenic activities and alteration on the natural environment leads to increasing UHIE as Infrastructures including roads, buildings, pedestrians, and other constructions minimizes urban vegetation cover (siti et al., 2013).

According to the study area LST result; the ‘Rural’ i.e. vegetation cover including street side greeneries relatively balanced the ‘Urban’ i.e. Buildings, roads, and other infrastructures area heat by provisioning cooling effect mainly through balancing Incoming solar energy from sun light and outgoing radiation from surfaces to the environment to manage excessive heating by regulating temperature (Ries, 2002 and Baccini et al., 2008).

Land surface temperature have an extensive impact on micro climate change and vegetation growth (Shahid, 2014) impact the surrounding area livelihood and road side activities including walking.

Urban built-up areas expansion which incorporates urban road expansion results decline of vegetation cover which contributes to an increases in LST and intensifies UHI (Warkaye et al., 2018 and Teferi et al., 2017). Because green spaces absorb heat mostly during the dry season, which lowers LST, reducing them due to urban growth will have a major detrimental impact on the environment (Samson et al., 2018).

Material selection in urban infrastructure plays a crucial role in mitigating UHIE (Voogt et al., 2003), as the main causes of UHIE is the high heat absorbing characters of pavements, concrete structures, and other various impervious surfaces by rising surface temperature in urban areas which leads to as increase in UHIE of the area. Higher albedo clearly lowers pavement surface temperatures, (Yang et al., 2015).

3.2.2. NDVI Dynamics

The most popular technique for analyzing the amount of vegetative coverage in an area using remote sensing images is the NDVI (Angadi et al., 2020, and Ghosh et al., 2020). In remote sensing, NDVI is a useful measure of vegetation cover (Mackey et al., 2012).

According to Figure 8 NDVI result, the average minimum annual NDVI for 2015, 2020, and 2024 is -0.06186, -0.25166, and -0.32952, respectively. The outcome demonstrates a decrease in vegetation over time. This decreasing trend in urban green spaces impacts the study areas UHIE as these green spaces have better cooling effect (Kong et al., 2014).

Land cover in urban environment plays significant role in providing ecosystem services (Bradley, 1995, and Bastian et al., 2002), including regulating service by controlling local temperature through absorbing and storing carbon dioxide majorly by vegetation cover; therefore decreasing trend in NDVI (Figure 8), showing a reduction in green coverage which implies vegetation cover in the area is incapable of provisioning ecosystem.

Change in Land use Land cover (LULC) by the conversion of green spaces in to impermeable surfaces have evolved extensive environmental problems including UHIE (Weng et al., 2001). As vegetation cover helps to mitigate UHIE through process such as evapotranspiration and cooling the environment through shading, enhancement of green coverage by fostering sustainable green infrastructure should be prioritized to enhance green coverage on the study area. Having a linear correlation, a ten percent (10%) increase of vegetation coverage would cool the air 0.23 C (Wong et al., 2005)

The ecology will be significantly impacted since vegetative cover is replaced by impermeable surfaces. An Increase in impervious surface i.e. asphalt roads, concrete pedestrian… etc. will linearly increase the LST in the area, while green infrastructures decreases it (Dai et al., 2019, and Li et al., 2016); areas with more green infrastructure shows less tendency of having highest LST.

According to Kong el al., in 2014; urban green areas including densely vegetated areas, street side green areas, green open spaces… etc. have a better cooling effect than urban water bodies (Kong et al., 2014) due to several reason mainly by the process of evapotranspiration as which they release moisture in to the air that will minimize the surface temperature and providing shading that can minimize the direct contact of sunlight to surface by absorbing solar radiation.

Changes in LULC primarily impacts the surface temperature of the urban area and its surrounding environments by replacing vegetated areas and open spaces with impermeable surfaces (Balew et al., 2020, and Sisay et al., 2019) by exposing the urban areas for direct solar radiation which increases the Surface urban heat island (SUHI). Therefore the decreasing trends in NDVI of the study area that means the loss of vegetation cover in the area will increase SUHI along the road side corridor which will have direct impact on walkability.

3.2.3. NDBI dynamics

NDBI algorithm is to detect changes over time in built-up environment by analyzing the built-up area using the NIR and Red bands (Varshney, 2013, and Xu, 2007). The findings of NDBI trend shows an increase from 2015 to 2020 with an implication of elevated built-up areas through urban expansion, surprisingly, this result shows a unexpected gradual decrease from 2020 to 2024 (Figure 9) due to the major reason investigated through historical imagery over time on the areas that low rise dense residences were demolished by corridor development project on road sides including buildings without proper setbacks and the other for ‘Chaka’ project expansion.

Based on this the result shows from 2015 to 2020 shows that there is a reduction in the mean NDBI value from -0.0808 to -0.1069 which suggests that there is a reduction in Built-up area. Through further investigation in the area through field observation and compiling the results with key informant’s information the mean result from NDBI is from the increased vegetation from the government initiative in the period. From the year 2020 to 2024 the mean NDBI result shows a noticeable increase which indicates there is a rise in built-up area which is directly linked mainly to the urban road expansion as it’s one of the major components in the study.

Based on the spatial scope of the study the expansion on the road i.e. ‘Megenagna’ to ‘Piassa’ road; which leads an increase in Built-up density and impervious surfaces alters urban landscapes to have a faster absorption rate and smaller thermal capacity (Bornstein, 1968; Rosenfeld et al., 1995; and Song, 2004) which will increase the LST and linearly elevates UHIE in the area.

LULC changes induced on by rapid urbanization are one of the biggest environmental concerns (Weng and Lo 2001 and Regassa et al. 2020) as the changes in LULC mainly related to expansion of built-up areas which directly alters the natural environment which increase the areas vulnerability to environmental issues such as increase in LST and increase in SUHI.

The study area NDBI result, which was computed by comparing the road before and after corridor development, primarily focuses on the road's extension from "Megenagna" to "Piassa" as a result of the corridor development, which intends to establish a new bicycle lane and extend the pedestrian line. According to field observation findings, a concrete pavement technology was used to create the bike and pedestrian lanes. Lighter-colored aggregates and cement binders can further cool concrete pavements, since studies of particularly lightened concrete have demonstrated solar reflectance levels of up to Eighty percent /80%/ (Levinson in 2001).

Additionally, various studies have explored strategies to enhance concrete pavement performance. Concrete pavement can be renovated by using a technique called white topping which uses fiber reinforcement to strengthen the pavement, keeping additional layers thinner and reducing the curing time (Lisa, 2008, and Hurd, 1997).

The enhancement of concrete pavements is significant due to their higher solar reflectance compared to conventional asphalt pavements. The concrete pavement with Forty five percent (45%) solar reflectance which is higher than asphalt pavement have ten percent (10%) solar reflectance (Lisa, 2008).

Various Previous studies on UHI have concentrated on assessing the relationship between LST and land cover composition (Chen et al., 2014; and Weng et al., 2004) this implication and the result from studies indicates that an increase in NDBI which is an effective indicator on identifying impervious surfaces in an area increases the Built-up land cover substantially rises the UHII.

3.2.4. UHI Dynamics

The finding of the research shows that the lowest UHII was recorded in 2015 with a value of -0.246969; increased to -0.257157 in 2020; and by 2024, the value of -0.273355 rises drastically, indicating a comparatively higher UHII than the previous years. This result should be seriously considered, as UHI adversely affect population health and intensify the effects of heatwaves, which have resulted in illnesses and death worldwide (Li et al., 2013 and Stone, 2012).

As the result on NDVI shows a continuously decreasing trend (Figure 4.11); Investigating the impact of UHI and SUHI, Using remote sensing to track shifts in LULC types and patterns of landscape provides essential information for the evaluation and analysis of SUHI (Korme et al., 2019) to statistically analyze the shifts mainly in NDVI as Vegetation cover is the main driving factor of UHI (Deliami et al., 2018).

By understanding the relationship specifically the correlation and regression between LST, NDVI, and NDBI (Isufi et al., 2021); the observed increasing dynamics in LST of the study area over time that have a strong linear correlation with NDBI with an increased value, and decreasing trend in NDVI implies that the area is experiencing an increasing trend on the aspects of UHIE.

4. Conclusion

UHII is a critical phenomenon extensively influenced by factors specifically LST, NDVI, and NDBI which shows the variations through interaction among the natural landscape and urban environment. The major finding of the research illustrated that the substantial increase in the UHII of the study area resulted from an intensification of built-up areas and reduction in amount and density of vegetation cover, which leads an upward trend in LST which linearly increases the UHII.

The finding of the research on the Primary objective on LST shows a noticeable change over time with an increasing trend on NDBI resulted mainly from expansion in impervious surfaces and decrease in NDVI due to a decrease in vegetation cover which minimizes the shading purposes to the impervious surfaces that will minimize the solar radiation and reduces the evapotranspiration that contributes to the substantial increase in UHII which reflects the root causes and impacts of urbanization and urban expansion on the environment which will have substantial implication on the urban resilience, environmental sustainability which gradually affects public health.

On the investigation aimed to attain the second objective on NDVI shows downward trend which have a linearly negative correlation with UHII implies an extensive increasing trend on LST. Additionally, reduction on vegetation cover will impact the thermal dynamics of urban areas by increasing their vulnerability to heat retention which results increase in LST which increases the susceptibility of the areas to higher UHII. Therefore enhancing green infrastructure with a proper scientific based approach considering various environmental factors and their purpose i.e. Shading, ornamental, perennial vegetation’s can mitigate UHII.

From the results of NDBI based on the third objective of the study, the extensive increasing trend in NDBI value that is negatively correlated with LST increases UHII. This increasing trend in NDBI is resulted from the road expansion due to corridor development that leads an increase in the impervious surfaces by altering the natural environment. This rise in UHII suggests an inclusive urban planning strategies for balancing both the urban environment and natural landscape to sustainable urban environment.

By utilizing remote sensing data, the research emphasized the interconnection among the main factors of UHII i.e. LST, NDVI and NDBI, to insight the major finding of this research resulted from combined impacts of reducing vegetation cover and rise in built-up area density implying an elevated UHII along roadway from ‘Megenagna’ to ‘Piassa’ corridor development which implies urban area expansion specifically road expansion including pedestrian and Bike lane leads to micro climate change by exposing higher thermal retention and increase in LST which simultaneously rises UHI.

As the study utilizes remote sensing, google earth engine, and geographic information system (GIS) it enhances how this systems can be effectively used for analyzing the spatial and temporal dynamics of urban areas UHII by investigating the LST, NDVI, and NDBI through the variation in vegetation cover and built-up density which will influence the surface temperature linearly with UHII.

Priority should be given to climate adaptive urban green strategy for provisioning the most efficient and effective species type that can regulate micro temperature by reducing the surface temperature in the area by cooling the environment, encouraging natural ecosystem preservation and conservation mechanism, promoting permeable pavement, and enhancing blue green infrastructure through adaptive urban planning strategies should be promoted to ensure sustainable and resilient urban environment by integrating the natural ecosystem with the urban environment and Nature-based solution with purpose-based plantation should be enhanced like shaded plants that reduce direct solar radiation.

Policy makers are expected to propose and implement a proactive inclusive policies, rules and enforcing regulations to minimize the adverse impacts of UHII on the environment to achieve sustainable resilient environment in urban areas. Future studies should explore in depth analysis through adaptive advanced approaches by integrating satellite imagery data with the Baseline situation (ground truth) for the accuracy and spatially detailed result to develop effective mitigation strategy.

Reference

Addis Ababa city roads authority (AACRA). The preparatory survey report for the project for upgrading road maintenance equipment in Addis Ababa city. 2019

Alfraihat, R., Mulugeta, G., & Gala, T.S. (2016). Ecological evaluation of urban heat island in Chicago City, USA. Journal of Atmospheric Pollution, 4(1), 23–29.

Baccini, M.; Biggeri, A.; Accetta, G.; Kosatsky, T.; Katsouyanni, K.; Analitis, A.; Anderson, H.R.; Bisanti, L.; D'Ippoliti, D.; Danova, J.; Forsberg, B.; Medina, S; Paldy, A.; Rabczenko, D.; Chindler, C. and Michelozzi, P. 2008. Heat effects on mortality in 15 European cities. Epidemiology 19:711-719. doi: 10.1097/EDE.0b013e318176bfcd.

Balew, A., & Korme, T. (2020). Monitoring land surface temperature in Bahir Dar City and its sur rounding using Landsat images. The Egyptian Journal of Remote Sensing and Space Science, 23, 371–386. https://doi.org/10.1016/j.ejrs.2020.02.001.

Balmford, A., Green, R. & Phalan, B. Proc. R. Soc. B 279, 2714–2724 (2012).

Bornstein, R. D. (1968). Observations of the urban heat island effect in New York City. Journal of Applied Meteorology, 7,575e582.

Bradley, G.A. 1995. Urban Forestry Landscapes: Integrating Multi-disciplinary Perspectives. Seattle: University of Washington Press. Washington. 111 pages.

Dai, Z., Guldmann, J.M. and Hu, Y., 2019. Thermal impacts of greenery, water, and impervious structures in Beijing’s Olympic area: A spatial regression approach. Ecological Indicators, 97, pp.77-88.

Deilami, K.; Kamruzzaman, M.; Liu, Y. Urban heat island effect: A systematic review of spatio-temporal factors, data, methods, and mitigation measures. Int. J. Appl. Earth Obs. Geoinf. 2018, 67, 30–42.

F. Chen, X. Yang, W. Zhu, 2014, WRF simulations of urban heat island under hot-weather synoptic conditions: The case study of Hangzhou City, China, Atmospheric Research, Vol. 138, Pages 364-377, ISSN 0169-8095, https://doi.org/10.1016/j.atmosres.2013.12.005.

Hurd, M.K. (1997) ‘Ultra-thin whitetopping’. Concrete Construction February

Imran, H.M.; Kala, J.; Ng, A.W.M.; Muthukumaran, S. Impacts of future urban expansion on urban heat island effects during heatwave events in the city of Melbourne in southeast Australia. Q. J. R. Meteorol. Soc. 2019, 145, 2586–2602.

Isufi, Florim & Berila, Albert & Bulliqi, Shpejtim. (2021). Measuring UHI using Landsat 8 OLI and TIRS data with NDVI and NDBI in Municipality of Prishtina. Disaster Advances. 14. 25-36. 10.25303/1411da2536.

Kong, F., Yin, H., James, P., Hutyra, L. R., & He, H. S. (2014). Effects of spatial pattern of greenspace on urban cooling in a large metropolitan area of eastern China. Landscape and Urban Planning, 128,35e47.

Ladson AR, Walsh CJ, Fletcher TD (2006) Improving stream health in urban areas by reducing runoff frequency from impervious surfaces. Australasian J Water Resour 10(1): 23-33.

Landsberg, H. E. (1981) the Urban Climate. New York, NY,Academic Press

Laurance, W. F., Goosem, M. & Laurance, S. G. W. Trends Ecol. Evol. 24, 659–669 (2009)

Levinson, R. and H.Akbari (2001) Effects of Composition and Exposure on the Solar Reflectance of Portland Cement Concrete. Berkeley, CA, Lawrence Berkeley National Laboratory: 51

Li, D., & Bou-Zeid, E. (2013). Synergistic interactions between urban heat islands and heat waves: The impact in cities is larger than the sum of its parts. Journal of Applied Meteorology and Climatology, 52, 2051–2064.

Lisa gartland, 2008. Heat islands: understanding and mitigating heat in urban areas

Liu, Q.; Xie, M.; Wu, R.; Xue, Q.; Chen, B.; Li, Z.; Li, X., (2021). From expanding areas to stable areas: Identification, classification and determinants of multiple frequency urban heat islands. Ecol. Indic., 130: 108046.

Li, X., Li, W., Middel, A., Harlan, S.L., Brazel, A.J. and Turner Ii, B.L., 2016. Remote sensing of the surface urban heat island and land architecture in Phoenix, Arizona: Combined effects of land composition and configuration and cadastral-demographic-economic factors. Remote Sensing of Environment, 174, pp.233-243.

Longley, Paul A., Kassa, Michael F. Goodchild, David J. Maguire, and David W. Rhind. 2015. Geographic Information Science and Systems. New York, NY: Wiley

Lütz, M. and Bastian, O. 2002. Implementation of landscape planning and nature conservation in the agricultural landscape-A case study from Saxony. Agriculture, Ecosystems and Environment 92(2–3): 159–170.

Mackey, C. W., Lee, X., & Smith, R. B. (2012). Remotely sensing the cooling effects of city scale efforts to reduce urban heat island. Building and Environment, 49, 348e358.

Mathias T. and Tebarek L., 2016. The city of Addis Ababa from 'forest city' to 'urban heat island': assessment of urban green space dynamics v.10, n.2, p.254-262

McGrane SJ (2016) Impacts of urbanisation on hydrological and water quality dynamics, and urban water management: A review. Hydrol Sci J 61(13): 2295-2311.Millard-Ball, A., 2022. The width and value of residential atreets. J. Am. Plan. Assoc. 88 (1), 30-43

Md Shahid, L. 2014. Land Surface Temperature Retrieval of Landsat 8 Data Using Split Window Algorithm- A Case Study of Ranchi District. International Journal of Engineering Development and Research 2 (4): 3840 3849.

Qaid, A., Lamit, H. B., Ossen, D. R., & Shahminan, R. N. R. (2016). Urban heat island and thermal comfort conditions at micro-climate scale in a tropical planned city. Energy and Buildings, 133, 577–595.

Regassa B, Kassaw M, Bagyaraj M (2020) Analysis of urban expan sion and modeling of LULC changes using geospatial techniques: the case of Adama City. Remote Sensing of Land, 4(1-2):40 58. https://doi.org/10.21523/gcj1.20040104

Ries, C.; Pillmann, W.; Kellner, K. and Stadler, P. 2002. Urban Green Space Management Information -Processing and Use of Remote Sensing Images and Scanner Data. Proceedings of Environmental Informatics 2002, Part 1: 503 510.

Rosenfeld, A. H., Akbari, H., Bretz, S., Fishman, B. L., Kurn, D. M., Sailor, D., et al. (1995). Mitigation of urban heat islands: Materials, utility programs, updates. Energy and Buildings, 22, 255e265.

Saghir, J., & Santoro, J. (2018). Urbanisation in Sub-Saharan Africa: Meeting Challenges by Bridging Stakeholders Center for Strategic and International Studies (CSIS). https://www.csis.org/analysis/urbanization-sub-saharan-africa

Samson w., K.V. Suryabhagavan and B. Satishkumar, 2018. Urban green areas to mitigate urban heat island effect: the case of Addis Ababa, Ethiopia 44 (4): 353-367, ISSN: 2320-5199

S. Das, D.P. Angadi, Land use-land cover (LULC) transformation and its relation with land surface temperature changes: a case study of Barrackpore Subdivision, West Bengal, India, Remote Sens. Appl.: Soc. Environ. 19 (2020 Aug 1) 100322.

Shuster WD, Bonta J, Thurston H, Warnemuende E, Smith DR (2005) Impacts of impervious surface on watershed hydrology: A review. Urban Water J 2(4): 263-275.

Sisay, D. C., Korme, T., & oda, . (2019). Understanding land surface temperature on rift areas to examine the spatial variation of urban heat island: the case of Hawassa, southern Ethiopia. GeoJournal. https://doi.org/ 10.1007/s10708-019-10110-5.

Siti, N.; Afzan, B.; Naim, W.M. and Alamah, M. 2013. Green Spaces Growth Impact on the Urban Microclimate. Procedia–Social and Behavioral Sciences 105: 547 557.

Song, Y. B. (2004). Influence of new town development on the urban heat island-the case of the Bundang area. Journal of Environmental Sciences (China), 17,641e645.

Stone, B., Jr (2012). The city and the coming climate: Climate change in the places we live. Cambridge University Press

Teferi, E., & Abraha, H. (2017). Urban heat island effect of Addis Ababa City: Implications of urban green spaces for climate change adaptation. In Climate change adaptation in Africa (pp. 539–552). Springer, Cham.

Varshney, A. 2013. Improved NDBI differencing algorithm for built up regions change detection from remote-sensing data: An automated approach. Remote Sensing Letters 4 (5): 504-512.

Vasenev, V., Varentsov, M., Konstantinov, P., Romzaykina, O., Kanareykina, I., Dvornikov, Y., & Manukyan, V. (2021). Projecting urban heat island effect on the spatial-temporal variation of microbial respiration in urban soils of Moscow megalopolis. Science of the Total Environment, 786, 147457.

Voogt, J.A. and Oke, T.R. 2003. Thermal remote sensing of urban climates. Remote Sensing of Environment 86: 370–384.

Warkaye, S., Suryabhagwan, K., & Satishkumar, B. S. E. (2018). Urban green areas to mitigate urban heat island effect: The case of Addis Ababa. Ethiopia International Journal of Ecology, 44, 353–367.

Weng, Q., & Lo, C. P. (2001). Spatial analysis of urban growth impacts on vegetative greenness with Landsat TM data. Geocarto International, 16(4), 17–25.

Weng, Q.; Dengsheng, Lu. and Schubring, J. 2004. Estimation of land surface temperature–vegetation abundance relationship for urban heat island studies. Remote Sensing of Environment 89: 467–483.

Wong, N. H., & Yu, C. (2005). Study of green areas and urban heat island in a tropical city. Habitat International, 29,547e558.

Xu, Hanqiu; Lin, Dongfeng; Tang, Fei, The impact of impervious surface development on land surface temperature in a subtropical city: Xiamen, China. International Journal of Climatology, 2013, Vol 33, Issue 8, p1873 ISSN 0899-8418 10.1002/joc.3554

Yang, J., Wang, Z-H., Kaloush, K.E., 2015. Environmental impacts of reflective materials: Is high albedo a ‘silver bullet’ for mitigating urban heat island ?. Renew. Sust. Energ. Rev. 47 (0), 830 – 843.

Xu, H. 2007. Extraction of urban built-up land features from Landsat imagery using a Thematic-oriented Index Combination technique. Photogrammetric Engineering & Remote Sensing 73 (12): 1381–1391.

Z. Dai, J. Guldmann, Y. Hu, 2019, Thermal impacts of greenery, water, and impervious structures in Beijing’s Olympic area: A spatial regression approach, Ecological Indicators, Vol. 97, Pages 77-88, ISSN 1470-160X, https://doi.org/10.1016/j.ecolind.2018.09.041.

Zhang, D.-L., Y.-X. Shou, and R. R. Dickerson, 2009: Upstream urbanization exacerbates urban heat island effects. Geophys. Res. Lett., 36, L24401, doi:10.1029/200

Annex 2 *Corridor development roads and Study Area Road*

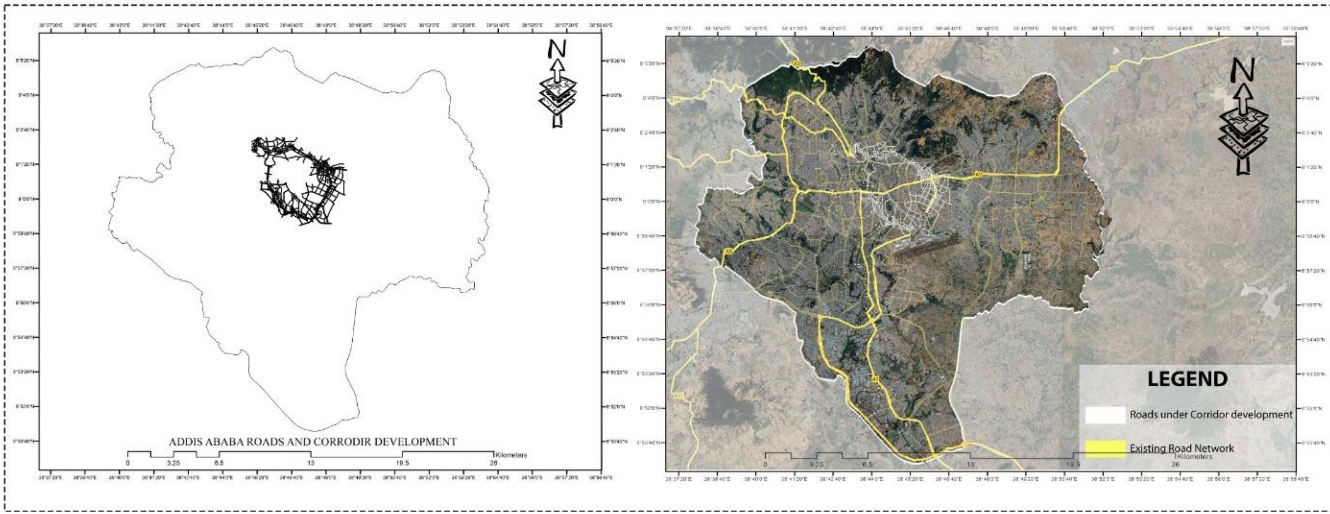

Addis Ababa boundary with corridor development roads

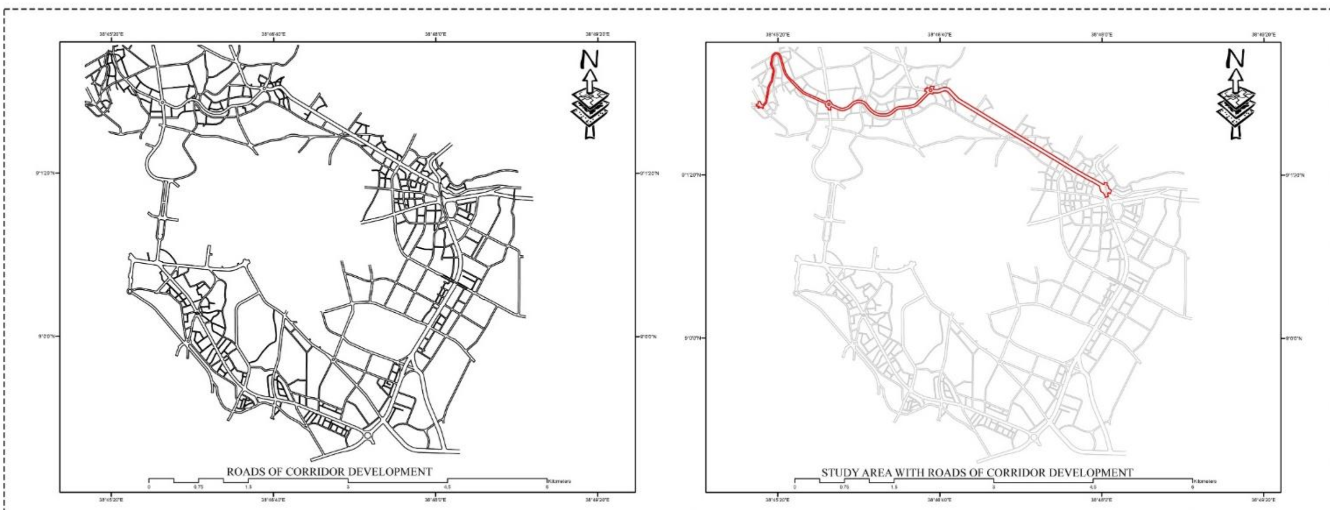

Annex 3 *Asphalt Pavement heat flow per day*

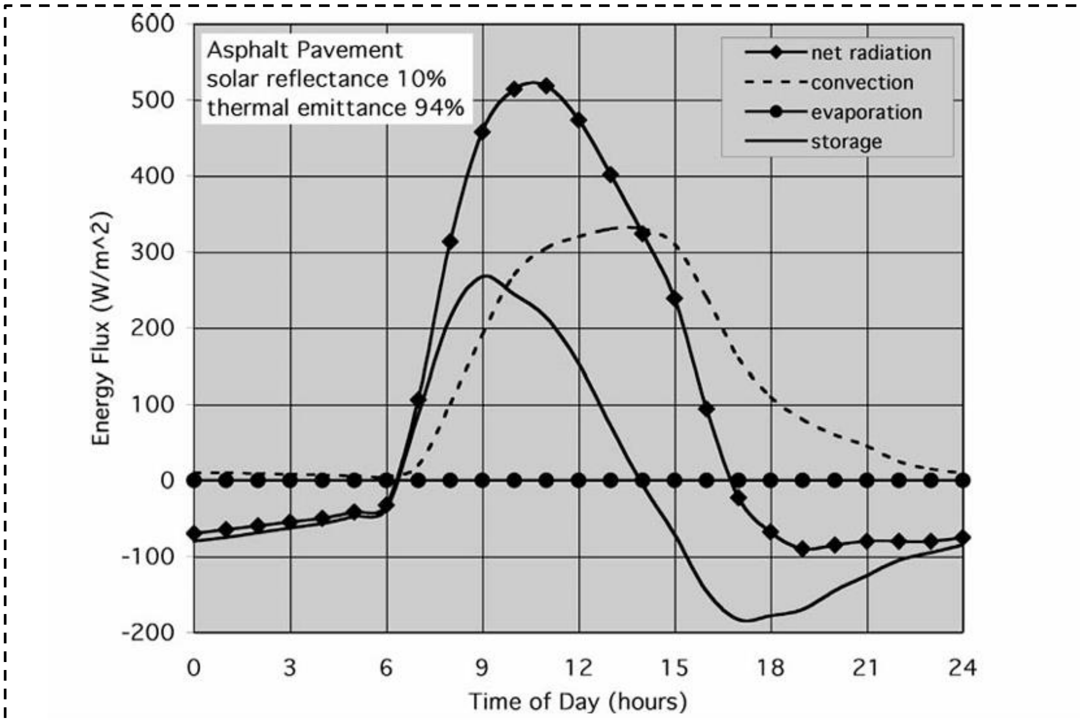

Source: Asaeda et al., 1996

Annex 4 *Variation of solar reflectance of asphalt and concrete pavement over time*

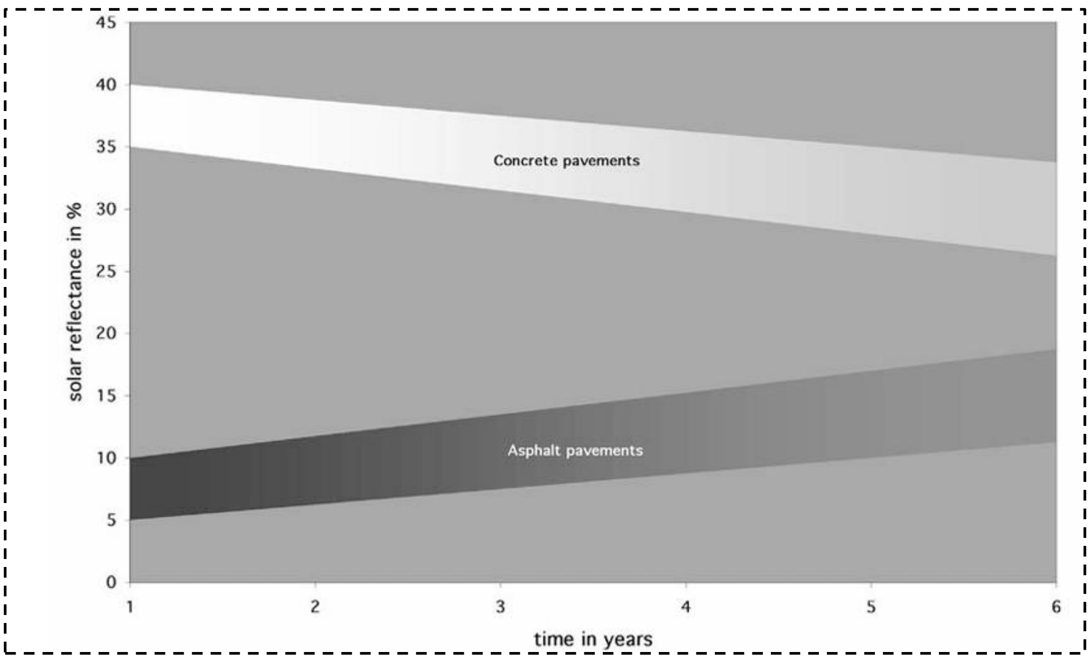

Source: Asaeda et al., 1996

Annex 5 *Concrete pavement temperature per day*

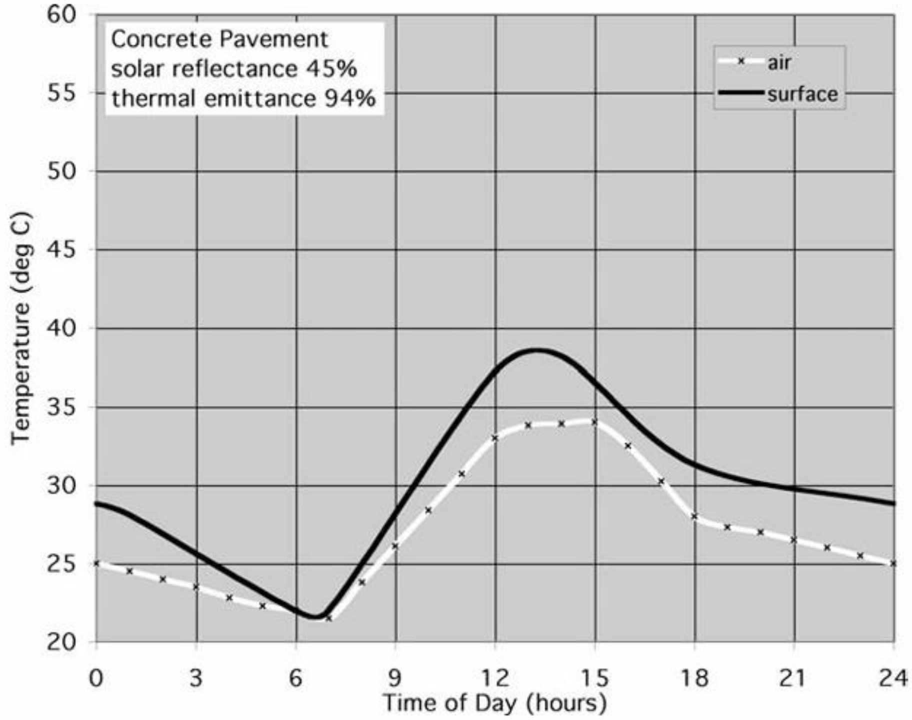

Source: Asaeda et al., 1996

Annex 6 *Addis Ababa mean, minimum, and maximum temperature*

Months	***Minimum***			***Maximum***			
	2015	**2020**	**2024**	**2015**	**2020**	**2024 Max**	**2024 Extreme**
January	7.96	10.482	7.5	23.841	24.18	23.7	28
February	10.171	11.875	9	23.841	25.5	24.8	29.1
March	10.789	13.606	10.6	23.841	26.351	25.3	31
April	12.503	13.562	11.4	23.841	25.955	24.9	30.5
May	13.643	13.19	11.2	23.841	24.783	25.2	30
June	13.083	11.996	10.7	23.841	23.203	23.5	29
July	12.435	12.244	11.1	23.841	20.606	21.2	27.2
August	12.2	12.244	11.1	23.841	20.917	21	31.8
September	12.093	12.165	10.5	23.841	22.032	21.9	26.2
October	12.016	10.377	8.3	23.841	23.99	23	28.5
November	8.143	9.234	6.4	23.841	24.26	23.1	30.1
December	10.209	8.5	6.5	23.841	23.787	23.2	26.6

Annex 7 *Temporal Trends in LST of Addis Ababa (2015, 2020, and 2024)*

Month	LST mean 2015	LST mean 2020	LST mean 2024
January	31.12296	28.499	33.748
February	33.84141	30.983	35.233
March	34.42367	31.584	34.219
April	36.29118	31.46	36.877
May	31.18678	31.879	34.12
June	26.60491	24.94	28.84
July	24.11921	24.154	27.283
August	25.88767	24.995	28.741
September	26.95352	27.5	30.714
October	30.99536	30.403	33.622
November	29.74201	30.649	34.743
December	29.33691	30.269	33.897
Average	30.04213	28.94294	32.66975

Annex 8 *Temporal Trends in LST of study area (2015, 2020, and 2024)*

Month	LST mean 2015	LST mean 2020	LST mean 2024
January	31.034	31.634	32.934
February	31.211	32.121	33.821
March	31.226	31.024	33.184
April	29.795	31.896	33.395
May	30.147	29.147	33.726
June	28.359	29.159	30.759
July	28.691	29.291	31.691
August	30.237	32.017	33.537
September	30.184	31.722	32.847
October	29.867	30.4867	32.567
November	30.06	30.995	33.396
December	30.117	30.639	32.039
Average	30.07733	30.84431	32.82467

Annex 9 *Tree, Shrub and grass species recommended for roadside*

Type	Common Name	Scientific Name	Family	Purpose	Height (M)	Spread (M)	Description
	Jacaranda	Jacaranda mimosifolia	Bignoniaceae	Ornamental, shade	7.5-15	6-9	Deciduous, fast-growing, drought-tolerant, termite resistant, sprouts easily if damaged Evergreen
	Siris tree	Albizial ebbeck	Fabaceae	Dense Shade,	15-20	12-20	Drought tolerant, adaptable, tolerate high temperature, umbrella like crown

Tree *species for roadside*				ornamental			
	African Tulip	Spathodea campanulata	Bignoniaceae	Ornamental, shade	10-25	Up to 10	Large leaf, broad crown; drought-resistant, termite resistant
	Flame tree	Delonix regia	Fabaceae	Ornamental, shade, wood, purification	8-15	Up to 12	Deciduous, spreading canopy; drought resistant, termite resistant
	Golden flower tree	Cassia fistula			10-15	6-8	Semi deciduous, Widely planted along roadside, spreading canopy
	Neem	Azadirachta indica	Meliaceae		15-20	2-6	Fast-growing, evergreen, drought and pest resistant
	Yellow cassia, Bombay blackwood (English)	Senna siamea	Fabaceae	ornamental, shade, Timber production	10-20	6-12	evergreen (drought resistant), fast-growing
	Tropical almond	Terminalia catappa	Combretaceae	ornamental, shade	15-25	10-20	Deciduous, Excellent road shade and pedestrian shade plant
	white cassia, mhomba (Kiswahili)	Senna spectabilis	Fabaceae		6-12	3-5	evergreen (drought resistant) fast-growing, boundary marker
	Chocolate Berry	Vitex payos	Lamiacae		4-10	2-7	Drought resistant tree found near rock outcrops, high water tables
	Indian Ashoka	Polyalthia longifolia	Annonaceae	ornamental, shade,	10-15	4-6	Provides shades, pollution tolerant, safe for sidewalks and paved areas
	brown ivory	Berchamia dischola r	Rhamnacea Rhamnaceae		10-15	Up to 20	Grows naturally, adaptable in semi-desert and grassland regions, large deciduous
	Bastard almond	Terminalia catappa	*Combretaceae*		Up to 35	Up to 18	evergreen tall tree, distinctive canopy and eatable nuts
	Prosea	Anthocephalus	Rubiaceae		20-30	10-15	evergreen Large foliage, tall tree

		chinensis					
	Golden shower tree	Cassia fistula	Fabaceae		10-15	6-10	Evergreen, medium-sized tree with large leaves, deciduous
	Tamarind tree	Tamarindus indica			12-25	15-20	Draught tolerant, good for street and urban planting
	Pongam	Pongamia pinnata			8-15	5-12	evergreen dense foliage, umbrella like
	Orchid tree	Bauhinia variegatta		Ornamental, shade	8-12	6-10	Shade with broad canopy, drought tolerance
	Bunyan tree	Ficus benghalensis	Moraceae		20-30	Up to 50	Semi evergreen spreading canopy and compact leaves
	Sacred Fig	Ficus religiosa			15-30	10-17	Semi evergreen shiny leaves
	Gmelina	Gmelina arborea	Lamiaceae	Shade, timber, eatable	25-30	8-12	Deciduous tree with hairy leaves
	Putranjiva	Putranjiva roxburghii	Putranjivaceae	Ornamental, shade,	8-15	6-10	evergreen shiny leaves tree
	Peepal tree	Ficus religiosa	Moraceae		20-30	15-20	Shade provider with its Rounded canopy, erosion control, air purification,
	Ficus tree	Ficus Benjamina			10-25	6-10	Provide shade, common as Street tree, suitable for urban environment
	Croton	Croton macrostachyus	Euphorbiaceae		12-25	4-10	evergreen well adapted to a dry climate and numerous side roots
	Bougainvillea	Bougainvillea spectabilis	Nyctaginaceae		6-12	6-10	Evergreen, climbing shrub producing stems up to 10 m long, ornamental
	Wild Sage	Lantana camara	Verbenaceae		0.5-2	2-3	Evergreen, can grow up to 2 m tall, erosion control

Shrub *for roadside*	Yellow oliander	Thevetia Peruviana	Apocynaceae		3-5	2-3	Attractive foliage, effective barrier plant, drought tolerant
	Common ironweed	Vernonia angustifolia	Asteraceae		1-3	1-4	Drought tolerant, ornamental, stalks
	Oleander	Nerium oleander	Apocynaceae		2-6	2-4	Evergreen, Drought tolerant, dense cover for wind break
	Yellow bells	Tecoma stans	Bignoniaceae		2-4	1-3.5	Commonly knowns as a roadside weed, ornamental, adapts well in tropical and subtropical environments
	Jungle flame	Ixora coccinea	Rubiaceae		1-3	1.5-2	Moderate light shade, Best for hedges and borders,
Grass *for roadside*	Sideoats grama/ mosquito grass	Bouteloua gracilis	Poaceae	Excellent drought tolerance			
	Prairie dropseed	Sporobolus heterolepis		Perennial, deciduous, ornamental grass with hair-like leaves			
	Kikuyu grass	Pennisetum clandestinum		Very fast-growing grass, good shade tolerance, excellent cold tolerance, and has the ability to smother weeds.			
	Pemba grass/ buffalo grass/ St. Augustine grass	Stenotaphrum secundatum		Excellent shade tolerance, completely			
	Zimbabwe grass	Chloris gayana		Shade tolerant grass, suitable for weed and erosion control			

Annex 10 *Interview Questions for Key informants*

This is to declare that all the answers in this interview question is forwarded without any external force, voluntarily with a full willingness to support the research in providing actual information based on my position, knowledge and data.

1. What was the baseline situation regarding roads, pedestrian, and road sides before corridor development?
2. What was the design objective and the plan formulated to achieve through the corridor development?
3. What was the general process from design to implementation?
4. What environmental consideration was employed in the design as well as execution phase? Is there any project team related to environmental concerns participated in the Design as well as execution?
5. What strategies do you utilize for enhancing green coverage in the project?
6. What key considerations was taken in material selection? Is there any consideration about permeable pavements?
7. Do you know about urban heat island effect? And is there any design consideration to mitigate the urban heat island effect in the area?
8. What was the major challenge you encounter in design as well as implementation and how do you resolved the issue?
9. What innovative technologies were employed to achieve the plan through design as well as implementation?
10. What prioritizing standards were taken for the urban road expansion?

    Is there any mitigating strategy employed for mitigating environmental impact due to the human intervention?